

INVESTIGATION OF FREQUENCY AND MOISTURE CONTENT
ON THE DEFORMATION CHARACTERISTICS OF SOIL

By

RICHARD GLENN NELSON //

Bachelor of Science
in Mechanical Engineering
Oklahoma State University
Stillwater, Oklahoma
1981

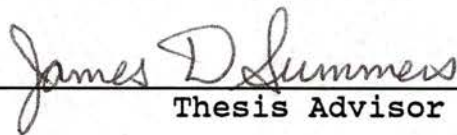
Master of Science
Oklahoma State University
1982

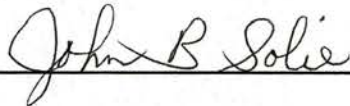
Submitted to the Faculty of the
Graduate College of the
Oklahoma State University
in partial fulfillment of
the requirements for
the Degree of
DOCTOR OF PHILOSOPHY
December, 1989

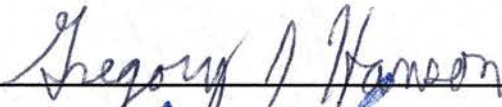
thesis
1989D
N 4296
cop-2

INVESTIGATION OF FREQUENCY AND MOISTURE CONTENT
ON THE DEFORMATION CHARACTERISTICS OF SOIL

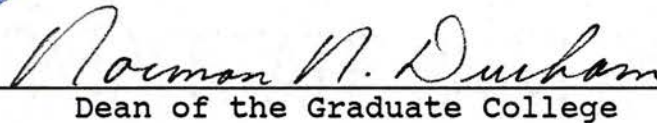
Thesis Approved:


Thesis Advisor








Dean of the Graduate College

ACKNOWLEDGEMENTS

I would like to thank my major advisor, Dr. James D. Summers for his patience, cooperation and understanding. Without his insight the completion of this project would not have been possible. I would also like to thank the remaining members of my committee; Dr. John B. Solie, Dr. Greg J. Hansen, Dr. John F. Stone and Dr. James N. Lange for the guidance they have provided. Their suggestions have helped me look at the questions and problems of this research with a new light and have helped me to better understand the research process.

I express gratitude and thanks to the Department of Agricultural Engineering, Oklahoma State University for their financial support throughout the duration of this project. Additional thanks goes to the personnel of the Agricultural Engineering Laboratory for their ideas in helping design and build the experimental equipment. I also wish to express thanks to Galen McLaughlin of the South Central Research Station at Chickasha for his help in obtaining the soil samples and in-situ data. Galen was instrumental in the outcome of this project and his ideas and insight were invaluable. There are two people that must be thanked because without their guidance and support I would not have been able to finish. These are Dr. Michael

F. Kocher, whose preliminary work in this area was invaluable and Kelvin P. Self for just telling me that things aren't really as bad as they seem.

Finally, I would like to thank my wife, Kristin for the many hours of love, understanding and patience during the time spent working on this program. I would also like to thank my parents for their understanding and my in-laws for their support and encouragement as well.

TABLE OF CONTENTS

Chapter	Page
I. INTRODUCTION AND OBJECTIVES.....	1
Introduction.....	1
Objectives.....	2
II. REVIEW OF LITERATURE.....	3
Time-Dependent Models.....	4
Three-Dimensional Models.....	4
Anisotropic Models.....	6
Plasticity Models.....	8
III. ONE-DIMENSIONAL EXPERIMENTAL EQUIPMENT AND PROCEDURE.....	14
Soil Samples.....	14
Testing Procedure.....	17
Sample Preparation.....	17
Modulus of Elasticity.....	18
Instrumentation.....	19
Amplitude and Frequency Testing.....	21
Moisture Content Determination.....	23
IV. THREE-DIMENSIONAL IN-SITU EXPERIMENTATION.....	26
Experimental Design.....	26
Experimental Equipment.....	31
Transmission of Data.....	33
V. RESULTS AND DISCUSSION.....	35
One-Dimensional Analysis.....	35
Dynamic Test Parameters.....	35
Acceleration to Displacement Conversion.....	36
Acceleration Curve Fits.....	37
Stress-Strain Plots.....	45
Frequency Variation Within a Moisture Content.....	45
Moisture Content Variation Within a Frequency.....	55
Dynamic Model Parameter Determination.....	66
Theory.....	67

Chapter	Page
Regression of Alpha and Xi as Functions of Moisture Content and Frequency.....	69
Three-Dimensional Analysis.....	76
Poisson's Ratio Determination.....	79
VI. CONCLUSIONS.....	89
VII. RECOMMENDATIONS FOR FURTHER RESEARCH.....	91
LITERATURE REVIEWED.....	93
APPENDIXES.....	97
APPENDIX A - ONE-DIMENSIONAL ACCELERATION DATA.....	98
APPENDIX B - THREE-DIMENSIONAL IN-SITU DATA.....	126

LIST OF TABLES

Table	Page
I. Moisture Contents for Amplitude and Frequency Testing for the Vertical Orientation.....	24
II. Moisture Contents for Amplitude and Frequency Testing for the Horizontal Orientation.....	25
III. Coefficients of Determination for Actual v. Generated Sine Wave Data for the Vertical Orientation.....	40
IV. Coefficients of Determination for Actual v. Generated Sine Wave Data for the Horizontal Orientation.....	40
V. Student's t Test Comparing the Slopes of Two Independent Regressions at One Frequency and Different Moisture Content Ranges.....	66
VI. Student's t Test Comparing the Slope, b_1 of the Equation $a, \xi = b_0 + b_1 \cdot MC$ Against a Value of Zero.....	75
VII. Average Values of a and ξ for Frequencies of 800 to 2000 Hz Within Their Respective Moisture Content Ranges.....	75
VIII. Average Values of Apparent Poisson's ratio for each Distance r from the Source of Input for all Three Input - Output Orientations.....	83
IX. Comparison of Calculated values of Apparent Poisson's ratio and Theoretical values based on Geometrical Damping for all Input - Output Orientations.....	84
X. Values of the Intercept, I and the Slope, S of the Regression $\nu' = I + S/r$ for each of the Three Input - Output Orientations.....	85

LIST OF FIGURES

Figure	Page
1. Map of South Central Research Station, Chickasha, Oklahoma showing Site of One and Three-Dimensional Experimental Areas.....	16
2. Electromagnetic Shaker.....	20
3. Low Amplitude Sinusoidal Waveform.....	22
4. High Amplitude Sinusoidal Waveform.....	22
5. Rectangular Parallelepiped Soil Mass.....	28
6. Schematic of a) Horizontal Input and Horizontal Output, b) Horizontal Input and Vertical Output and c) Vertical Input and Horizontal Output.....	30
7. Spring Loaded Impulse Generator.....	32
8. Graphs of a) Displacement, x , b) Velocity, \dot{x} and c) Acceleration, \ddot{x} for a Continuous System Subject to Harmonic Motion.....	38
9. Comparison of Generated Sine Wave Data to Actual Experimental Sine Wave Data for a) Bottom Accelerometer and b) Top Accelerometer. Vertical Orientation, Low Amplitude.....	41
10. Comparison of Generated Sine Wave Data to Actual Experimental Sine Wave Data for a) Bottom Accelerometer b) Top Accelerometer. Vertical Orientation, High Amplitude.....	42
11. Comparison of Generated Sine Wave Data to Actual Experimental Sine Wave Data for a) Bottom Accelerometer and b) Top Accelerometer. Horizontal Orientation, High Amplitude.....	43
12. Variation of Stress-Strain Values with Frequency for a Vertically Oriented Soil Sample at a Moisture Content Level of 14.5%.....	46

13.	Variation of Stress-Strain Values with Frequency for a Vertically Oriented Soil Sample at a Moisture Content Level of 17.2%.....	47
14.	Variation of Stress-Strain Values with Frequency for a Vertically Oriented Soil Sample at a Moisture Content Level of 17.8%.....	48
15.	Variation of Stress-Strain Values with Frequency for a Vertically Oriented Soil Sample at a Moisture Content Level of 18.5%.....	49
16.	Variation of Stress-Strain Values with Frequency for a Horizontally Oriented Soil Sample at a Moisture Content Level of 16.9%.....	50
17.	Variation of Stress-Strain Values with Frequency for a Horizontally Oriented Soil Sample at a Moisture Content Level of 17.7%.....	51
18.	Variation of Stress-Strain Values with Frequency for a Horizontally Oriented Soil Sample at a Moisture Content Level of 17.9%.....	52
19.	Variation of Stress-Strain Values with Frequency for a Horizontally Oriented Soil Sample at a Moisture Content Level of 18.6%.....	53
20.	Variation of Stress-Strain Values with Moisture Content for a Vertically Oriented Sample Vibrated at a Frequency of 300 Hz.....	56
21.	Variation of Stress-Strain Values with Moisture Content for a Vertically Oriented Sample Vibrated at a Frequency of 800 Hz.....	57
22.	Variation of Stress-Strain Values with Moisture Content for a Vertically Oriented Sample Vibrated at a Frequency of 1000 Hz.....	58
23.	Variation of Stress-Strain Values with Moisture Content for a Vertically Oriented Sample Vibrated at a Frequency of 1500 Hz.....	59

24.	Variation of Stress-Strain Values with Moisture Content for a Vertically Oriented Sample Vibrated at a Frequency of 2000 Hz.....	60
25.	Variation of Stress-Strain Values with Moisture Content for a Horizontally Oriented Sample Vibrated at a Frequency of 800 Hz.....	61
26.	Variation of Stress-Strain Values with Moisture Content for a Horizontally Oriented Sample Vibrated at a Frequency of 1000 Hz.....	62
27.	Variation of Stress-Strain Values with Moisture Content for a Horizontally Oriented Sample Vibrated at a Frequency of 1500 Hz.....	63
28.	Variation of Stress-Strain Values with Moisture Content for a Horizontally Oriented Sample Vibrated at a Frequency of 2000 Hz.....	64
29.	Variation of α with Moisture Content for Vertically Oriented Samples.....	71
30.	Variation of α with Moisture Content for Horizontally Oriented Samples.....	72
31.	Variation of ξ with Moisture Content for Vertically Oriented Samples.....	73
32.	Variation of ξ with Moisture Content for Horizontally Oriented Samples.....	74
33.	Horizontal Input and Horizontal Output at a Distance of 0.114 Meters.....	77
34.	Horizontal Input and Vertical Output at a Distance of 0.227 Meters.....	78
35.	Variation of Apparent Poisson's Ratio with the Inverse Distance for the Horizontal Input-Horizontal Output Orientation.....	86
36.	Variation of Apparent Poisson's Ratio with the Inverse Distance for the Horizontal Input-Vertical Output Orientation.....	87
37.	Variation of Apparent Poisson's Ratio with the Inverse Distance for the Vertical Input-Horizontal Output Orientation.....	88

LIST OF SYMBOLS

A	- Cross sectional area of the soil sample
A_1, A_2	- Waveform amplitudes
E_1, E_0	- Static stress-strain modulus
E^*	- Dynamic stress-strain modulus
F	- Force
j	- Imaginary number
k	- As defined in the text
L	- Length of soil sample
L_1	- Initial length
L_f	- Final length
m	- Mass of soil sample
mc	- Moisture content
ν'	- Apparent Poisson's ratio
r	- Distance from input source
t	- Time
u	- Displacement of a point within the soil sample
x, y, z	- Cartesian coordinate directions
x	- Displacement
\dot{x}	- Velocity
\ddot{x}	- Acceleration
α	- Parameter in the second-order viscoelastic stress-strain equation
ϵ	- Strain

ϵ_j	- Strain in direction j
ϵ_Y'	- Yield strain
$\dot{\epsilon}$	- Strain rate
$\ddot{\epsilon}$	- Second derivative of strain with respect to time
ϵ''	- Plastic strain
$\dot{\epsilon}''$	- Plastic strain rate
λ	- Magnitude of the maximum displacement at the bottom of the soil sample
ϕ'	- As defined in the text
ξ	- Parameter in the second-order viscoelastic stress-strain equation
ρ	- Wet bulk density
σ	- Stress
$\sigma_x, \sigma_y, \sigma_z$	- Stresses in each of the Cartesian coordinate directions
σ_Y'	- Yield stress
σ_0, σ_1	- Initial stress
$\dot{\sigma}$	- Stress rate
ω	- Vibration frequency

CHAPTER I

INTRODUCTION AND OBJECTIVES

Introduction

One of the most important parameters that nearly all agricultural operations depend upon is soil. Soil provides a support system for the growth of crops. To be able to produce the food and fiber that the world will require in the future, a better understanding of soil and its behavior is required.

Most soils are not in the correct condition for crop growth and require some preparation by machine before planting. The design of soil working machines must be directed toward producing an optimum soil condition for maximum crop yield. In order to accomplish this, an understanding of how the soil reacts to the varying forces is important.

Understanding how soil yields when forces are applied to it requires knowledge about the strength of the soil. Gill and Vanden Berg (1968) concluded that the way to describe soil strength is through the use of stress-strain relationships.

Objectives

The overall objective of this research is to develop a criterion for the tensile failure of soil located at the South Central Research Station, Chickasha, Oklahoma. The specific objectives are as follows:

1. Determine the effect of moisture content on the stress-strain behavior of soil.
2. Determine if a significant plastic region exists in soil during tension and determine a tensile failure criterion.
3. Develop a stress-strain relationship based on the second-order viscoelastic stress-strain equation so that all three dimensions are encompassed with the primary planes being horizontal and vertical.
4. Develop an experimental procedure and equipment to validate the model in-situ.

CHAPTER II

REVIEW OF LITERATURE

Many investigators have developed models that relate stress to strain (force to displacement). However, due to the complex nature of soil and its response to the many variables that affect it, a description that encompasses all stress-strain behavior would be difficult if not impossible to formulate. Soil is a multiphase medium consisting of granular particles, water and air. At different temperatures and moisture contents, the physical nature of soil can change dramatically as well as the properties that describe its behavior. It is possible for simple elastic medium to a non-Newtonian fluid, and because of this, models based on only one state are not very practical.

Vanden Berg (1961) said that elastic and plastic theory have their place in the development of stress-strain theory but are not developed enough to reliably use. Kitani and Persson (1967) stated a need for two-dimensional relationships to solve practical problems associated with soil deformation.

Vanden Berg (1961) expressed a need for soil behavior theory to include large strains and volumetric changes. He also mentioned the need for soil stress-strain relations to

express changing strength due to mass compaction. He commented that this might be the most difficult area to model.

Time-Dependent Models

Johnson et al. (1972) and Vanden Berg (1961) realized that in dynamic systems which affect soil, the relation between stress and strain is time dependent and should be included in any analysis. Johnson et al. (1972) developed a relationship between time and a length scale for soil samples. Ram and Gupta (1972) observed that soil behaved non-linearly, viscoelastically. They concluded soil could be modeled by a stress-strain-time relationship.

Smith et al. (1978) proposed a first-order viscoelastic stress-strain model for evaluating the dynamic behavior of prosthetic urethane compounds. This model included a static component as well as a term to describe the first time derivative of strain.

Prevost (1980) stated a need for the transient response of the soil to be included in the modeling process and suggested that an extension of Biot's theory into the non-linear anelastic range to accomplish this.

Three-Dimensional Models

Baladi and Rohani (1978) developed a three-dimensional, elastic-plastic, isotropic constitutive model for geologic materials to simulate a wide range of stress-strain-pore pressure responses for fully saturated cohesionless soils.

Baladi (1979) investigated multiphase drained and undrained soil samples to develop a three-dimensional elastic-plastic model to simulate the stress-strain behavior of geologic materials. He stated that a two or three-phase constitutive model would predict the deformation path(s) better than a single-phase model would.

Khan (1979) stated that, in general, soil behaves neither like an elastic solid nor a Newtonian fluid but that it possesses certain viscous characteristics. He formulated a general relationship to predict the stress-strain characteristics of soils for all stress paths. A limitation of his model is that it is only accurate for small deformations (elastic state) and is an approximation for large, non-linear displacements. Rohani (1972) reviewed seven mathematical models describing the stress-strain-time behavior of non-linear materials. These models were only valid for homogeneous and isotropic media with small displacement gradients (linear approximations).

Other areas of modeling that are pertinent deal with changes in strength occurring as moisture content changes. Gill (1959) concluded that the soil strength varies not with moisture content but with moisture loss.

Another modeling approach to stress-strain relationships is the concept of the "spatial mobilized plane" or SMP (Matsuoka and Nakai, 1974; Matsuoka, 1976;

planes among the three principal stress axes. The three planes comprise one resultant plane on which the soil particles are assumed to slide. Stress-strain relationships of soils can be uniquely expressed respective to the resultant plane. These models employ a total strain increment consisting of an elastic strain, plastic strain due to consolidation, and plastic strain due to shear. However, strain-rate dependence or anisotropic effects are not mentioned or included.

Anisotropic Models

While each of the models previously mentioned has made a contribution to the overall understanding of the soil deformation process, many assumptions have been made to arrive at the working models. One of the most critical assumptions has been that of isotropy. It is known and generally realized that most materials, soil included, are not homogeneous and isotropic, but are nonhomogeneous and anisotropic, meaning that the soil structure is not uniform and its properties have a preference for a specific direction. Arya et al. (1980) concluded stress and strain significantly varied from the isotropic case to the anisotropic case for creep in spherical vessels. Lopes and Feijoo (1982) developed an approach to modeling soil creep through a stress-strain-time relationship that used volumetric and deviatoric creep strains. Several researchers (Arthur and Menzies, 1972; Miura and Toki, 1984;

Green and Readies, 1975; and Ochiai and Lade, 1983) have worked with sand to determine how anisotropic fabric affects the stress-strain behavior. Ochiai and Lade (1983) have concluded that data concerning three-dimensional behavior is not always consistent. Part of the problem is no clear and concise method exists to distinguish between inherent and induced anisotropy.

Other researchers (Hansen and Clough, 1982; Banerjee et al., 1981; and Yuen et al., 1978) investigated the influence of anisotropy on clay samples. Banerjee et al. (1981) derived a mathematical model accounting for initial (inherent) anisotropy due to depositional stress history and subsequent alteration during plastic deformation. Prevost et al. (1980) developed a three-dimensional, non-linear, anisotropic, elasto-plastic and path-dependent stress-strain-strength model for use on offshore structure foundations. These authors felt very strongly that any past history effects must be taken into consideration. They used multiple yield surfaces to describe deformation of soil and felt that anisotropy of soil could be described by the position of yield surfaces as the material deforms. They concluded that the non-linearity and anisotropy are a direct result of the plasticity associated with soil deformation. Nakase and Kamei (1983) also felt that anisotropy resulted from plastic deformation of soil and defined anisotropy in terms of a plasticity index. As the plasticity index becomes more pronounced, anisotropy becomes less important.

Miura and Toki (1984) used a plastic potential function in conjunction with a yield function to help provide an answer to the problem of anisotropic effects. But Banerjee et al. (1981) stated existing theories of plastic volumetric strain hardening (critical state models) are inadequate for large plastic deformation in soil structures.

Plasticity Models

Because soil is a complex medium and its behavior can change subject to many variables, modeling by an elastic relationship alone will not adequately define a stress-strain relation. Prevost and Hoeg (1975) stated elastic theory alone cannot properly account for observed soil behavior and that an incremental plastic theory provides a very promising complementary tool for describing stress-strain-strength models. They proposed to model soil as an elastic-plastic, strain-hardening or strain-softening frictional material. Their model accounted for non-linear behavior through the use of yield functions and an associated flow rule. The major drawback was no provision for anisotropic effects.

Most authors feel that elastic-plastic models hold promise for defining the constitutive relationships for soil media. Baladi (1979) and Baladi and Rohani (1977, 1978) developed three-dimensional, elastic-plastic constitutive models for geologic materials through the use of an incremental plastic theory. However, all models assumed

isotropy. Elastic-plastic models developed by Lade and Duncan (1975) and Richter (1979) were similar but made no allowance for anisotropy.

Prevost and Hoeg (1977) improved on earlier models with an analytical model that described anisotropic, elastic-plastic and path-dependent stress-strain properties of soils. Anisotropy is due to deviatoric plastic flow. They used yield surfaces to define a "field of plastic moduli" to determine expansions or contractions of the soil. Prevost (1985) developed a similar model for cohesionless soils and was able to account for hysteretic behavior associated with cyclic plastic flow. Baladi and Rohani (1982) created three-dimensional, elastic-viscoplastic and work-hardening constitutive relations for geologic materials that would also reproduce the hysteric behavior of a material under a certain state of stress. The authors alluded to the fact that two types of models have potential to accurately describe material response to stress. The first was a viscoelastic-plastic model in which both the elastic and plastic responses were rate sensitive. The second model was a elastic-visco-plastic model in which the elastic portion was rate-independent and the plastic portion was rate-dependent.

To better understand dynamic behavior of soil and formulate rate-dependent relationships, an understanding of wave propagation is helpful. DeRoock and Cooper (1967) proposed using propagation velocity of a mechanical force

which could be related to the strength of the soil. Kocher and Summers (1988) used one-dimensional wave propagation theory to evaluate of several dynamic soil stress-strain models. They employed a vibrational test on a cylindrical soil sample to obtain acceleration parameters to verify their dynamic models.

Most stress-strain models presented are variations on Hooke's law, i.e., they contain a direct linear or non-linear relationship between stress and strain with no strain rate dependence (first, second or higher order derivative terms). Shackel (1973) proposed that each strain present in the soil was a function of all principal stresses and that the problem associated with stress-strain relationships was to find the correct form of those functionals relating all six principal stresses to the individual strains.

For some applications, the models obtained the desired results but for others such as problems involving large deformations, they fell short of accurate prediction. Thus a need arose to modify existing stress-strain theories with the addition of strain-rate affects for soils. Early investigators such as Prandtl (1928) proposed the form:

$$\sigma = \phi (\epsilon'', \dot{\epsilon}'') \quad (1)$$

where ϵ'' = plastic strain

$\dot{\epsilon}''$ = plastic strain rate. Deuthler (1932) found that the logarithmic form

$$\sigma = \sigma_1 + A \ln \frac{\dot{\epsilon}''}{B} \quad (2)$$

was a good model for tensile test data. In 1951, Malvern proposed the following flow law:

$$E_0 \dot{\epsilon} = \dot{\sigma} + g(\sigma, \epsilon) \quad (3)$$

for plastic deformation. The last term on the right hand side, $g(\sigma, \epsilon)$ models the elastic line above the initial yield strain, ϵ_y' . This implies that the material is brought to a state of incipient plastic flow after a given elastic strain. The plastic flow requires some time in which to become appreciable resulting in the additional strain beyond ϵ_y' is initially mainly elastic. Malvern performed numerical integration on the equations describing longitudinal waves of plastic deformation to arrive at the following form of the expression $g(\sigma, \epsilon)$:

$$g(\sigma, \epsilon) = k[\sigma - f(\epsilon)] \quad (4)$$

where k is a constant. The plastic strain rate is proportional to $\sigma - f(\epsilon)$ which is the excess stress over the stress at the same strain in a static test. Therefore, Malvern's stress-strain identity becomes:

$$E_0 \epsilon = \sigma + k[\sigma - f(\epsilon)] \quad (5)$$

Sokolovsky (1948) independently derived the same basic equation as Malvern's but for a special case of an elastic-viscous-plastic material without workhardening in which

$g(\sigma - \sigma_{y'})$ is only a function of the excess of the instantaneous stress over the initial yield stress $\sigma - \sigma_{y'}$. Malvern did further studies on strain rate effects by investigating dynamic compression measurements on annealed aluminum specimens and longitudinal compressive plastic wave propagation experiments. These experiments were performed in relation to the rate-dependent theory of plastic wave propagation. He studied rate-dependency with respect to temperature and concluded that as temperature increased so did the rate dependency of the material. From this analysis, he formulated the following relation between stress and strain:

$$\sigma = \sigma_0 \left(1 + \frac{k}{\sigma_0 \ln \dot{\epsilon}} \right) \quad (6)$$

Pisarenko (1984) investigated stress and strain waves with large amplitudes in a condensed medium not describable by Hooke's law. He postulated stress was a function of not only first-order derivatives of strain but second, third, and higher order ones as well. Sokolovsky's and Malvern's equations are defined for when the process affecting the medium proceeds slowly. A variant of their equations, for when the processes proceed quickly, was developed by Vasin et al. (1975) and is as follows:

$$f(\sigma, \epsilon) \dot{\epsilon} = \dot{\sigma} + g(\sigma, \epsilon) \quad (7)$$

The most relevant work to date has been that of Kocher and Summers (1988). Their use of longitudinal vibration of cylindrical soil samples was used to evaluate four different stress-strain models. These models were a complex modulus, viscous, and first and second-order viscoelastic. Each of the models was used in conjunction with the wave propagation analysis to help determine which of the four models best described the dynamic behavior of the soil. The second-order viscoelastic model was the one that best described the additional dynamic complexities of the soil and is as follows:

$$\sigma = E_0 \epsilon + \alpha \dot{\epsilon} + \xi \ddot{\epsilon} \quad (8)$$

Tests were performed on soils samples taken from field cores originally oriented vertically and horizontally.

CHAPTER III

ONE-DIMENSIONAL EXPERIMENTAL EQUIPMENT AND PROCEDURE

The purpose of performing experimentation on cylindrical soil samples was to determine the effect of frequency and moisture content on the stress-strain behavior of soil.

Kocher and Summers (1988) have shown that the second-order stress-strain equation

$$\sigma = E\epsilon + \alpha\dot{\epsilon} + \xi\ddot{\epsilon} \quad (9)$$

very effectively models dynamic behavior of soil. The propagation of stress waves through a cylindrical soil sample was used to provide information concerning the effect of moisture on the parameters of equation (9). Wave propagation data were used to determine if a failure criterion for soil could be established.

Soil Samples

Investigation of the moisture content effects on the second-order stress-strain equation involved obtaining experimental soil samples at different moisture levels. The samples were obtained at the South Central Research Station

at Chickasha, Oklahoma. The textural analysis (% sand, % silt, and % clay) of the soil used for the one-dimensional experimentation was 19% sand, 68% silt and 14% clay. The textural analysis of the soil used for the in-situ portion of this study was 28% sand, 61% silt and 12% clay. The soil at both locations was a Reinach silt loam. Figure 1 is a map of the South Central Research Station and shows the locations at which both portions of this study were conducted. Kocher and Summers (1988) analyzed soil samples from the same location and found the parameters of Equation (9) vary with sample orientation. Because of this finding, soil samples were taken such that the longitudinal axis was originally in both vertical and horizontal directions.

To extract samples in the vertical orientation from the ground, an auger was employed to drill approximately 400 mm into the ground and remove a cylindrical shaped core of soil. Soil cores were divided into sections approximately 50-75 mm in length. If a core sample was broken as a result of drilling it was discarded if shorter than 50 mm. Soil cores with cracks or other physical damage were removed from consideration. Once a core had been broken into the desired lengths, each of the pieces were placed in a plastic bag and stored in a cushioned box for transport to the Agricultural Engineering Laboratory at Stillwater, Oklahoma. Samples were transferred to a refrigerator to keep the moisture level from decreasing until experimentation began.

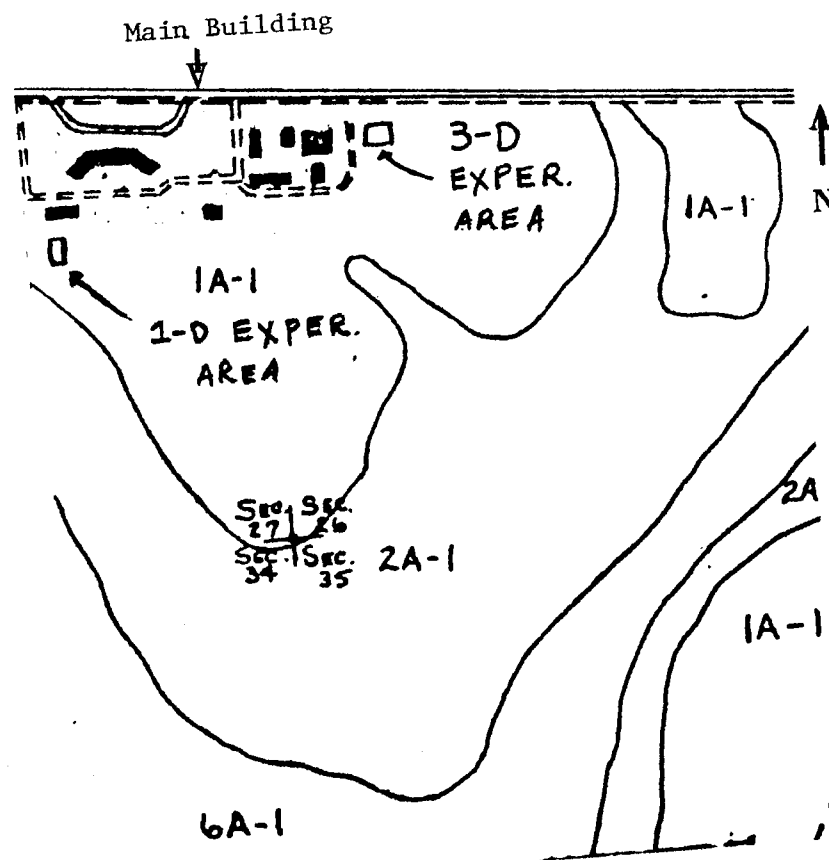


Figure 1. Map of South Central Research Station, Chickasha, Oklahoma showing Site of One and Three-Dimensional Experimental Areas

To extract horizontal samples, a metal box was pushed into the ground using a tractor mounted loader. This box had one open side and a circular hole cut into one end. The box containing the soil mass was removed from the ground and placed on its longitudinal axis. The auger used to obtain vertical samples was used to drill into the soil mass contained in the box. Using this procedure, the longitudinal axis of the sample lay in the horizontal plane of the soil.

To obtain samples at different moisture content levels, a field plot measuring 0.258 meters squared was flooded with water using a garden sprinkler. The area was watered until water stood throughout a majority of the plot. The water was given time to infiltrate the ground, two days after application the first samples were taken. Approximately 15 cores were taken, each yielding 2 to 4 samples. After another 2 to 3 days when the moisture content of the soil was felt to have changed sufficiently, another set of samples was obtained. This process was repeated until samples at three moisture content levels were obtained.

Testing Procedure

Sample Preparation

Soil samples were prepared before testing by cutting into 35-50 mm lengths. Once a sample was cut to an appropriate length, both ends were trimmed to form a flat surface perpendicular to the longitudinal axis of the

sample. The length and diameter of each sample were measured using digital calipers and recorded. Three length and diameter measurements were made for each sample. The length and diameter measurements were averaged before recording. Each sample was then weighed on a scientific scale for use in determining moisture content. The mass of the sample when wet divided by its volume calculated from length and diameter data provided wet bulk density.

Modulus of Elasticity

One of the coefficients used in the second-order viscoelastic stress-strain equation is the modulus of elasticity, E . To determine this constant, a static measurement was required. The static measurement consisted of a compression test on each sample. Soil samples were placed between two porous stones with the sample mounted vertically on the static stress-strain test stand with its longitudinal axis oriented vertically. At the top of the sample, a dial indicator was bolted to a mounting bracket to measure sample deflection as the top of the sample was loaded. The tip of the dial indicator was adjusted such that 5 mm of vertical travel remained once the tip deflected. Lead weights with a mass of 5 grams each were placed two at a time on top of the porous stone and the resulting deflection was read from the dial indicator and recorded. This was repeated every 30 seconds to 1 minute until a 100 gram load rested on the sample.

Since this was a static test, Hooke's Law, $\sigma = E\epsilon$ can be used to determine the modulus of elasticity, E . The stress, σ , was calculated as the quantity of the mass of the lead weights and porous stone times the acceleration constant divided by the area of the sample. The strain, ϵ , was calculated as the measured deflection divided by the original length of the sample. Both of these quantities were recorded after every addition of 10 grams to the top of the sample. A linear regression routine was used to determine the slope of σ versus ϵ which is E . Coefficient of determination values for the slope (E) ranged from .91 to .99.

Instrumentation

The testing procedure involved the use of an electromagnetic shaker shown in Figure 2 that produced a sinusoidal oscillation, $\lambda \sin \omega t$, to the base of the soil sample. A Ling Dynamics model V-408 exciter with a model T-400 base were selected. The sinusoidal excitation of the shaker was produced by a power amplifier (Model PA-400) consisting of a variable frequency adjustment and master gain control setting for amplitude level adjustment. Attached to the armature of the shaker was an accelerometer on which the soil sample was placed. Another accelerometer was placed at the top of the soil sample. These were Kistler model 8002 quartz accelerometers. This is shown in Figure 2. The sample was attached to the bottom

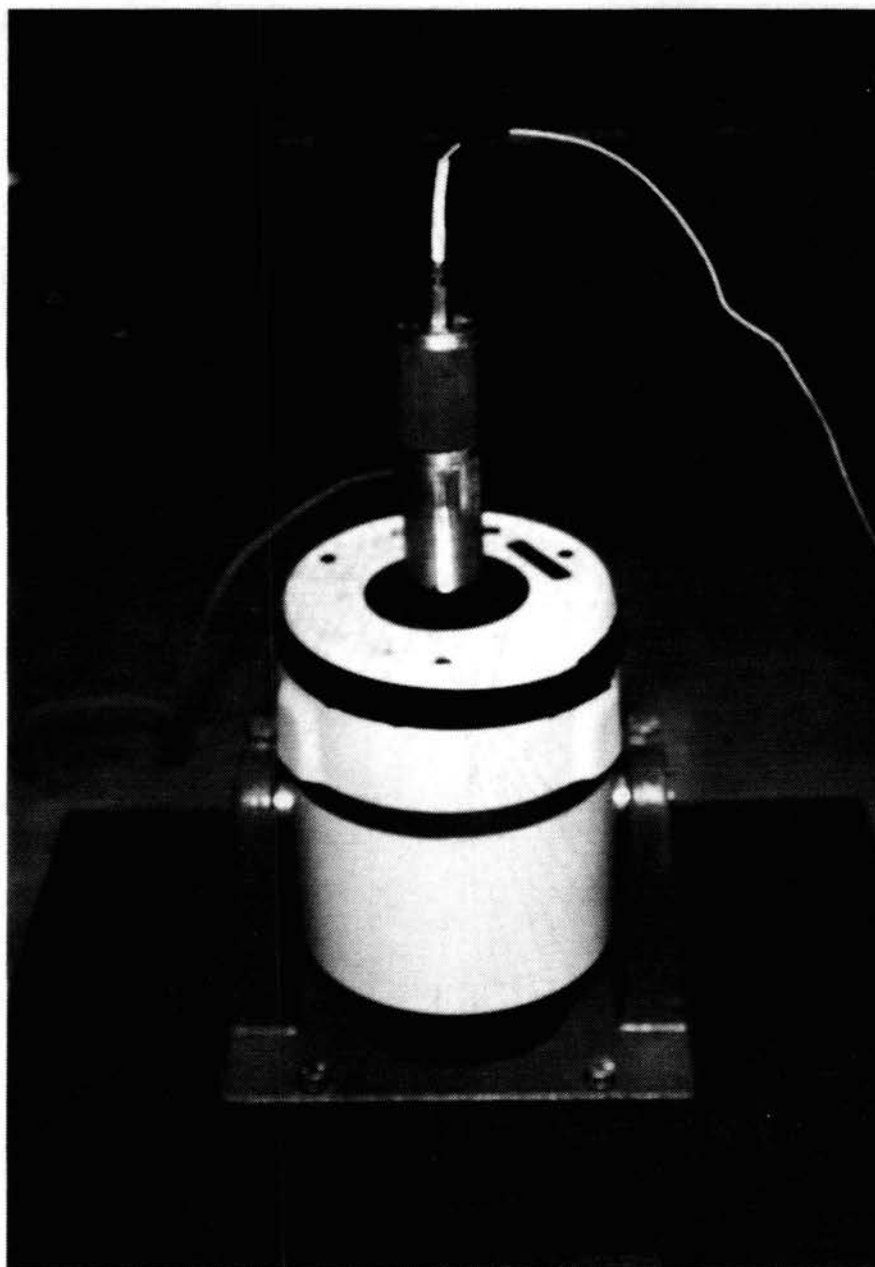


Figure 2. Electromagnetic Shaker

accelerometer using a thin layer of beeswax to ensure that it would not vibrate loose from the test apparatus during testing. A thin layer of beeswax was used to hold the top accelerometer onto the top end of the sample. The accelerometer attached to the bottom of the sample measured the input acceleration and the accelerometer at the top of the sample measured the acceleration wave propagated through the soil sample. The charges produced by the accelerometers were converted to voltages by Kistler model 5004 dual mode charge amplifiers.

A Nicolet 2090 digital storage oscilloscope with a RS-232C port was used to display the voltage-time data obtained from the accelerometers. The screen data consisted of two sinusoidal waveforms, imposed on each other, representing the bottom (input) and top (output) acceleration waves. Figures 3 and 4 show typical voltage-time waveforms displayed on the oscilloscope screen. A computer program written by Kocher (1986) was used to convert the voltage data to acceleration data and save it on floppy disk.

Amplitude and Frequency Testing

Each sample was to be tested at one frequency and several amplitude settings. The different amplitude settings corresponded to different stress levels applied to the base of the soil sample. It was hoped that by increasing the amplitude, information concerning the plasticity or a failure criterion of soil could be

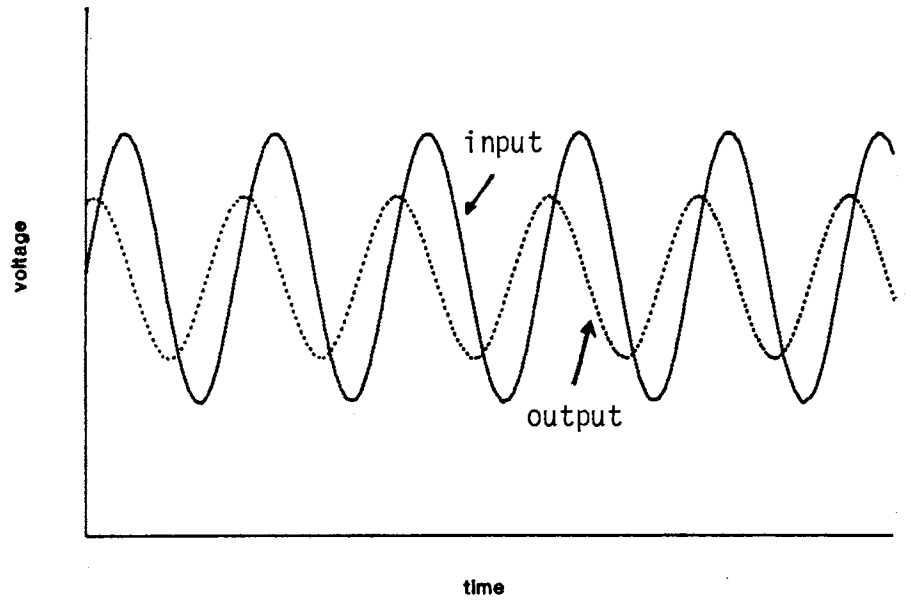


Figure 3. Low amplitude Sinusoidal Waveform.

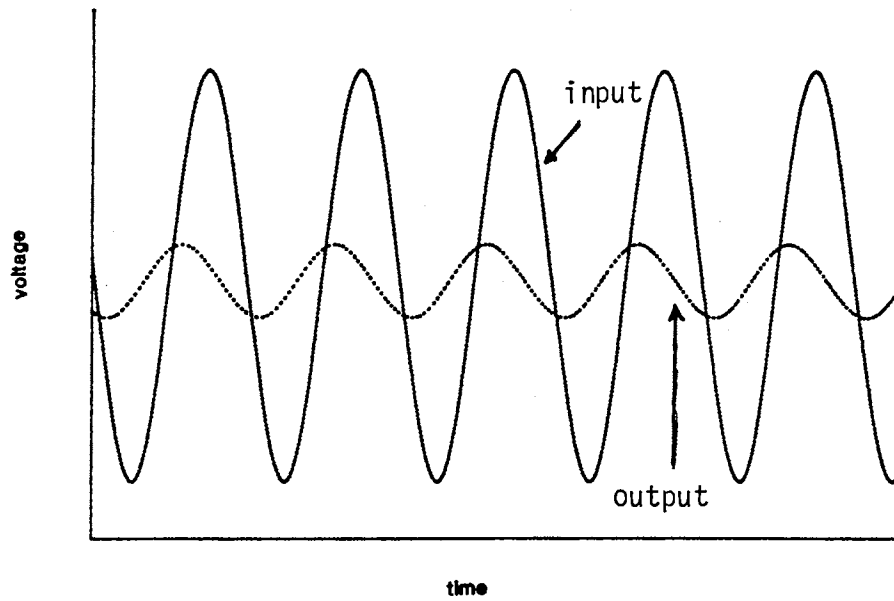


Figure 4. High Amplitude Sinusoidal Waveform

determined. It was felt that seven frequencies ranging from 200 to 2000 Hz would provide a reasonable cross-section of data concerning the effect of frequency on soil of different moisture contents. The test frequencies were 300, 800, 1000, 1300, 1500, 1700 and 2000 Hz. These frequencies were determined from work done by Kocher and Summers (1988). The anticipated natural frequencies were felt to lie in the 1300-1700 Hz range.

Soil samples were vibrated at a selected amplitude for a short period of time. Data were stored by the oscilloscope and transferred to a microcomputer data file. After the data were stored on floppy disk, the next amplitude level from the master gain control on the power amplifier was input to the sample. This process was repeated for up to nine different amplitude levels at one frequency or until the signal on the screen became indistinguishable from noise.

Moisture Content Determination

The moisture content of each sample was determined by drying each sample after dynamic testing. After testing had been completed, each sample was taken from the test stand and placed in a container along with any particles that fell off during testing. The container was transferred to an oven and the sample was dried for 24 hours at 105 degrees Celsius. The sample was weighed and the moisture content

was determined on a dry basis according to the following equation:

$$\%mc = \frac{(\text{wet weight} - \text{dry weight})}{\text{dry weight}} * 100\% \quad (10)$$

The range of moisture contents for the experimental samples for both orientations was 13.1% to 22.55%. Tables I and II show the moisture contents that were tested at each frequency for both orientations.

The percent saturations and wet bulk densities of each sample were calculated and recorded. These are presented for each sample in Appendix A.

TABLE I
MOISTURE CONTENTS FOR AMPLITUDE AND
FREQUENCY TESTING FOR THE
VERTICAL ORIENTATION

Frequency, Hz	Moisture Content, % Dry Basis		
300	13.1	17.2	20.0
800	15.1	17.2	19.8
1000	16.4	18.5	21.7
1300	14.5	17.3	21.5
1500	15.5	18.0	21.5
1700	14.5	16.3	18.4
2000	16.4	17.1	18.0

TABLE II
MOISTURE CONTENTS FOR AMPLITUDE AND
FREQUENCY TESTING FOR THE
HORIZONTAL ORIENTATION

Frequency, Hz	Moisture Content, % Dry Basis		
300	16.9	18.6	19.2
800	17.1	18.6	21.4
1000	16.9	18.2	20.5
1300	16.7	18.6	19.6
1500	16.7	17.6	18.5
1700	16.5	17.8	20.1
2000	16.5	18.3	20.3

CHAPTER IV

THREE-DIMENSIONAL IN-SITU EXPERIMENTATION

The objective of this section was to develop an experimental procedure for obtaining in-situ data to formulate a three-dimensional soil deformation relationship. Experimentation in the field consisted of obtaining in-situ acceleration data in three dimensions. This data was used to formulate a relationship for the deformation of soil in the three principal directions each perpendicular to each other.

Experimental Design

The main purpose of performing three-dimensional in-situ experimentation on a soil mass was to study the relationship between a force applied in one direction and the soil's response in a direction perpendicular to the force. Of particular interest was the resulting deformations at the point of input as well as the point of output response.

To investigate the effects of input force to output responses that are perpendicular to each other, a Cartesian coordinate system was employed. These axes were designated

x, y and z. The x and y axes were oriented horizontally and the z axis was oriented vertically downward.

To study the three-dimensional behavior of soil in-situ, a mass of soil in the shape of a rectangular parallelepiped was cut into the ground by removing soil around the desired soil mass as shown in Figure 5. Four faces of the parallelepiped were vertical planes and the top face was a horizontal plane. The bottom face remained attached to the earth. Two of the vertical planes were perpendicular to the x-axis and the other two vertical planes were perpendicular to the y-axis. The top face was perpendicular to the z-axis. The depth and height of the parallelepiped were 0.28 m and the length was 0.33 m. By constructing the soil mass in this manner, all three principal directions were available for any combination of input and output. The following three cases of input and output were examined:

- (1) Horizontal input and output
- (2) Horizontal input and vertical output
- (3) Vertical input and horizontal output

In this manner, output displacements in any perpendicular orientation can be found as a function of an input force in any direction perpendicular to it.

The acceleration input to the soil face varied due to the amplitude of the applied force which excited the soil mass. The force applied to one of the faces deformed the soil at some frequency. The experimental design calls for



Figure 5. Rectangular Parallelepiped Soil Mass

the output response or deformations to be measured at five different locations away from the input source. This design was applied to all three orientations.

For the horizontal to horizontal orientation, the input was made at the center of one of the vertical faces. The output was measured on another vertical face at distances of 0.114, 0.144, 0.183, 0.227 and 0.274 m from the point at which the input was made.

The horizontal to vertical orientation had the same design except that the output was measured on the top face at the same distances from the input source as the horizontal input and output case.

The vertical to horizontal orientation calls for the input to be made on the top face and the output to be measured on one of the vertical planes (horizontal face).

Figure 6 illustrates each of the orientations.

Each location on the soil mass was tested at four different stress inputs. After one of the locations had been subjected to the four inputs, the output accelerometer was moved to the next location and the process was repeated until all five locations had been tested. There were no changes made to the soil mass during the time of experimentation. Following this, the next orientation of input and output was tested in the same manner.

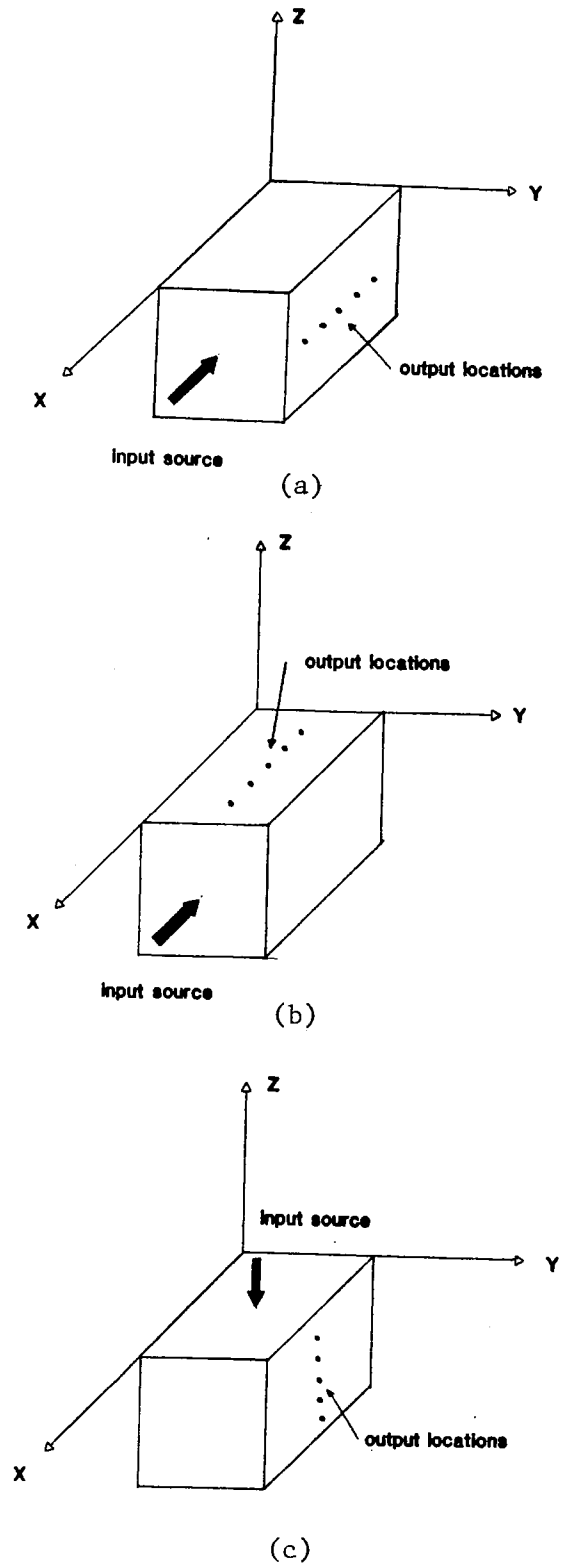


Figure 6. Schematic of a) Horizontal Input and Horizontal Output, b) Horizontal Input and Vertical Output and c) Vertical Input and Horizontal Output

Experimental Equipment

The sinusoidal shaker used in the laboratory could not be made adaptable for field work so several methods were used in an attempt to provide an excitation to the soil mass. These included a conventional hammer, pendulum, and spring loaded impulse generator. The hammer and the pendulum were precluded because of damage to the soil face. The spring loaded impulse generator shown in Figure 7 best achieved the desired results.

The impulse generator consisted of a flat disk constructed of aluminum and measured 0.1 m in diameter and 0.0127 m thick. The disk was attached to a sleeve of roller bearing. Mounted on the back of the sleeve was a handle to help slide the bearing on the cylindrical shaft which was screwed to a mounting plate located at the back of the base. By sliding the sleeve and disk against the spring, the spring was compressed. When the sleeve and disk were released, the disk struck the soil face causing the soil to be excited at its natural frequency.

The spring was compressed several different distances to examine how the soil reacts to the different levels of excitation. When the spring was compressed to roughly one-quarter of its length, the impulse generator jumped at the soil face and did not strike the soil in a flush manner. To remedy this situation, a 45 kg block of steel was bolted to the base plate of the generator. Marks were made on the shaft at every 0.0127 m and the front face of the disk was

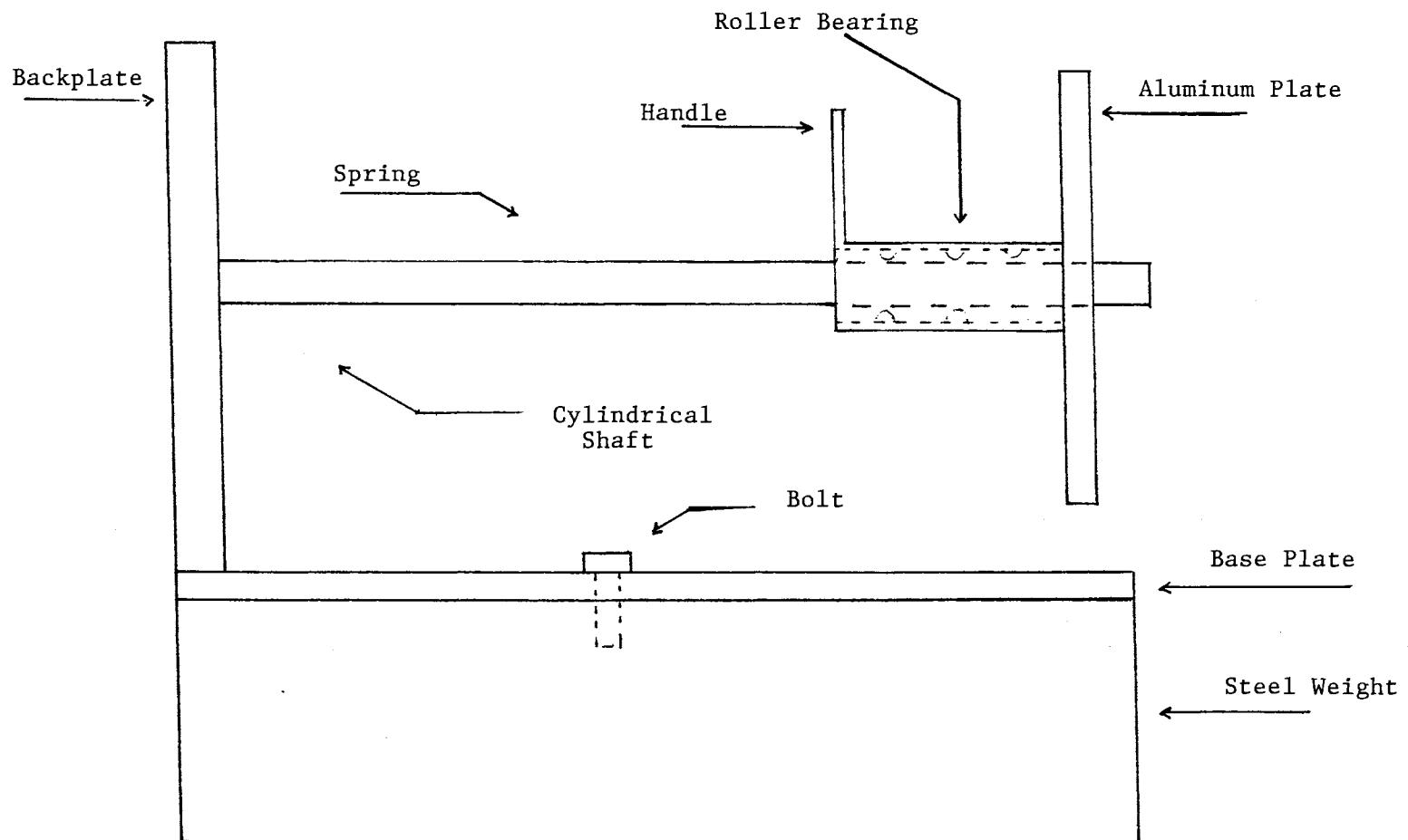


Figure 7. Spring Loaded Impulse Generator

made even with the first four marks to provide the four stress inputs. These stress input levels provided reasonable variability in input and output amplitudes for all lengths.

Transmission of Data

The input and output signals of the accelerometers were transmitted to a computer disk for storage. The instrumentation from the one-dimensional study was used. Before data were transmitted from the oscilloscope to the computer for permanent storage, each signal was checked to insure that the complete signal had been captured.

Three areas of signal capture must be reviewed before transmission. The first involved the start of each signal. To insure that the trigger had properly caught the start of both input and output, the vertical cursor on the oscilloscope screen was placed at approximately 25 time steps from the left-hand side of the edge of the screen. The values to the left of the cursor were zero so the starts of both signals were guaranteed to be caught.

Secondly, the amplitude of input and output signals were checked to see that they had not eclipsed the top and bottom of the screen resulting in lost or false values. If data escaped the screen, the charge amplifier gravitational constant was too low and needed to be reset.

The last requirement involved the end of the signal. After the soil was excited, the excitation waveform dampened

out. This means a region of steady-state response was at the end of the signal. If all three of these conditions were met then the signals were stored on disk.

CHAPTER V

RESULTS AND DISCUSSION

One-Dimensional Analysis

Tests were conducted on cylindrical soil samples of varying moisture content. The purpose of these tests was to subject soil samples to different axial forces of varying frequency and amplitude and determine if either a plastic region exists or if a soil failure criterion can be formulated.

Dynamic Test Parameters

The measured acceleration data were sinusoidal in nature for both bottom and top waveforms. These waveforms were stored in data files on floppy disk and a computer program was written to read both files and determine frequency, phase lag and maximum accelerations of both waveforms. The program determined the times at which a full sinusoidal cycle started and stopped for both files. For each file, the program read and averaged acceleration values over one complete cycle. This average value is an indication of the bias or drift in the acceleration data recorded by the measurement system. The value of the bias

was subtracted from each acceleration value over a full cycle.

The phase angle or phase lag between input and output waveforms was calculated using the difference in the start times of the two cycles multiplied by the frequency in radians per second.

The maximum acceleration over the period of one cycle for both files was found. The maximum acceleration of each of the files is the amplitude of the acceleration waveform. The maximum top acceleration divided by the maximum bottom acceleration was defined as the acceleration ratio.

Acceleration to Displacement Conversion

As engineering materials are subjected to stress, they also experience strain. This applies to soil as well. Strain is defined as the difference between the final and initial lengths, L_f and L_i respectively, divided by the initial length. This relationship is:

$$\epsilon = (L_f - L_i)/L_i \quad (11)$$

The numerator of equation (11) is the change in length or displacement the material experiences due to being stressed. The input to the base of the soil sample from the electromagnetic shaker was $A \sin(\omega * t)$, where A is the amplitude and ω is the frequency. To determine the total displacement that occurs at each end of the soil sample due to this excitation, recorded acceleration data was converted

to displacement data. This was accomplished in the following manner.

From classical harmonic motion theory, a displacement x can be written as:

$$x = A \sin(\omega * t). \quad (12)$$

Successive differentiation of equation (12) with respect to time yields the following relationships for velocity and acceleration:

$$\dot{x} = \omega * A * \cos(\omega * t) = \omega * A * \sin(\omega * t + \pi/2) \quad (13)$$

$$\ddot{x} = -\omega^2 * A * \sin(\omega * t) = \omega^2 * A * \sin(\omega * t + \pi) \quad (14)$$

The acceleration \ddot{x} , is harmonic as well and is proportional to displacement but leads it by 180 degrees. This is demonstrated graphically by Figure 8. This graph demonstrates that the displacement of a continuous system can be determined directly from its acceleration curve provided the acceleration curve is sinusoidal.

Acceleration Curve Fits

To use either the graphs or equations (12) and (14) for obtaining sample displacements, it must be determined that the experimental acceleration waveforms reasonably approximate harmonic or sinusoidal motion. From earlier analysis, the amplitude and the frequency of the experimental acceleration data are known. A 'perfect' experimental sine wave would be $A \sin(\omega * t)$, where A is the

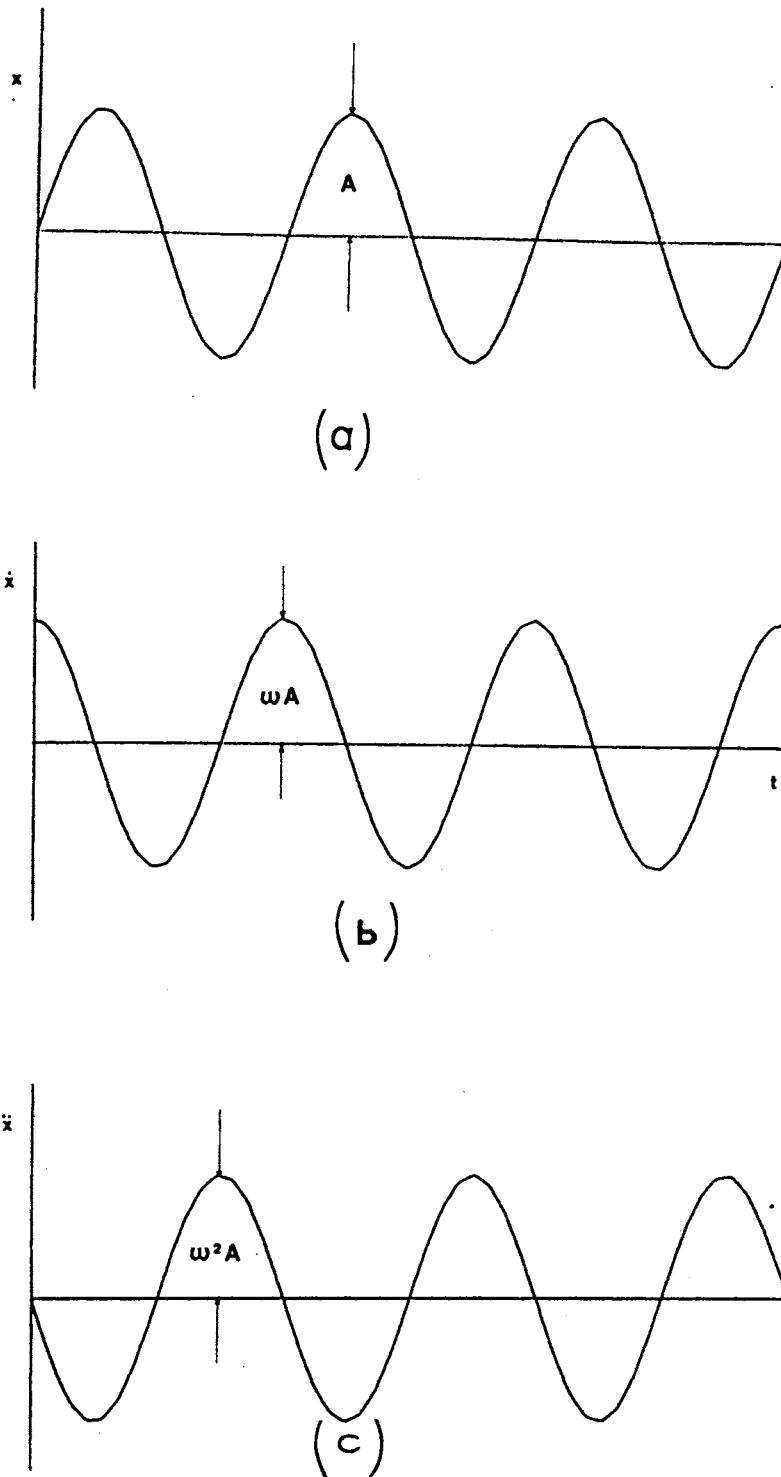


Figure 8. Graphs of a) Displacement, x , b) Velocity, \dot{x} and c) Acceleration, \ddot{x} for a Continuous System subject to Harmonic Motion

amplitude of the experimental waveform and ω is the frequency. Regression analysis provides a coefficient of determination or R^2 between the generated and actual experimental data and is a measure of how well the recorded data actually approximates a generated sine wave of the same amplitude and frequency. Regressions were conducted for all seven frequencies for both low and high amplitude settings and both bottom and top waveforms.

Tables III and IV show the coefficient of determination between actual experimental data and generated waveform data for both orientations. Figures 9, 10 and 11 show a comparison of actual experimental acceleration data to generated acceleration data.

Since the experimental waveforms are excellent approximations of harmonic motion at their respective frequencies, the use of classical vibratory theory was used to generate displacement data directly from experimental acceleration data. Referring to Figure 8, the values of displacement over the same time period as the acceleration waveform are the negative of the acceleration waveform values divided by the frequency. If the amplitude of the acceleration waveform is a value $A \cdot \omega^2$, then the amplitude of the displacement waveform is $-A / \omega^2$.

The computer program, having already found the amplitude and frequency of the experimental acceleration

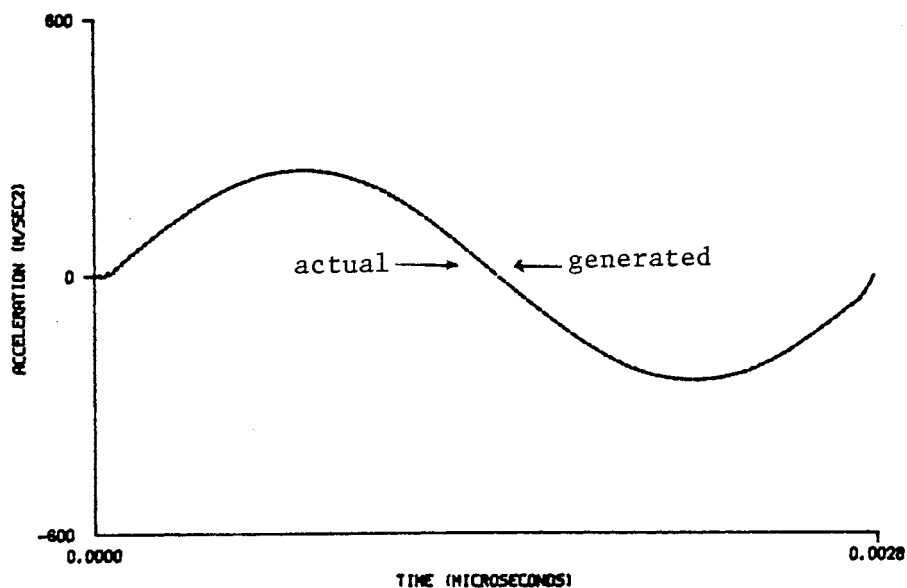
TABLE III
COEFFICIENTS OF DETERMINATION FOR ACTUAL
VERSUS GENERATED SINE WAVE DATA FOR
THE VERTICAL ORIENTATION

Frequency, Hertz	Bottom Acceleration Amplitude		Top Acceleration Amplitude	
	<u>Low</u>	<u>High</u>	<u>Low</u>	<u>High</u>
300	.999	.999	.924	.936
800	.999	.999	.987	.965
1000	.999	.999	.961	.950
1300	.997	.996	.940	.972
1500	.997	.995	.982	.964
1700	.998	.992	.970	.935
2000	.999	.999	.996	.965

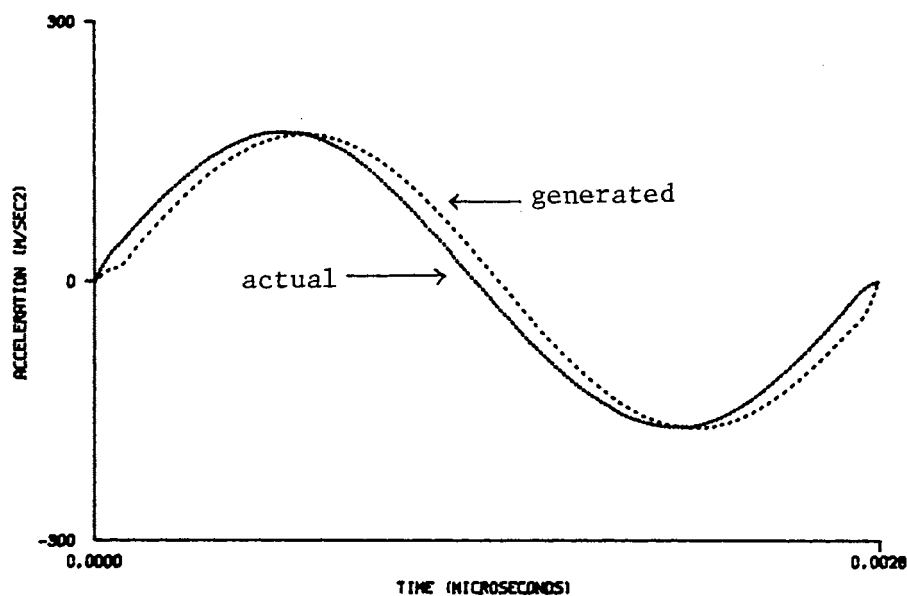
TABLE IV
COEFFICIENTS OF DETERMINATION FOR ACTUAL
VERSUS GENERATED SINE WAVE DATA FOR
THE HORIZONTAL ORIENTATION

Frequency, Hertz	Bottom Acceleration Amplitude		Top Acceleration Amplitude	
	<u>Low</u>	<u>High</u>	<u>Low</u>	<u>High</u>
300	.999	.999	.976	.961
800	.999	.999	.990	.987
1000	.997	.996	.975	.940
1300	.999	.996	.990	.982
1500	.990	.996	.985	.965
1700	.996	.997	.973	.961
2000	.998	.997	.950	.944

waveforms, multiplied a sinusoidal function $\sin(\omega * t)$ by the negative of the maximum acceleration amplitude divided by

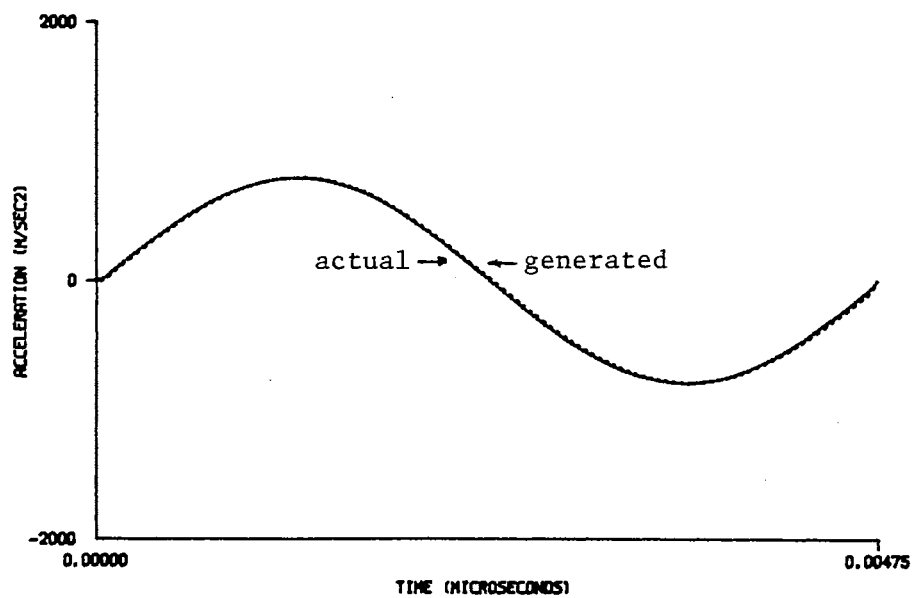


(a)

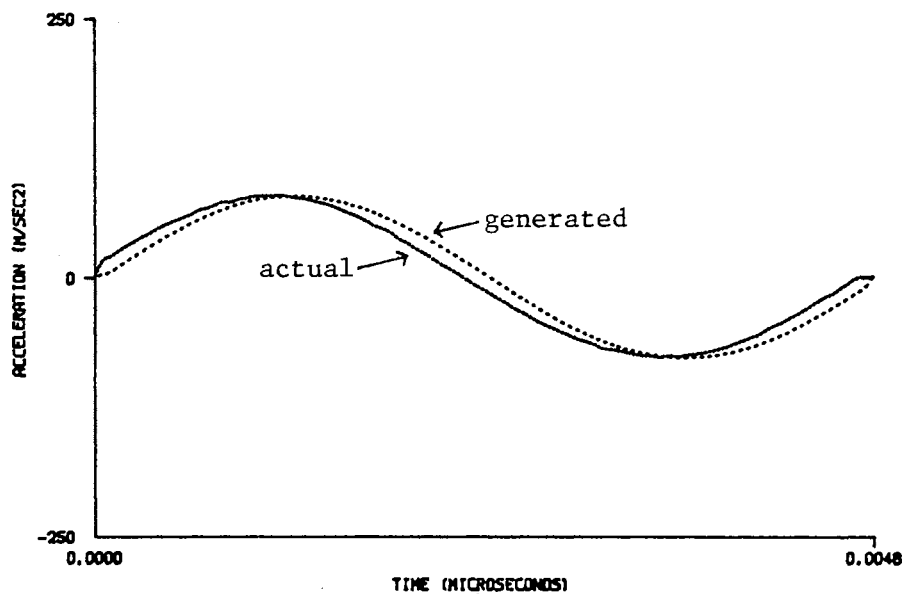


(b)

Figure 9. Comparison of Generated Sine Wave Data to Actual Experimental Sine Wave Data for a) Bottom Accelerometer and b) top Accelerometer. Vertical Orientation, Low Amplitude



(a)



(b)

Figure 10. Comparison of Generated Sine Wave Data to Actual Experimental Sine Wave Data for a) Bottom Accelerometer b) Top Accelerometer Vertical Orientation, High Amplitude

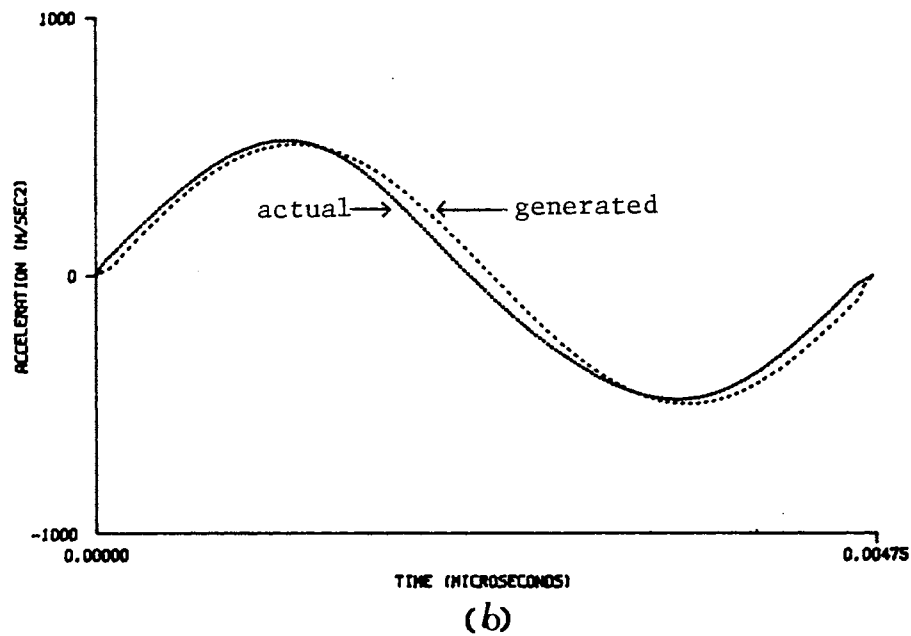
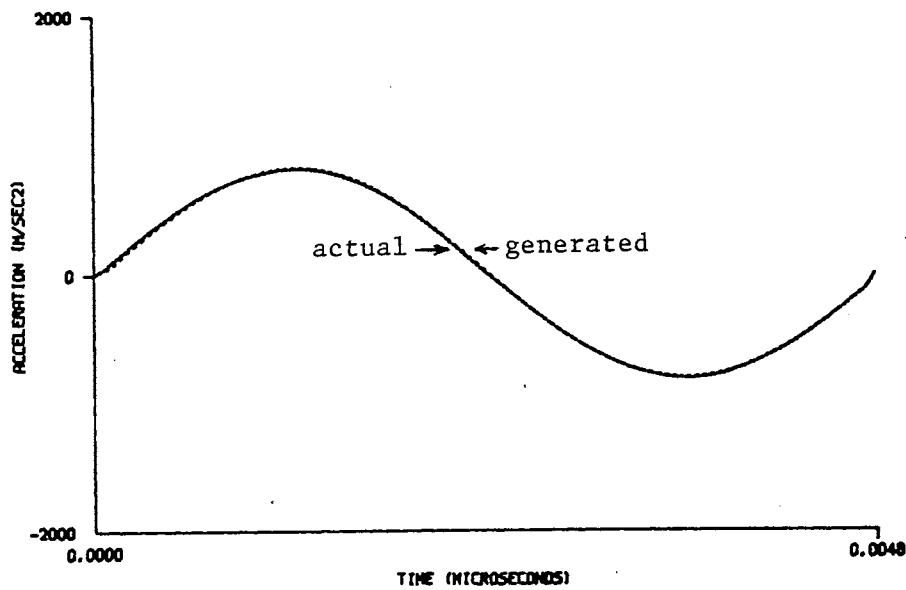


Figure 11. Comparison of Generated Sine Wave Data to Actual Experimental Sine Wave Data for a) Bottom Accelerometer and b) Top Accelerometer Horizontal Orientation, High Amplitude

the frequency squared through the same time period as the acceleration cycle. This was done for both bottom and top waveforms.

To find the relative displacement or deformation at each time through one cycle, displacement values of the bottom waveform were subtracted from displacement values of the top waveform. The maximum tensile strain experienced by the soil sample was the largest deformation present in the cycle divided by the original length of the soil sample.

The maximum stress applied to the soil sample was a function of the maximum acceleration experienced at the base of the sample. Using Newton's Second Law of Motion, the maximum force applied to the base of the soil sample was equal to the mass of the sample multiplied by the maximum acceleration. The applied stress was equal to that force divided by the area of the soil sample. This is shown by equation (15).

$$\sigma = \frac{F}{A} = \frac{m\ddot{x}}{A} \quad (15)$$

As the master gain was increased on the power amplifier, the amplitudes of both waveforms increased. As the amplitudes increased, the maximum acceleration at the bottom of the soil sample became larger resulting in a greater applied stress. Strain is defined by the relative displacement or deformation between the top and bottom of the soil sample. This deformation is also a direct function of the amplitudes

of both waveforms. Therefore, any increase in amplitude resulted in a greater strain.

By increasing the amplitude, it may be possible to approach yielding and more importantly a failure criteria might be established.

Stress-Strain Plots

Graphs of stress-strain values were generated for several soil samples of each orientation. These plots were divided into two categories. The first set concerns stress-strain values for both orientations at one particular moisture content. These are shown in Figures 12-19. The second set of plots involve stress-strain values at four different frequencies with a variation of moisture content within that one frequency. These are plotted in Figures 20-28.

Frequency Variation Within a Moisture Content

Figures 12-19 show the variation of stress-strain values for both orientations letting frequency vary at one particular moisture content. All graphs show that the variation of strain with stress is linear. The maximum force provided by the electromagnetic shaker was approximately 115 N. This limitation in equipment meant that stress levels input to the base of the soil sample were not large enough to create permanent plastic deformation.

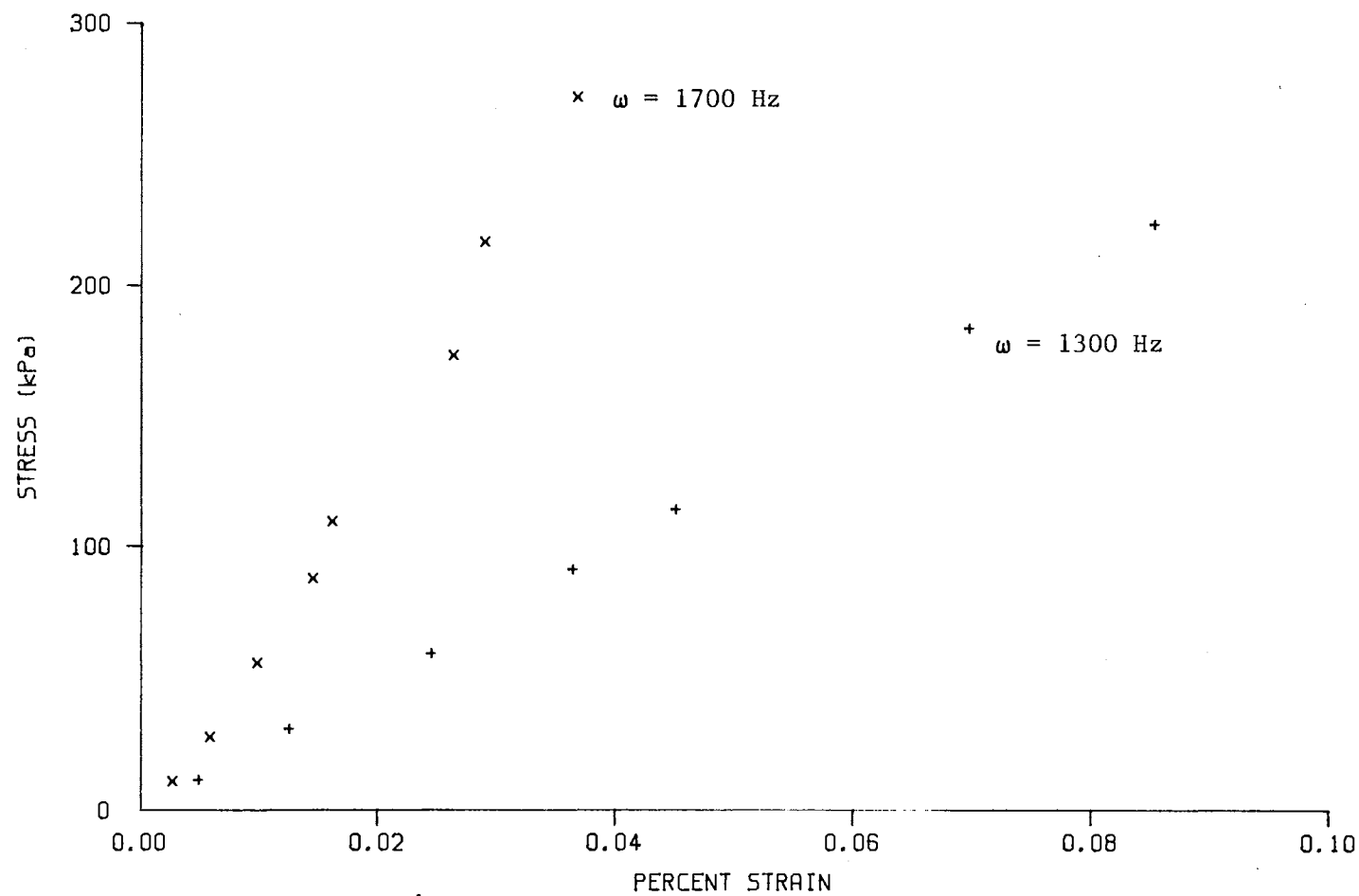


Figure 12. Variation of Stress-Strain Values with Frequency for a Vertically Oriented Soil Sample at a Moisture Content Level of 14.5%

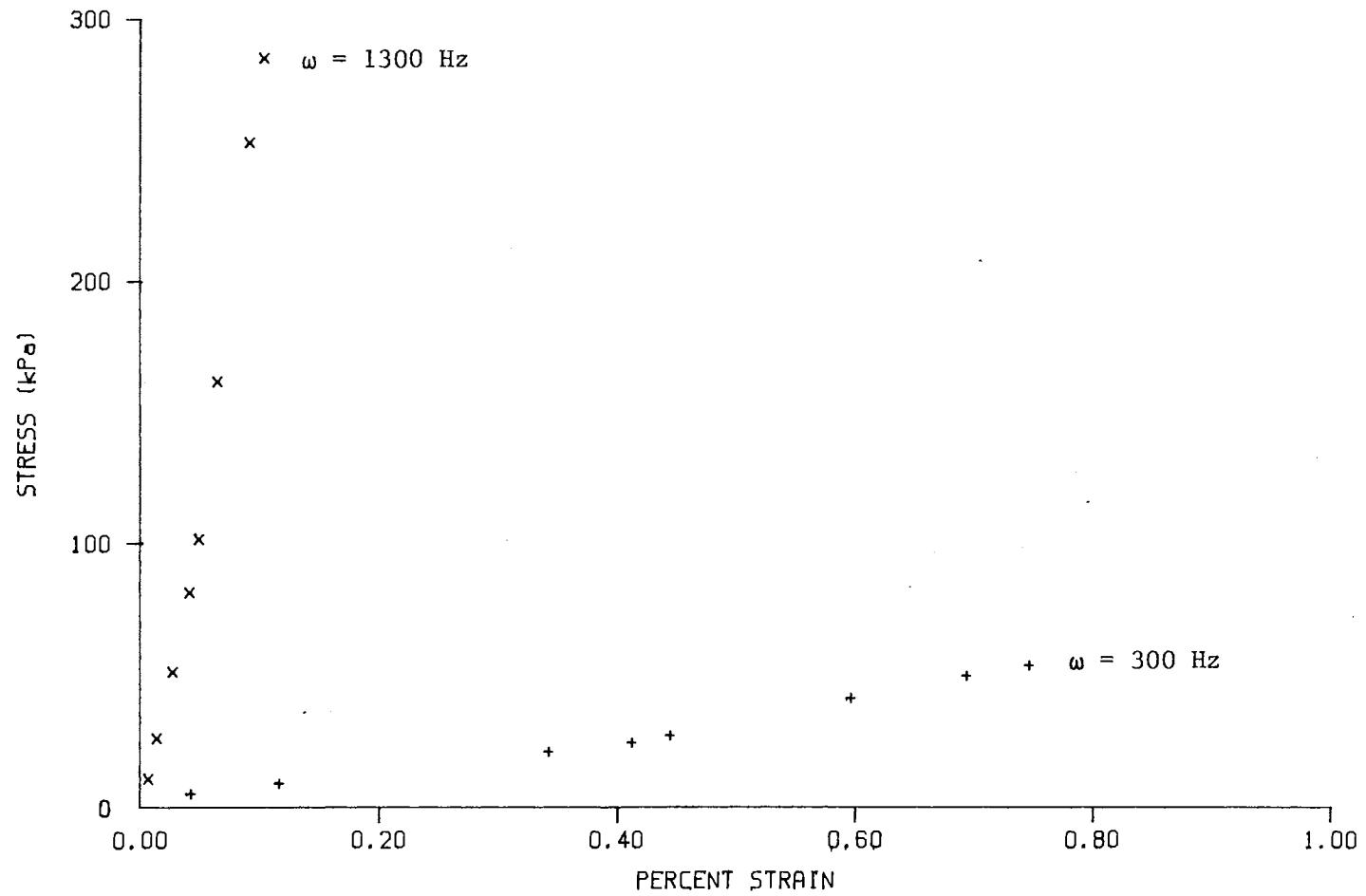


Figure 13. Variation of Stress-Strain Values with Frequency for a Vertically Oriented Soil Sample at a Moisture Content Level of 17.2%

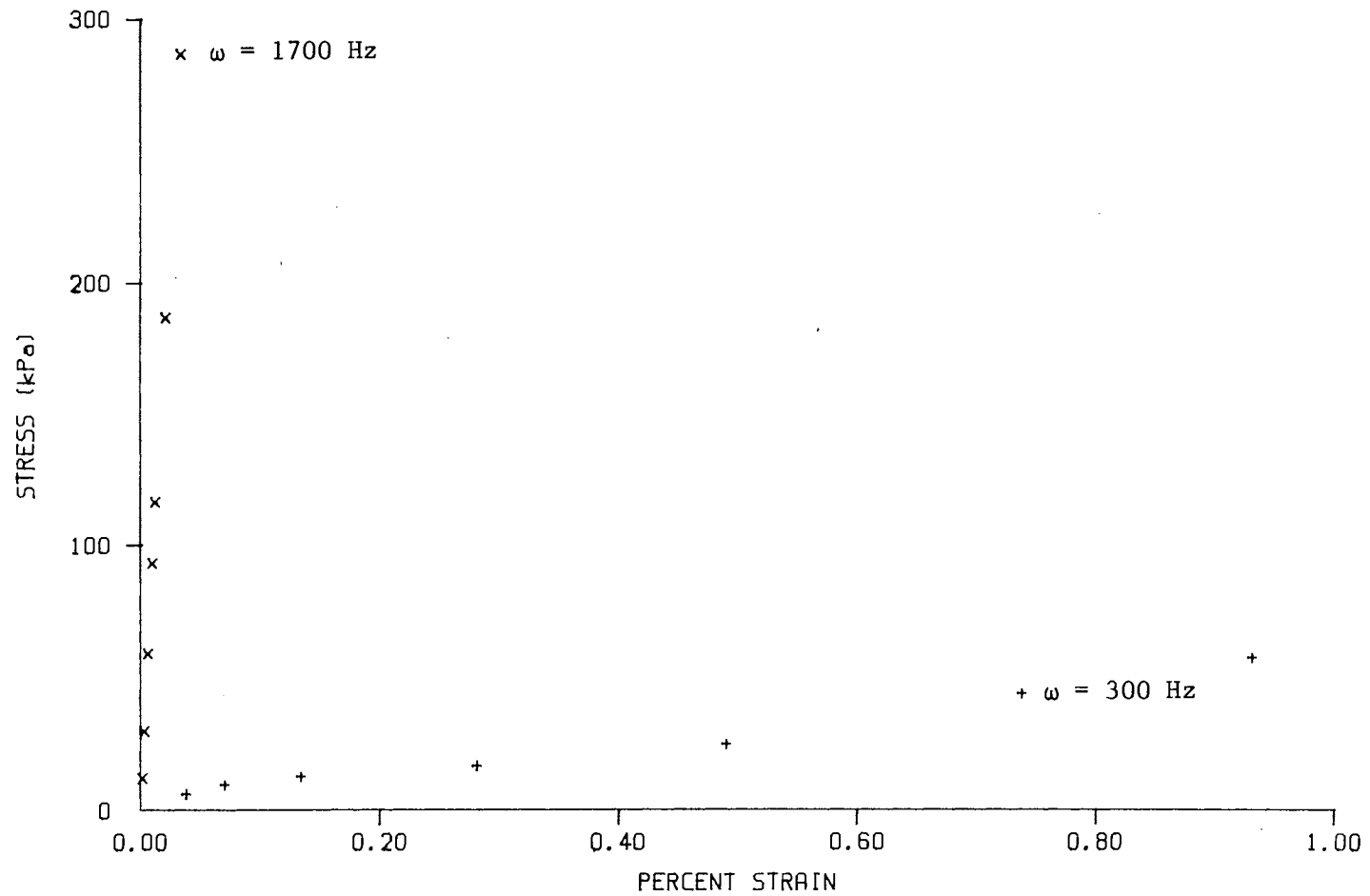


Figure 14. Variation of Stress-Strain Values with Frequency for a Vertically Oriented Soil Sample at a Moisture Content Level of 17.8%

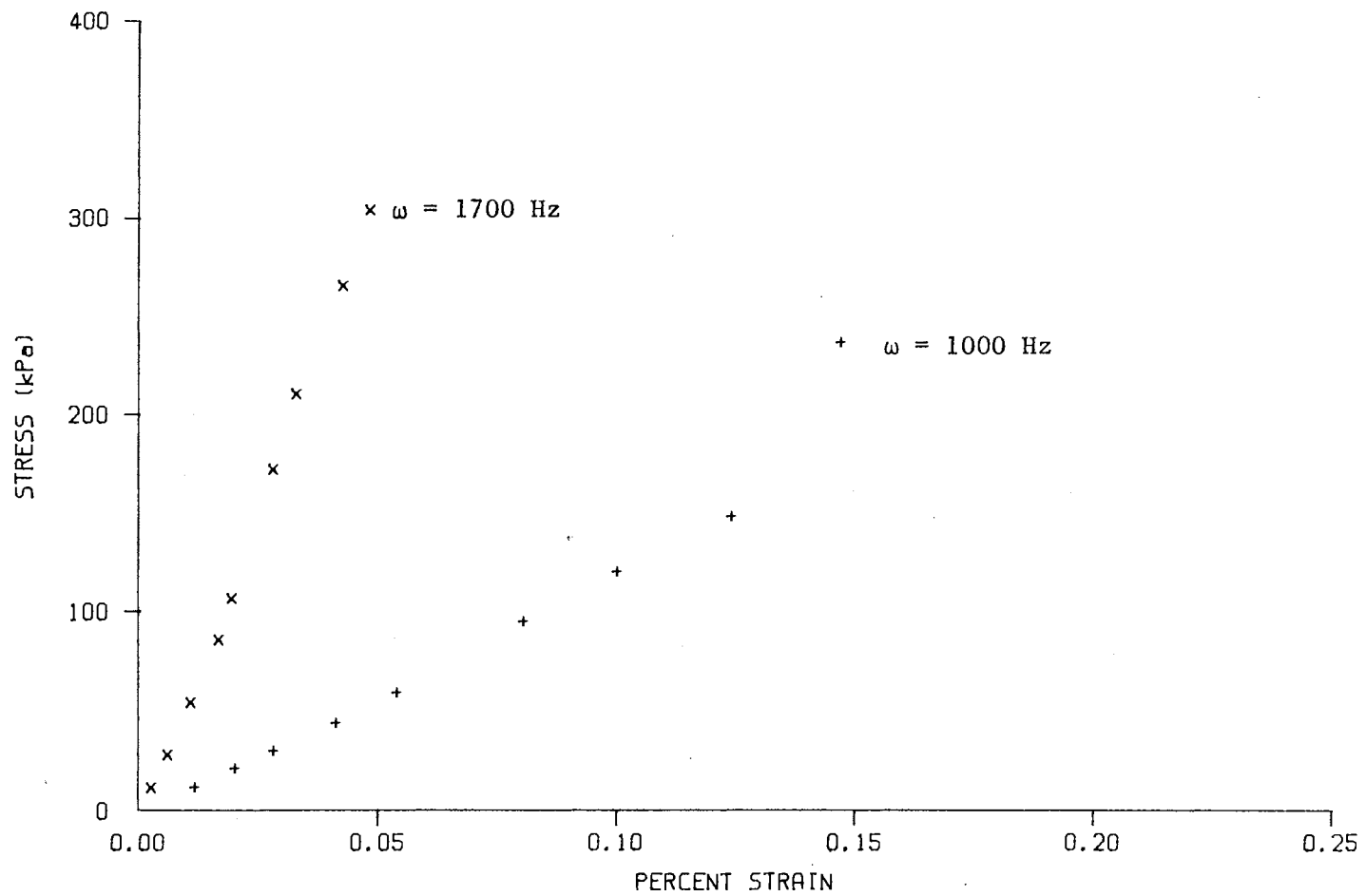


Figure 15. Variation of Stress-Strain Values with Frequency for a Vertically Oriented Soil Sample at a Moisture Content Level of 18.5%

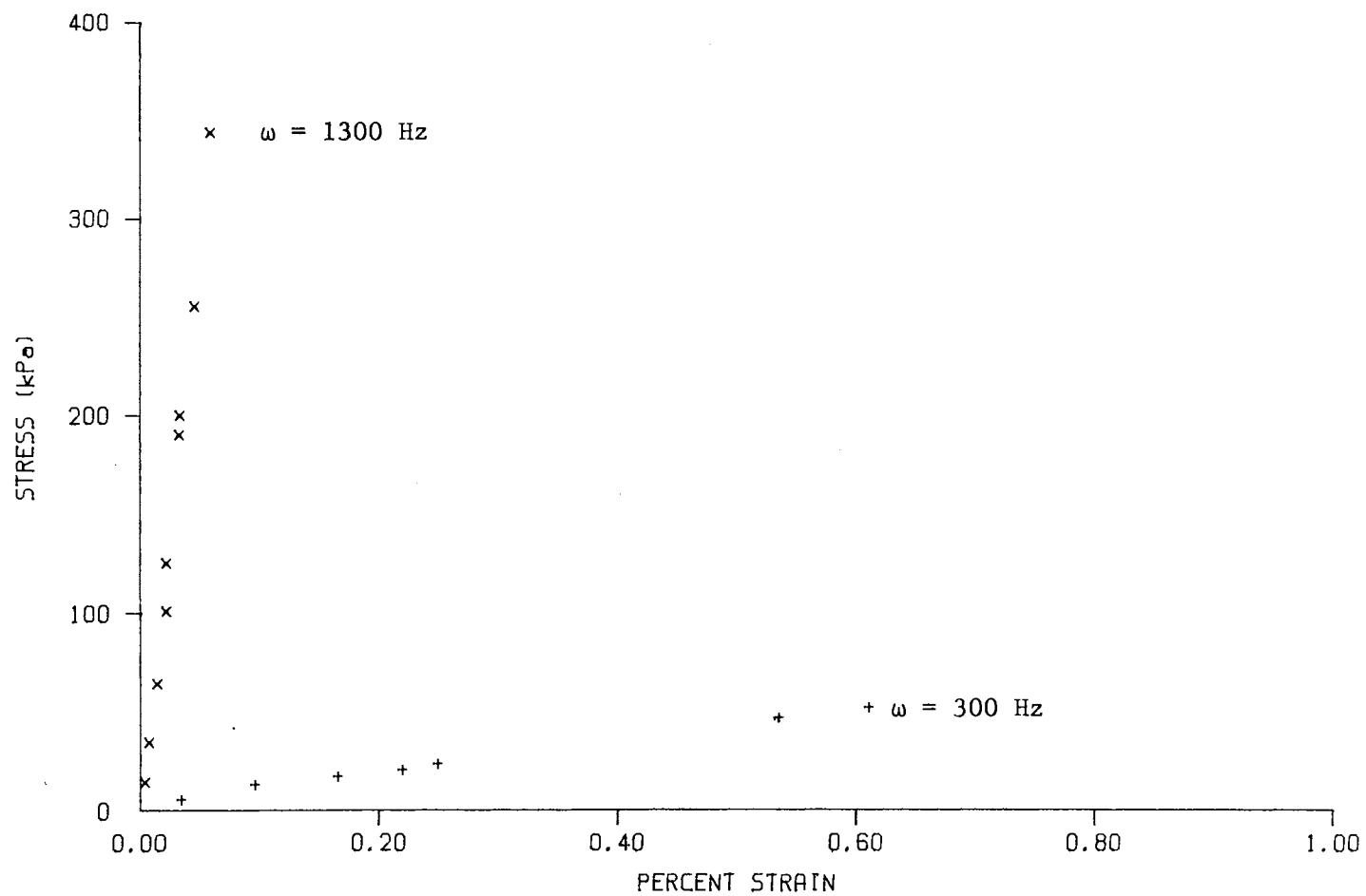


Figure 16. Variation of Stress-Strain Values with Frequency for a Vertically Oriented Soil Sample at a Moisture Content Level of 16.9%

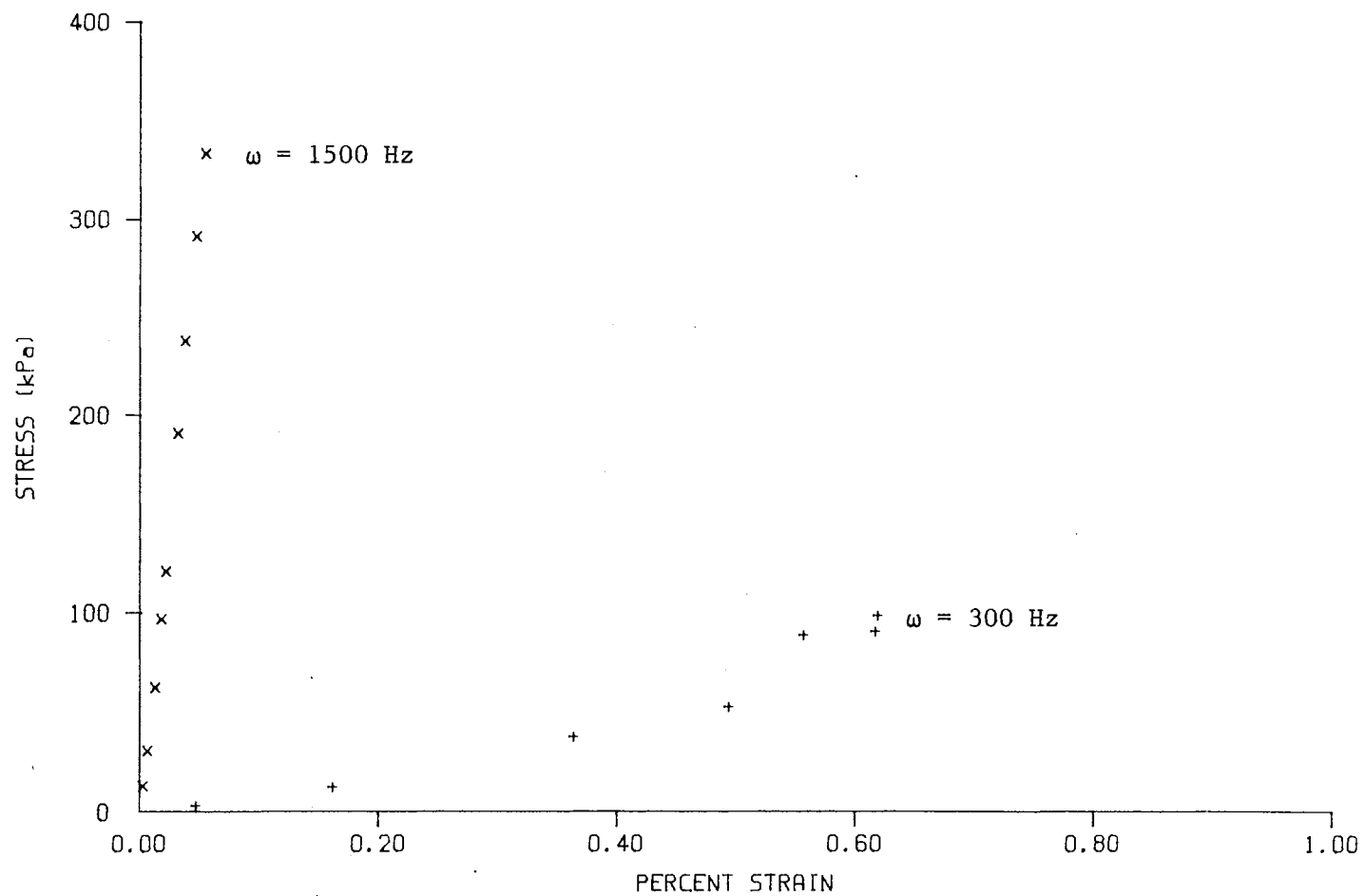


Figure 17. Variation of Stress-Strain Values with Frequency for a Vertically Oriented Soil Sample at a Moisture Content Level of 17.7%

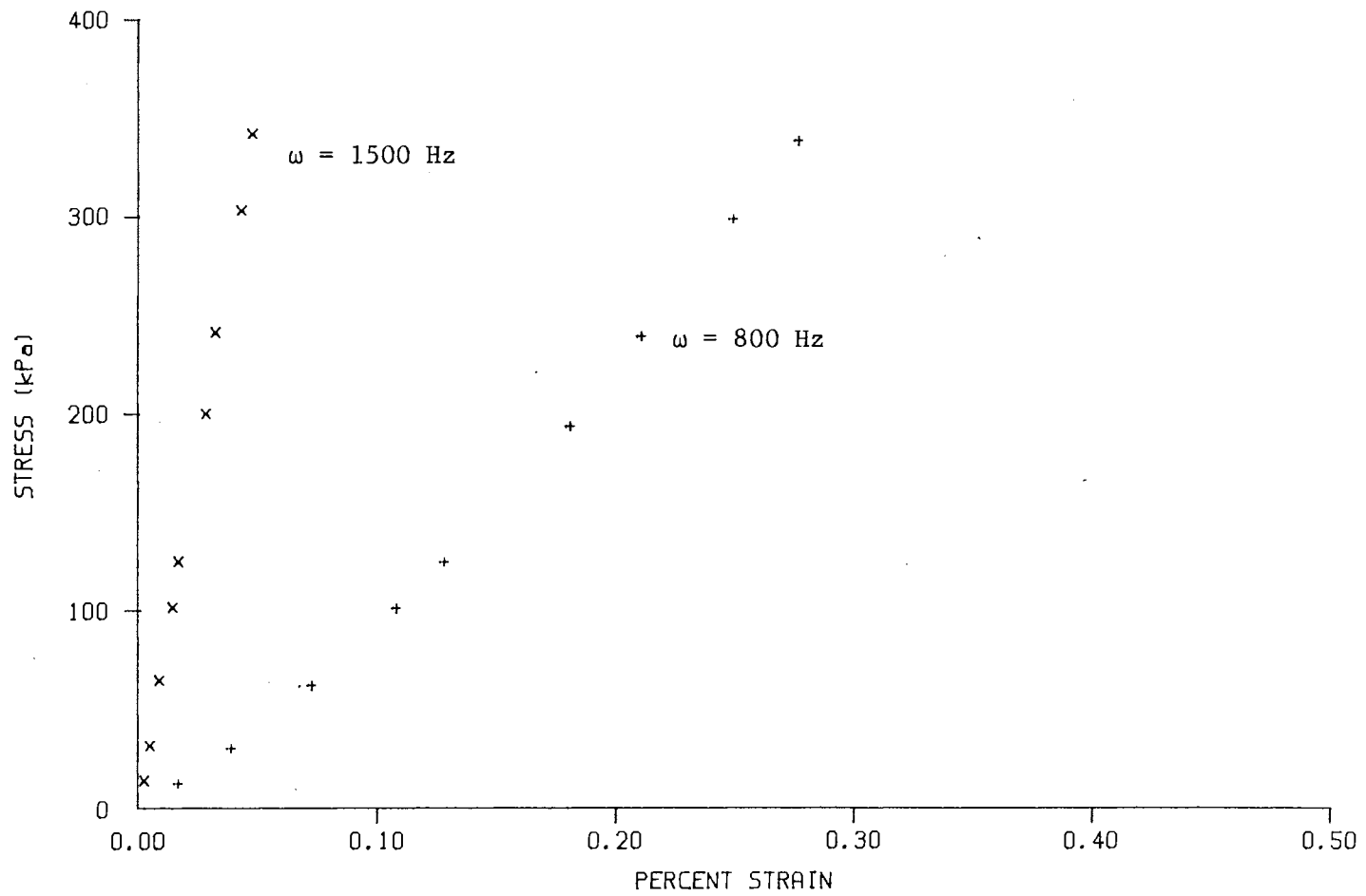


Figure 18. Variation of Stress-Strain Values with Frequency for a Horizontally Oriented Soil Sample at a Moisture Content Level of 17.9%

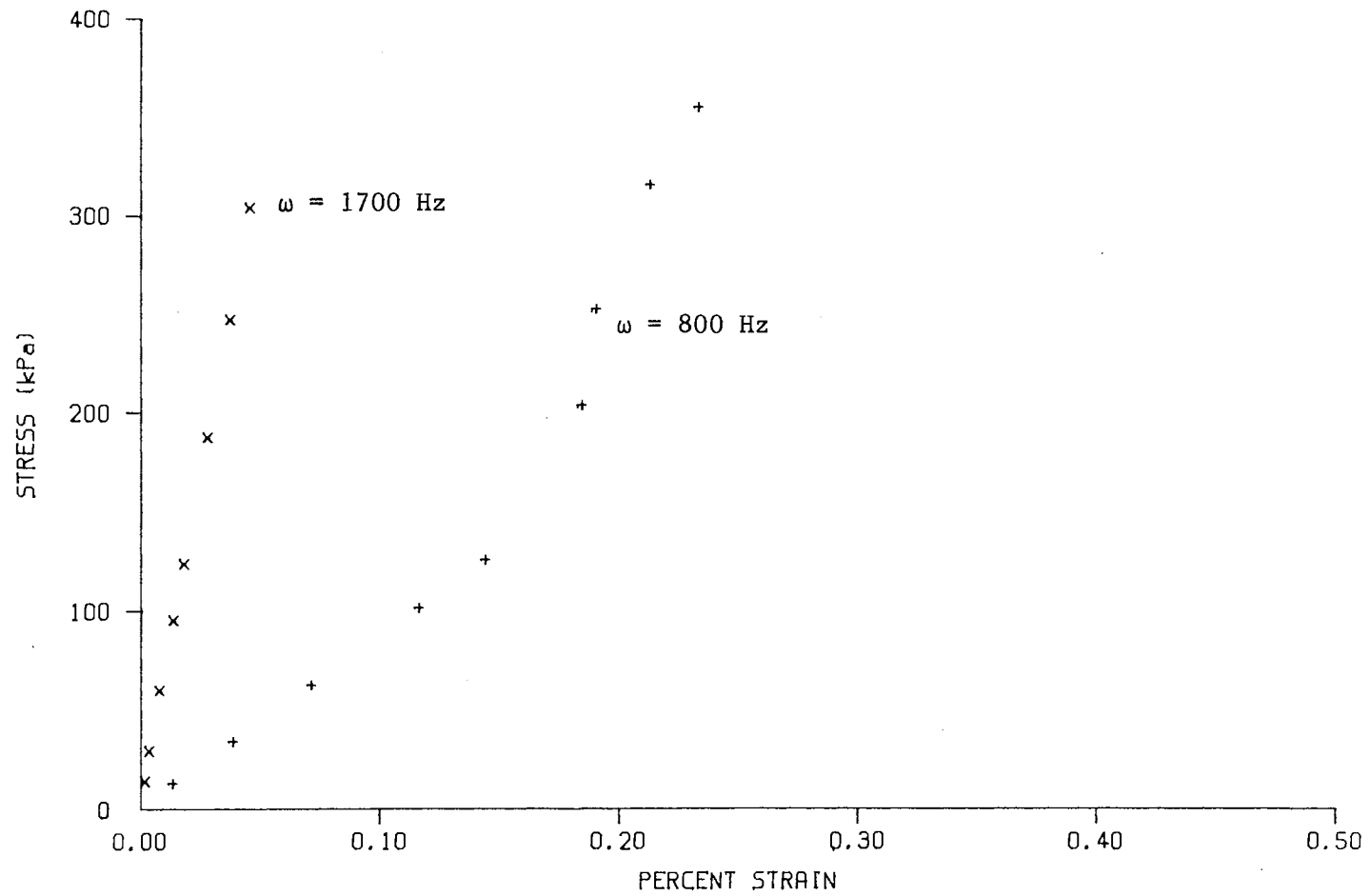


Figure 19. Variation of Stress-Strain Values with Frequency for Horizontally Oriented Soil Sample at a Moisture Content Level of 18.6%

This is not to say that the soil samples are not capable of achieving plasticity at higher stress levels.

Figure 13 shows the variation of stress-strain values for a vertically oriented sample at a moisture content level of 17.2%. The maximum achievable stress when tested at a frequency of 1300 Hz was 285 kPa and the greatest strain experienced was .1%. When a soil sample of the same moisture content was vibrated at a frequency of 300 Hz, the maximum achievable stress was only 53.52 kPa and the strain was .746%. This was almost 7.5 times the deformation experienced by the other sample.

Figure 16 demonstrates the same concept for a horizontally oriented sample at a moisture content level of 16.9%. The maximum attainable stress for the sample vibrated at 1300 Hz was 343 kPa with only a .059% strain while a sample tested at a frequency of 300 Hz experienced a .61% strain but only achieved a stress level of 50.5 kPa.

For both orientations and all moisture contents investigated, tremendous variation of stress existed between two different frequencies at any particular level of strain. As frequency increased, higher stresses were developed at lower strains. The fact that higher stresses were developed does not necessarily imply that a higher frequency will produce failure. Possible soil failure criteria within the range of moisture content levels cannot be extrapolated from the data of Figures 12-19.

Moisture Content Variation Within a Frequency

Figures 20-28 show the variation of stress with strain for both vertically and horizontally oriented soil samples of different moisture contents tested at one frequency. This is shown by Figures 20 through 24 for vertically oriented samples and Figures 25 and 28 for horizontally oriented samples. The variation of stress within a frequency was not as pronounced in this case as it was for the case of stress within a particular moisture content level except at the frequency of 300 Hz for vertically oriented samples as shown in Figure 20. In this case, there is a significant difference between stress and strain values over the given moisture content range.

Figure 21 shows only a 7.5% difference in maximum achievable stresses between a samples of 15.1% and 19.8% moisture content level when tested at 800 Hz. Figure 23 shows a 10.0% increase in achievable stresses between samples of moisture content levels between 15.5% and 21.5% when tested at 1500 Hz. The same argument can be made for other soil samples tested at the other frequencies.

Similar behavior was noticed for horizontally oriented samples. Figure 25 shows only a 5.4% increase in maximum achievable stress levels for samples vibrated at 800 Hz between the low and high moisture content levels of 17.1% and 21.4%. In Figure 28, the two moisture contents considered were 16.5% and 18.9%. These samples were tested

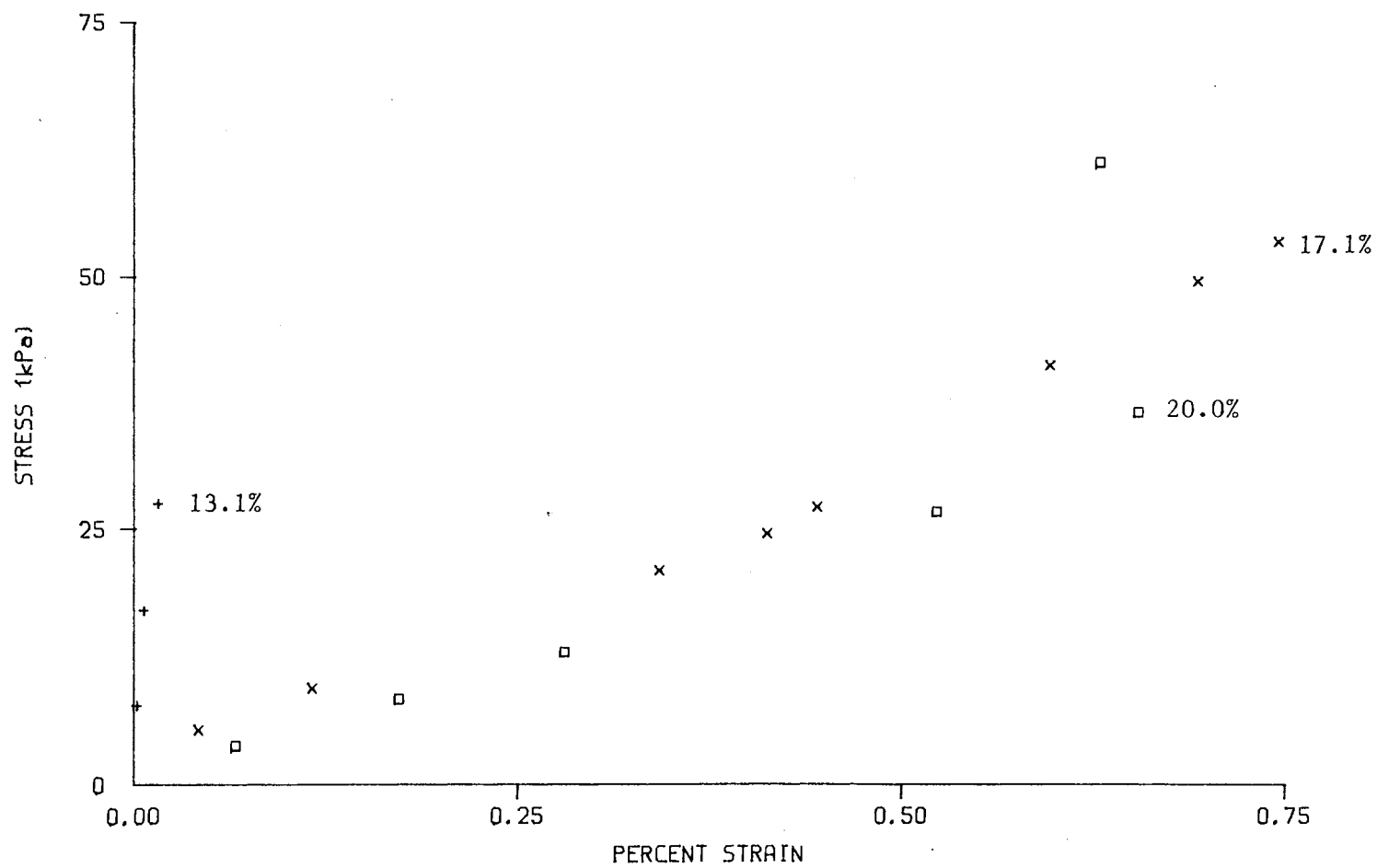


Figure 20. Variation of Stress-Strain Values with Moisture content for a Vertically Oriented Sample Vibrated at a Frequency of 300 Hz

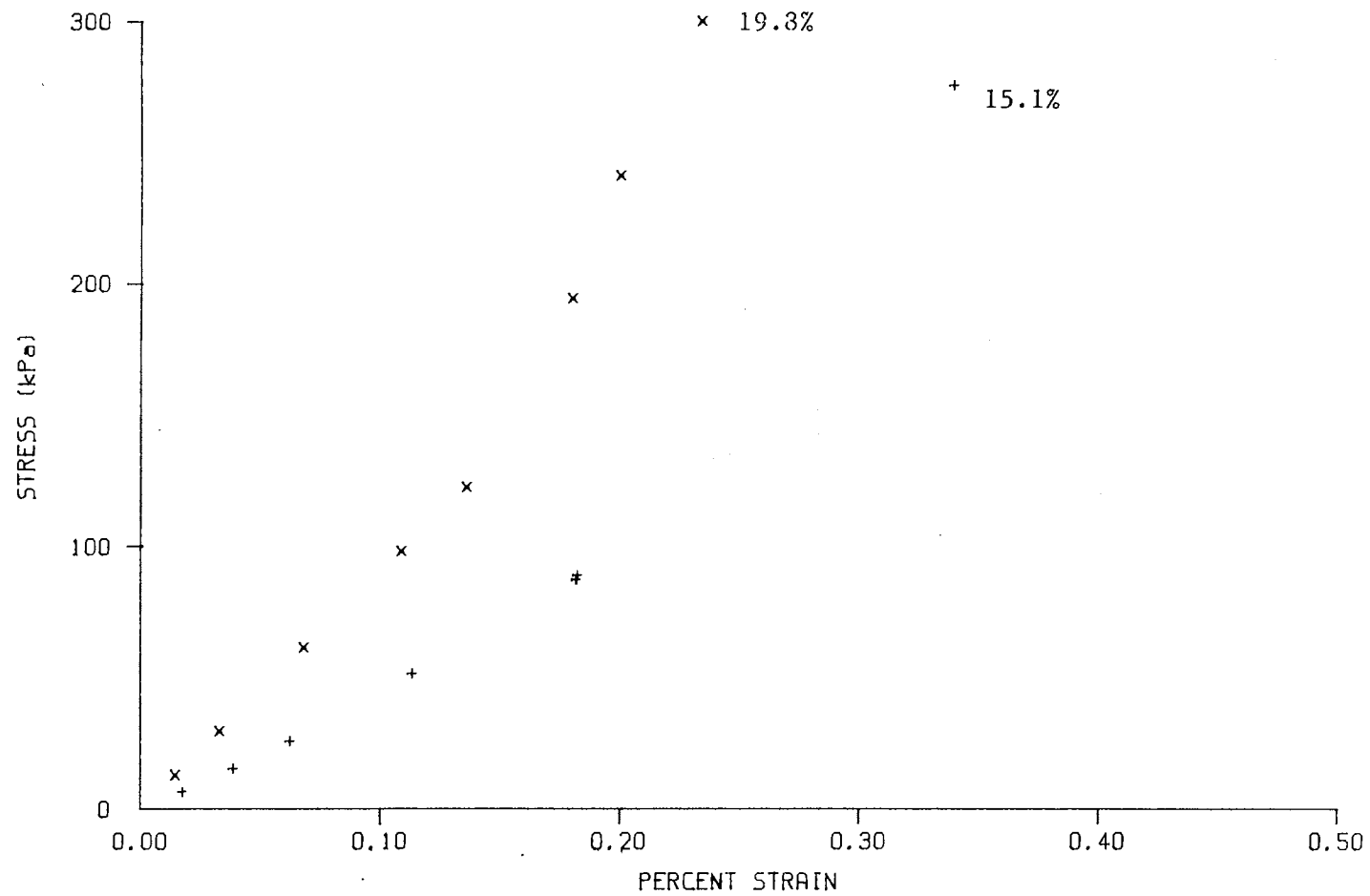


Figure 21. Variation of Stress-Strain Values with Moisture content for a Vertically Oriented Sample Vibrated at a Frequency of 800 Hz

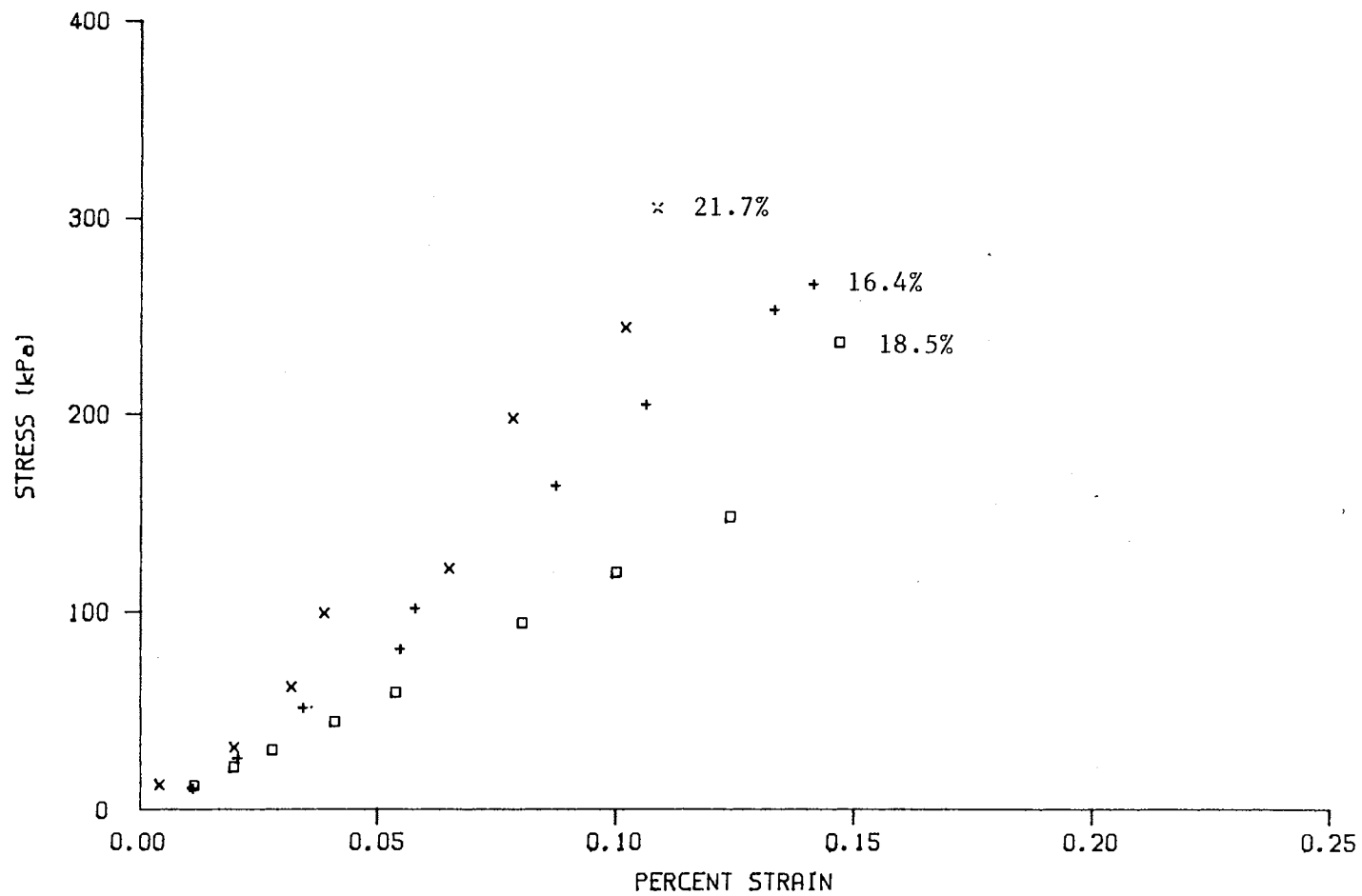


Figure 22. Variation of Stress-Strain Values with Moisture content for a Vertically Oriented Sample Vibrated at a Frequency of 1000 Hz

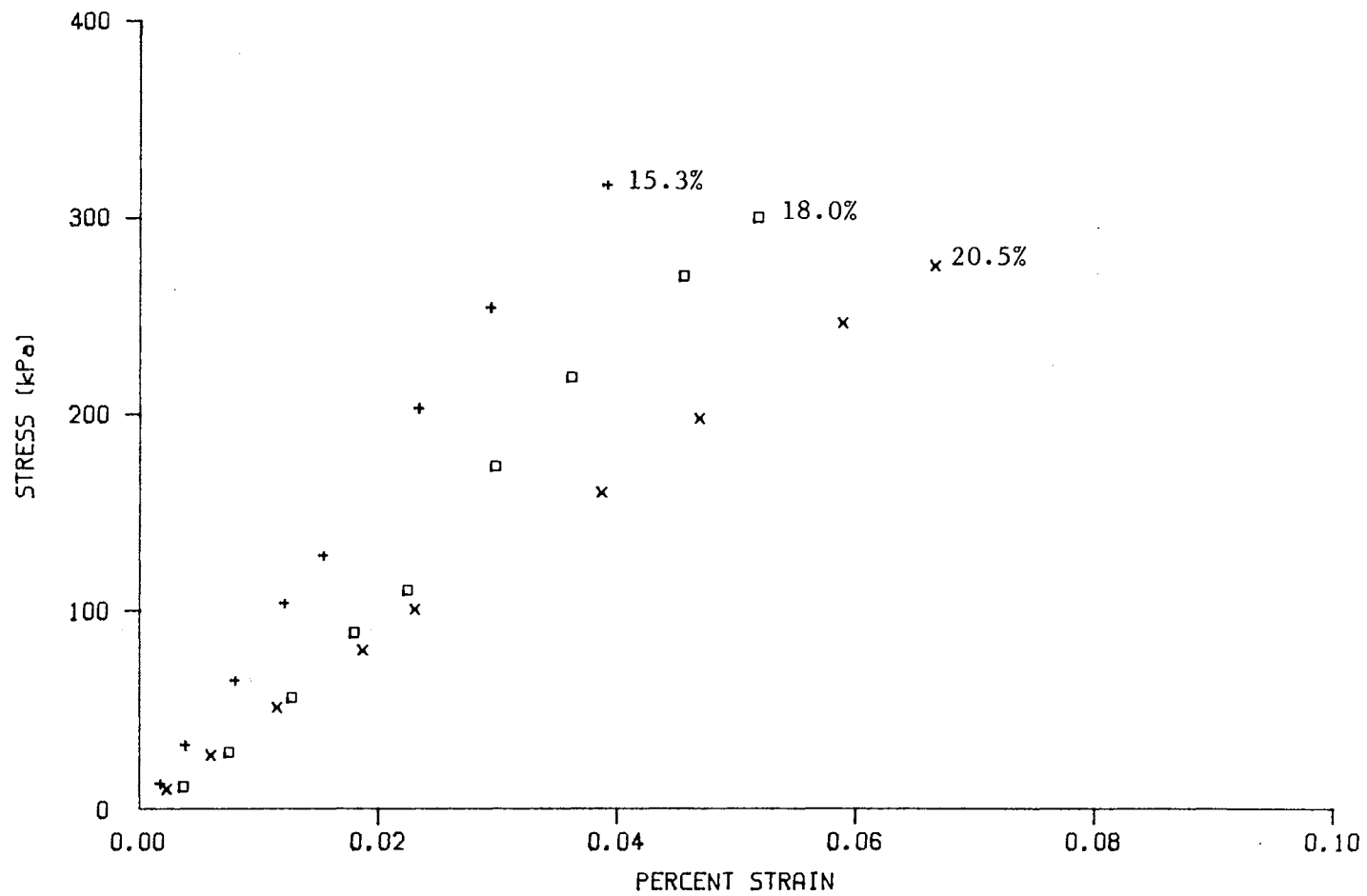


Figure 23. Variation of Stress-Strain Values with Moisture content for a Vertically Oriented Sample Vibrated at a Frequency of 1500 Hz

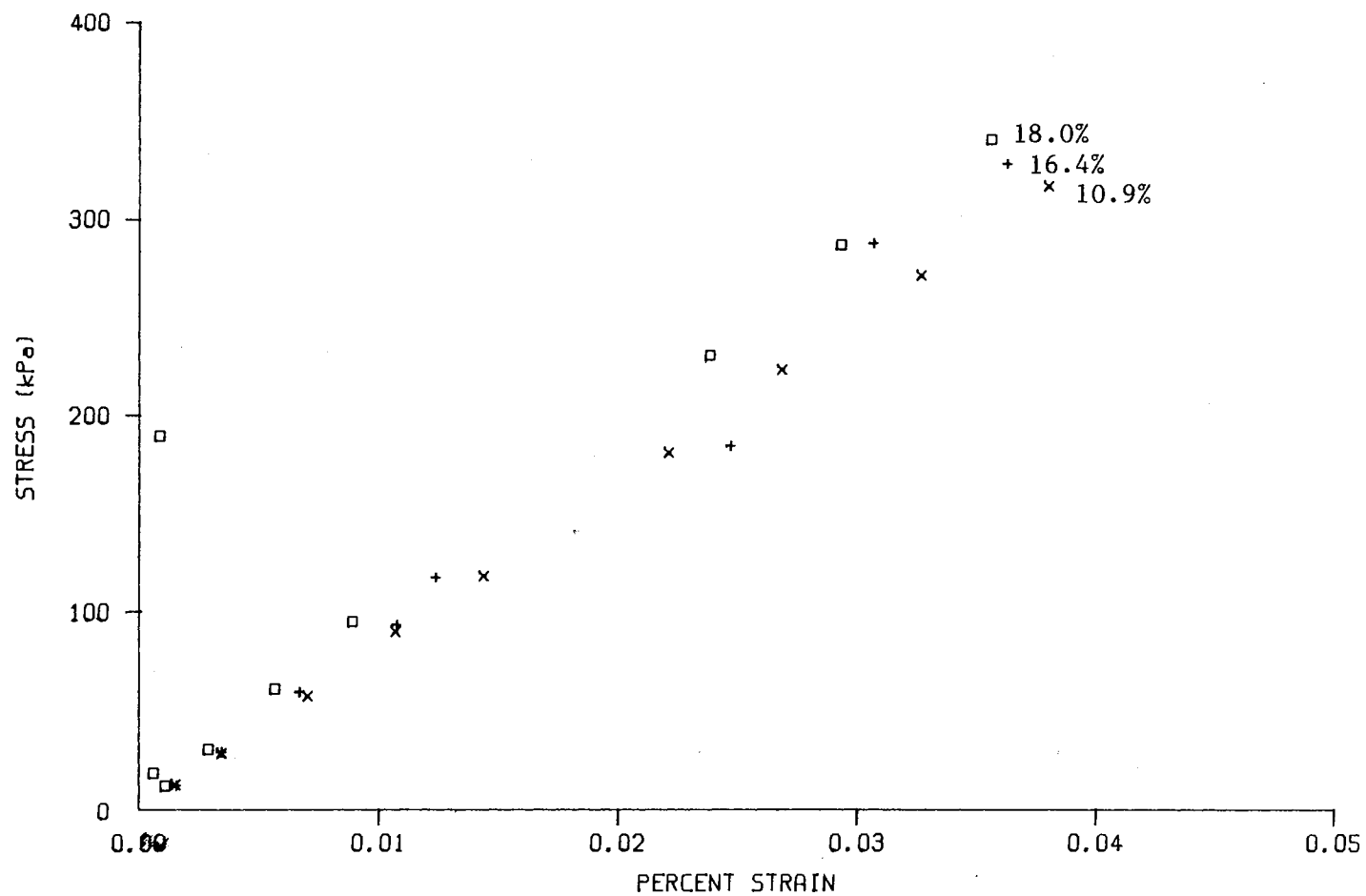


Figure 24. Variation of Stress-Strain Values with Moisture content for a Vertically Oriented Sample Vibrated at a Frequency of 2000 Hz

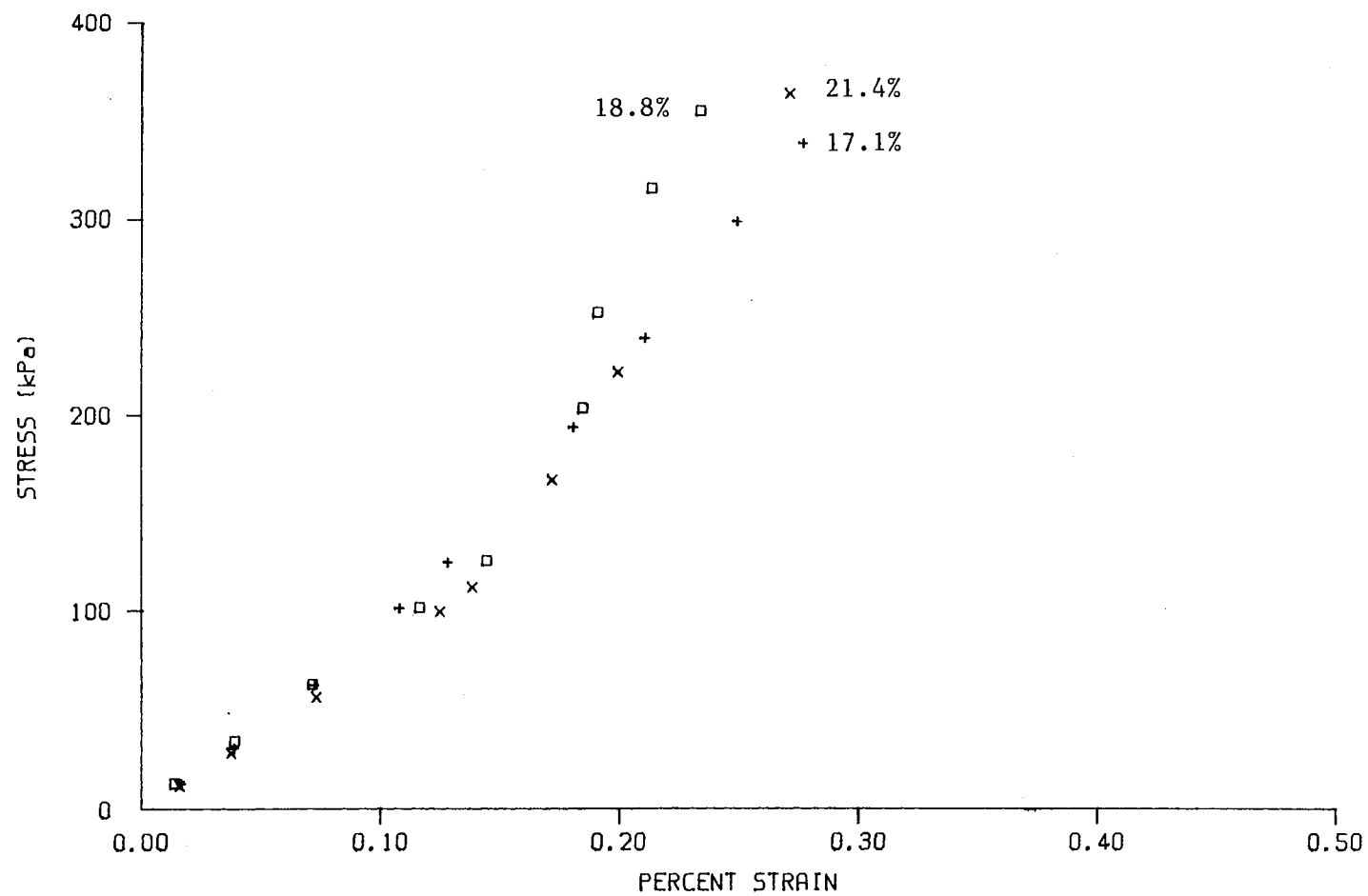


Figure 25. Variation of Stress-Strain Values with Moisture Content for a Horizontally Oriented Sample Vibrated at a Frequency of 800 Hz

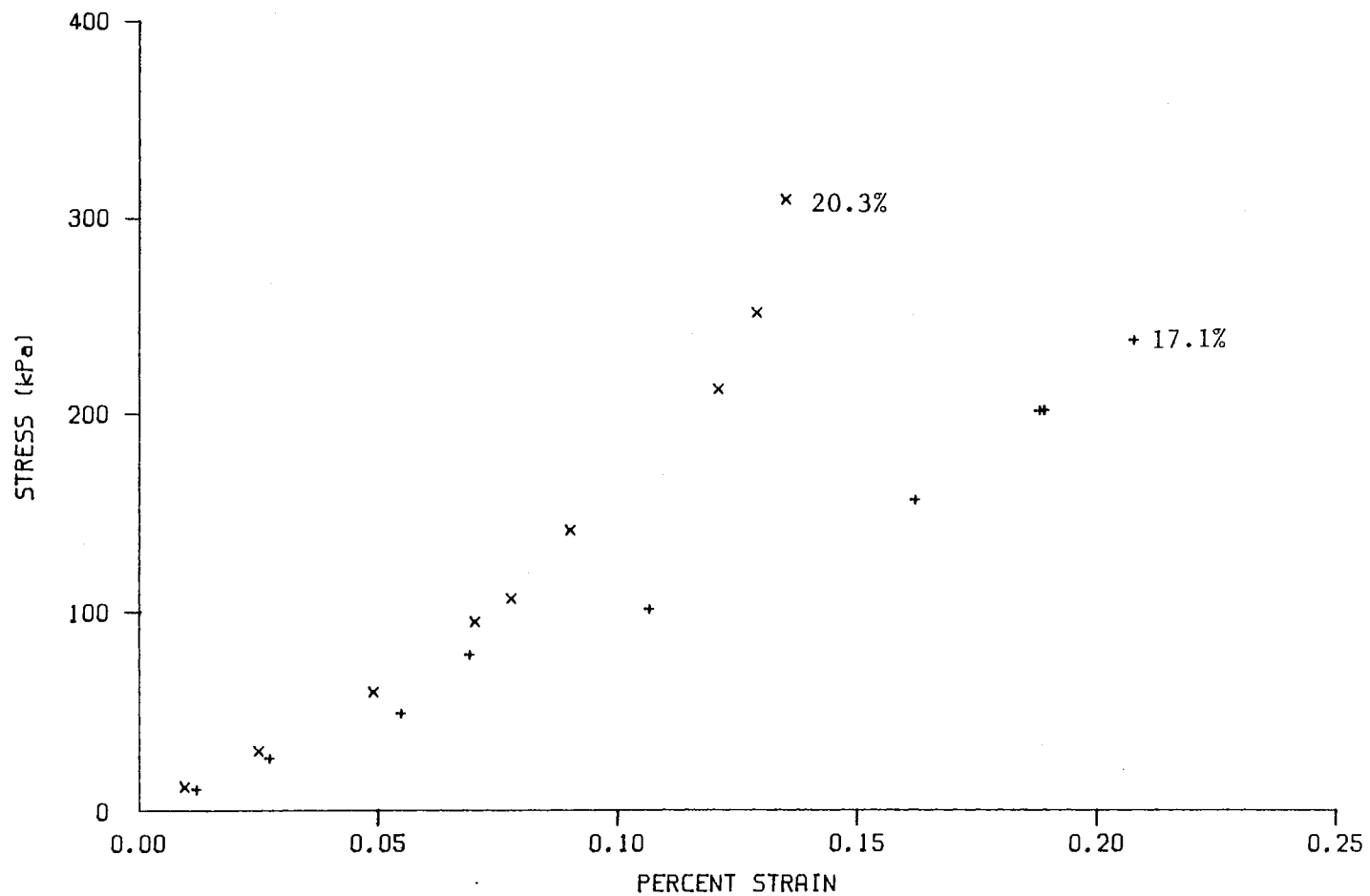


Figure 26. Variation of Stress-Strain Values with Moisture Content for a Horizontally Oriented Sample Vibrated at a Frequency of 1000 Hz

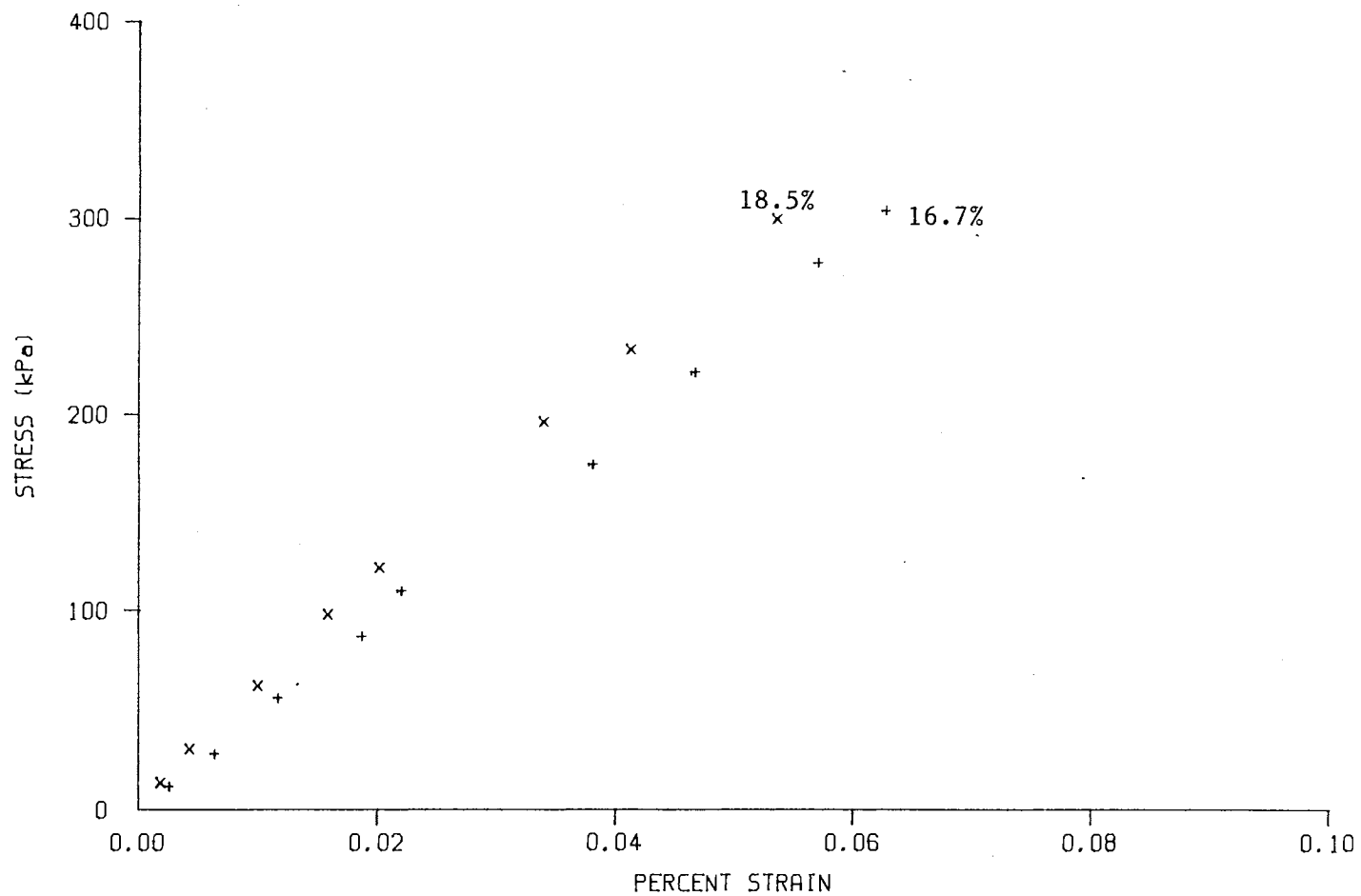


Figure 27. Variation of Stress-Strain Values with Moisture Content for a Horizontally Oriented Sample Vibrated at a Frequency of 1500 Hz

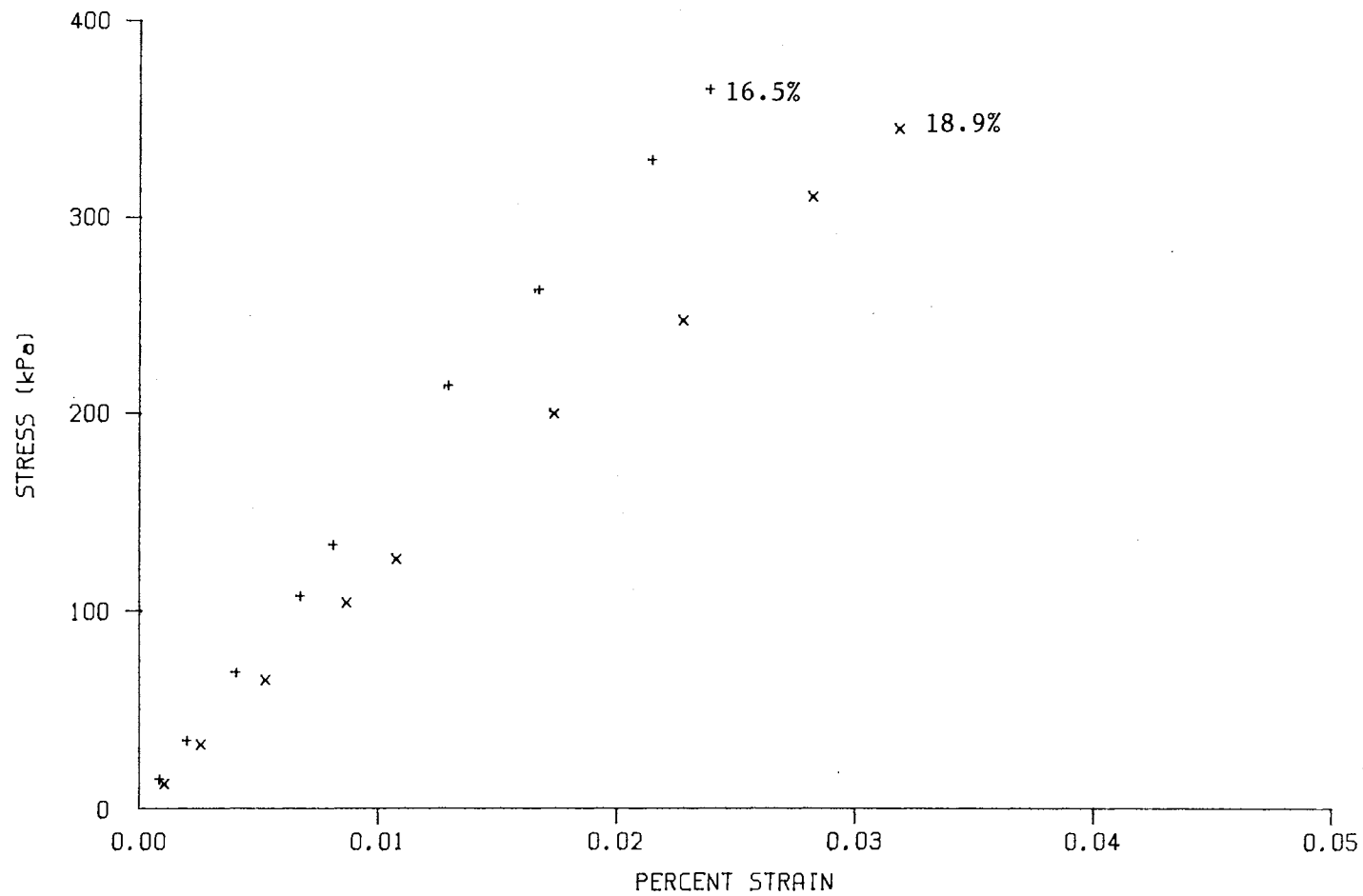


Figure 28. Variation of Stress-Strain Values with Moisture Content for a Horizontally Oriented Sample Vibrated at a Frequency of 2000 Hz

at a frequency of 2000 Hz. The maximum attainable stresses of the two samples varied by only 3.6%.

The data from the previous figures suggest that the stress-strain behavior of soil may not be significantly affected by the range of moisture contents to which the samples were exposed. To test the hypothesis that moisture content may not effect the stress-strain behavior within the given moisture content range except at a low frequency such as 300 Hz, a Student's t test given by equation (16) comparing the difference between two independent regressions was performed.

$$t = b_1 - b_2 / \sqrt{s_p^2 (1/ \sum (X_1 - \bar{X}) + 1/ \sum (X_2 - \bar{X}))} \quad (16)$$

This analysis involved comparing the slopes of each of the stress-strain curves for a particular frequency and determining if a statistical difference existed between them over the particular moisture content range. Table V shows a comparison between the Student's t at 300 Hz and the t values obtained for the other frequencies of 800, 1000, 1500, and 2000 Hz for both orientations. In all cases, with the exception of samples tested at 300 Hz, there was no statistical difference between the slopes of each of the curves within the moisture content range specified. The t values for samples tested at 1300 and 1700 Hz showed no significant difference between slopes either.

Therefore, the hypothesis that moisture content does not play a role in determining stress-strain behavior

through the range of moisture contents presented can not be rejected at any standard level of significance. This analysis implies that the deformation and possible failure of soil are not as sensitive to the moisture content level at which the soil resides as compared to the frequency at which it is excited.

TABLE V

STUDENT'S t TEST COMPARING THE SLOPES OF TWO INDEPENDENT STRESS-STRAIN REGRESSIONS AT ONE FREQUENCY AND DIFFERENT MOISTURE CONTENT RANGES

Frequency, Hz	Vertical Orientation	Horizontal Orientation
300	12.572	0.870
800	0.740	0.070
1000	0.532	1.120
1500	1.130	0.230
2000	0.134	0.676

Dynamic Model Parameter Determination

It is known from previous work, Kocher and Summers (1988), that calculation of stresses in soil as functions of strain requires evaluation of the parameters α , α and

ξ . This involves use of both experimental data in conjunction with theoretical relationships.

Theory

Kocher and Summers (1988) have shown the displacement function u to be

$$u = \lambda e^{j\omega t} [\cos(k'x) + \tan(k'L + \phi') \sin(k'x)] \quad (17)$$

where

$$k' = \omega \sqrt{\frac{\rho}{E - \xi \omega^2 + j\alpha \omega}}$$

$$\phi = \tan^{-1} \left[\frac{m}{A - \sqrt{\rho(E - \xi \omega^2 + j\alpha \omega)}} \right]$$

The constant λ is equal to the maximum acceleration at the bottom of the sample divided by the frequency squared.

From experimental data the acceleration ratio is known. To determine the parameters α and ξ , the experimental value of the acceleration ratio is compared with the theoretical value. The theoretical value of the acceleration ratio is the second time derivative of displacement and is:

$$\frac{\partial^2 u}{\partial t^2} = -\lambda \omega^2 e^{j\omega t} [\cos(k'x) + \tan(k'L + \phi') \sin(k'x)] \quad (18)$$

Equation (18) is evaluated at $x=0$ and $x=L$ to produce expressions for acceleration at the top and bottom of the sample respectively.

$$\frac{\partial^2 u(0,t)}{\partial t^2} = -\omega^2 \lambda e^{j\omega t} \quad (19)$$

$$\frac{\partial^2 u(L,t)}{\partial t^2} = -\omega^2 \lambda e^{j\omega t} [\cos(k' L) + \tan(k' L + \phi') \sin(k' L)] \quad (20)$$

The theoretical acceleration ratio is equation (19) divided by equation (20). This is shown in equation (21).

$$\frac{\text{top acceleration}}{\text{bottom acceleration}} = \cos(k' L) + \tan(k' L + \phi') \sin(k' L) \quad (21)$$

The experimental acceleration ratio is a complex number and can be divided into its real and imaginary parts. The real part of the experimental acceleration ratio is the acceleration ratio multiplied by the cosine of the phase angle and the imaginary part is the acceleration ratio multiplied by the sine of the phase angle. Equation (21) can also be divided into its real and imaginary parts with only α and ξ as unknowns.

An iterative procedure was applied to make the experimental acceleration ratio numerically the same as the theoretical acceleration ratio. This was accomplished in the following manner.

An initial guess of α and ξ was made and the error between the experimental and theoretical acceleration ratios was determined. To decrease the error, one parameter, either α or ξ , was held constant while the other was varied greater and smaller than the original guess. The value of the

varied parameter that provided the smaller error was then varied again in the same manner as before and the process was repeated until the error was a minimum. This parameter was held constant while the other parameter was varied in the same manner as above until the smallest possible error was obtained. The process was repeated until the error between the experimental and theoretical acceleration ratios was within an acceptable limit. The α and ξ values were determined for that particular sample at the given frequency and moisture content. This process was performed for all samples of both orientations. For each soil sample, several amplitude settings (λ) were tested each yielding an α and ξ value. These data are presented in Appendix A.

Regression of Alpha and Xi as Functions of Moisture Content and Frequency

Kocher and Summers (1988) have shown α and ξ to be functions of frequency. Since the present work is concerned with the relation of stress-strain as a function of moisture content, it is possible that α and ξ are functions of moisture content as well.

To be able to make a realistic determination of how α and ξ vary in relation to moisture content, average values of α and ξ at each frequency were used. Average values were used because there was not a consistent trend of variation (fluctuation between positive and negative slopes) in α and ξ as the gain increased. These values were

plotted against the moisture content of the sample for the frequencies of 300, 1000, 1500, and 2000 Hz and are shown in Figures 29 through 32.

From the data provided by Figures 29 and 32, a model of α and ξ as a linear function of moisture content for each frequency was tried. The purpose of this was to determine if moisture content was significant in modeling α and ξ over the given range of moisture contents.

To determine if α and ξ are functions of moisture content, the slopes of these equations were tested against the hypothesis that they were numerically equal to zero meaning no variation in α and ξ with moisture content. A Student's t Test was performed on α and ξ for both orientations at each particular frequency. Table VI presents the results of these tests. It can be seen that α and ξ at frequencies of 800 to 2000 Hz do not vary within the moisture content range at which they were tested. Therefore, the hypothesis that they are independent of moisture content within this particular range should not be rejected at any standard level of significance with the exception of a few values and average values of α and ξ can be used for analysis. These average values of α and ξ for the frequencies of 800 to 2000 Hz for both orientations are listed in Table VII. The data for vertically oriented samples vibrated at 300 Hz shows that moisture content does effect parameter behavior. Equations for α and ξ tested at 300 Hz are given below.

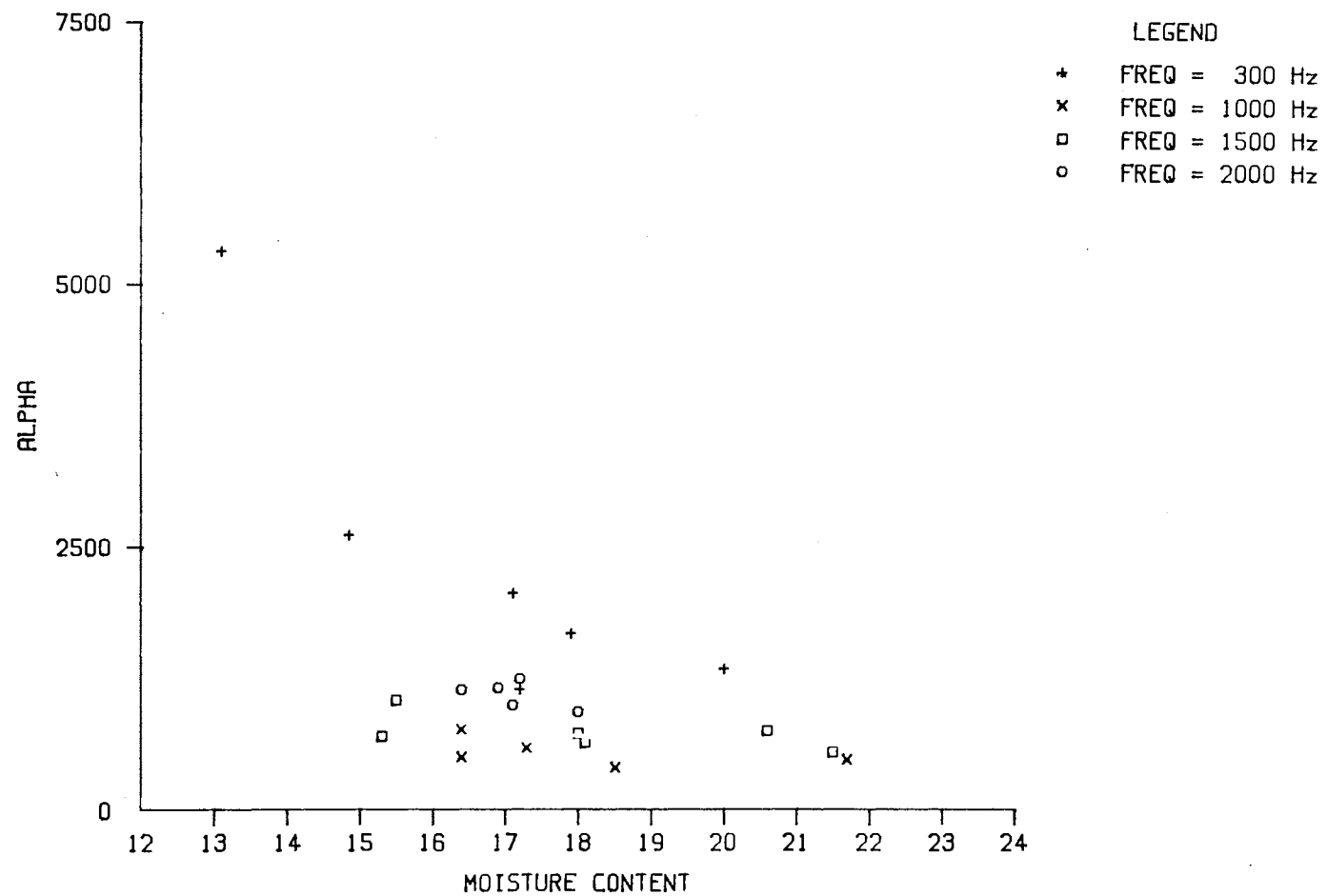


Figure 29. Variation of α with Moisture content for Vertically Oriented Samples

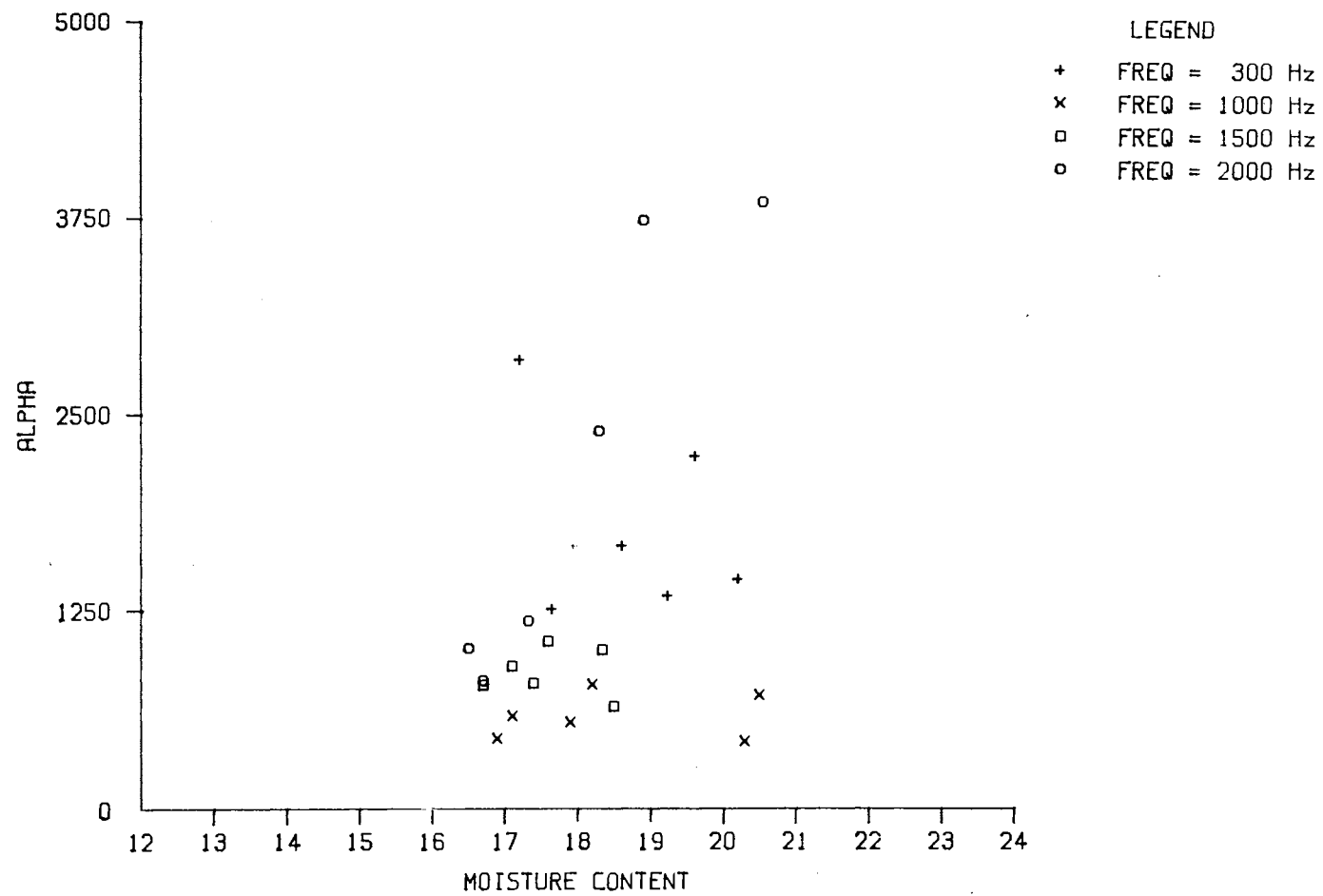


Figure 30. Variation of α with Moisture Content for Horizontally Oriented Samples.

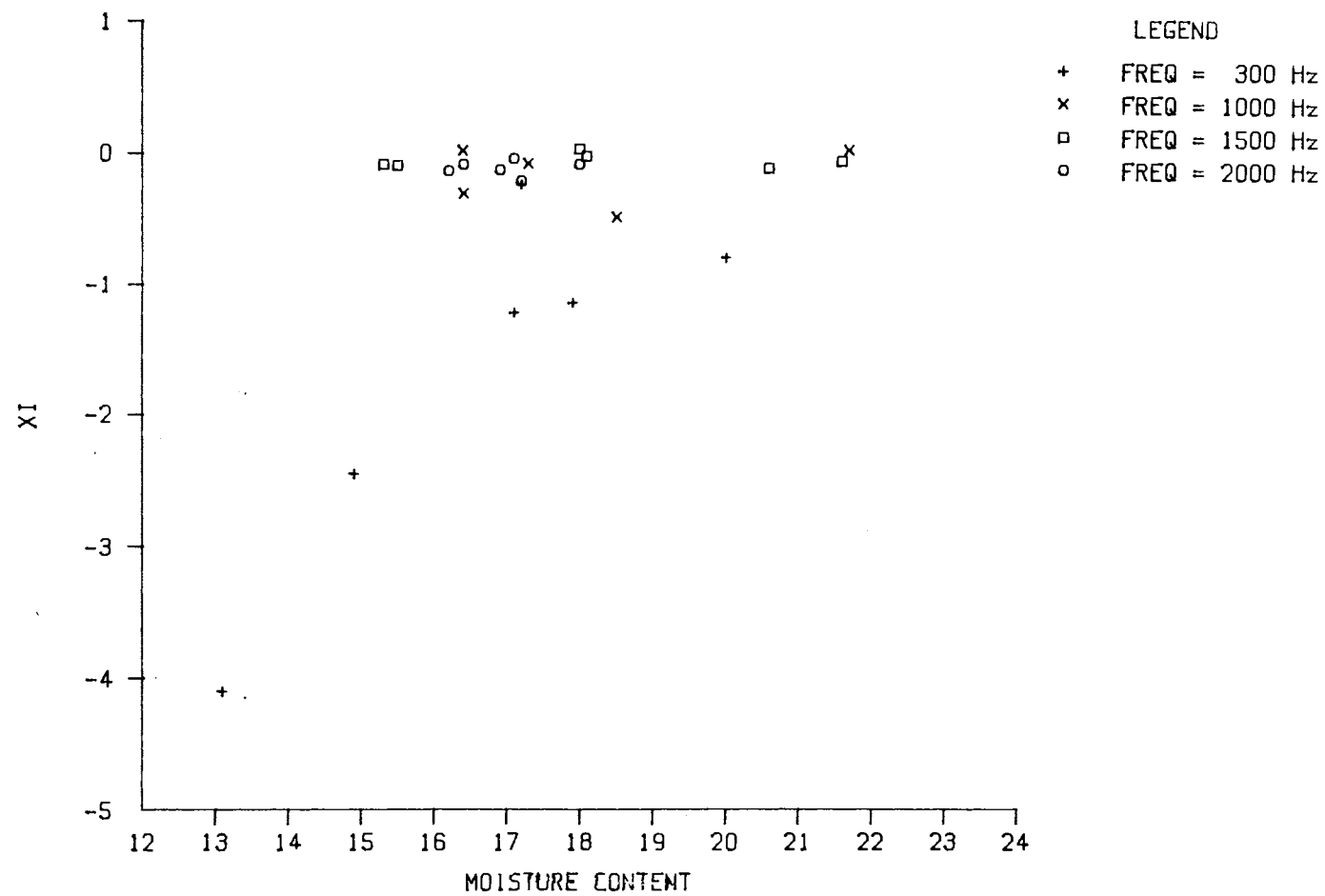


Figure 31. Variation of ξ with Moisture Content for Vertically Oriented Samples

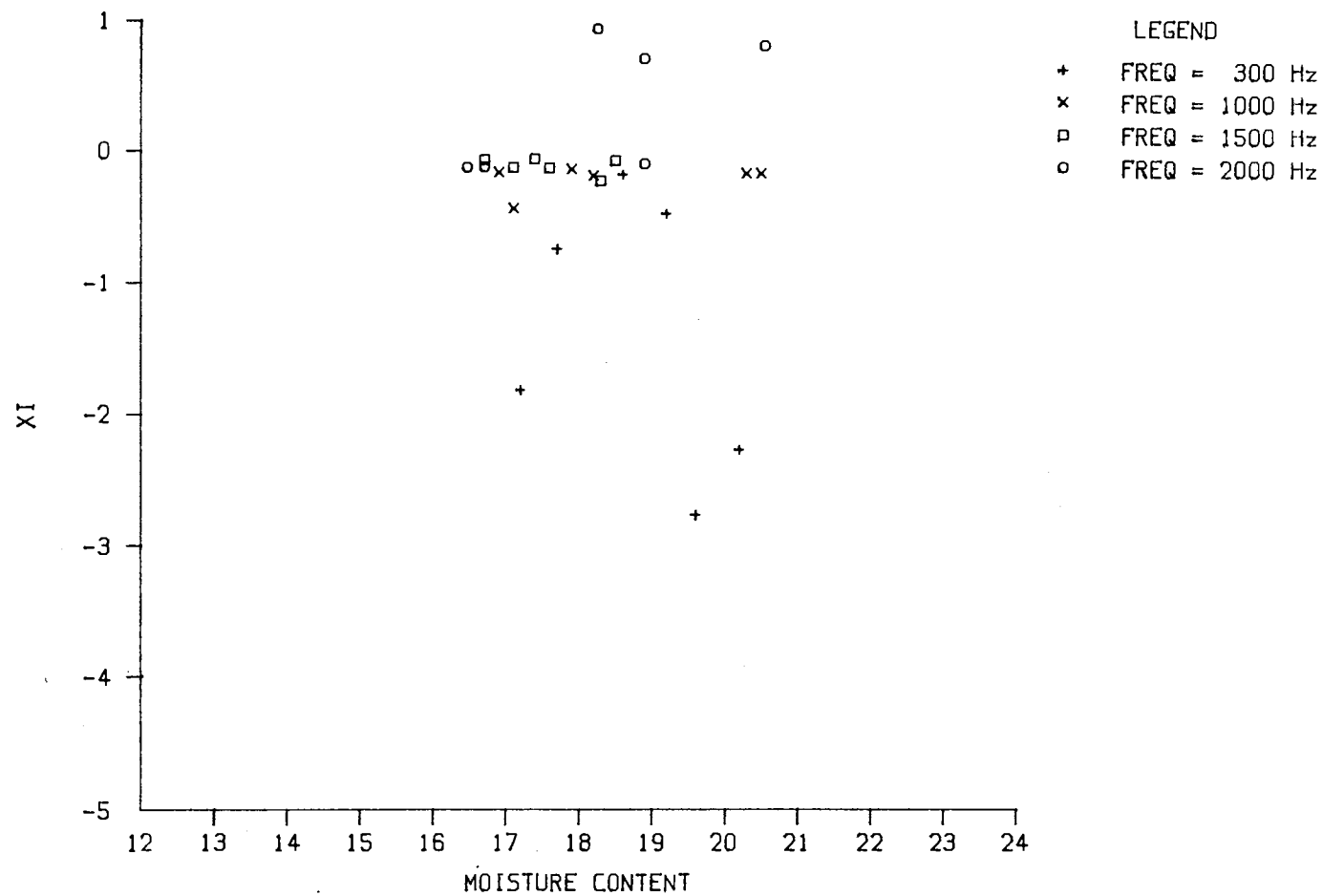


Figure 32. Variation of ϵ with Moisture Content for Horizontally Oriented Samples

TABLE VI

STUDENT'S t TEST COMPARING THE SLOPE, b_1
 OF THE EQUATION $\alpha, \xi = b_0 + b_1 \cdot MC$
 AGAINST A VALUE OF ZERO

FREQUENCY, Hz	α_V	α_H	ξ_V	ξ_H
300	3.42	0.85	3.44	0.74
800	1.24	1.12	0.21	0.26
1000	1.04	0.29	2.74	0.17
1300	2.82*	1.50	1.71	0.05
1500	1.50	0.04	0.94	0.45
1700	0.54	0.08	1.44	1.27
2000	1.26	5.45	0.88	1.72

*Significant at the 5% level

TABLE VII

AVERAGE VALUES OF α AND ξ FOR FREQUENCIES
 OF 800 TO 2000 Hz WITHIN THEIR RESPECTIVE
 MOISTURE CONTENT RANGES

Frequency, Hz	α_V	α_H	ξ_V	ξ_H
800	1050	580	-0.834	-0.273
1000	542	580	-0.176	-0.222
1300	776	689	-0.173	-0.162
1500	680	860	-0.067	-0.122
1700	754	868	-0.067	-0.155
2000	1091	2160	-0.124	-0.124

$$\alpha_V = -6845 + 1.5E05/mc \quad (22)$$

$$\xi_V = 6.65 - 136.36/mc \quad (23)$$

Three-Dimensional Analysis

Data acquired from in-situ experimentation provided acceleration waveforms concerning an input excitation and the response of the soil mass at a certain distance from this excitation. Typical recorded waveforms are shown in Figures 33 and 34. The data were used to determine Poisson's ratio of the soil mass subject to an input frequency and differing lengths between input source and output response which are perpendicular to each other.

A waveform such as the one shown in Figure 34 can be divided into three sections consisting of the time before signal collection (section A), oscillatory portion of the signal (section B) and steady-state portion (section C). Section A is the time before signal capture and reflects an improper 'zeroing' of the signals. Because the signals could not always be 'zeroed', they were shifted up or down from the time axis. This shift biased the voltage values and needed to be removed. To accomplish this, the values of section A are averaged until the start of the oscillatory portion of the signal and this average was subtracted from all acceleration values contained in the waveform.

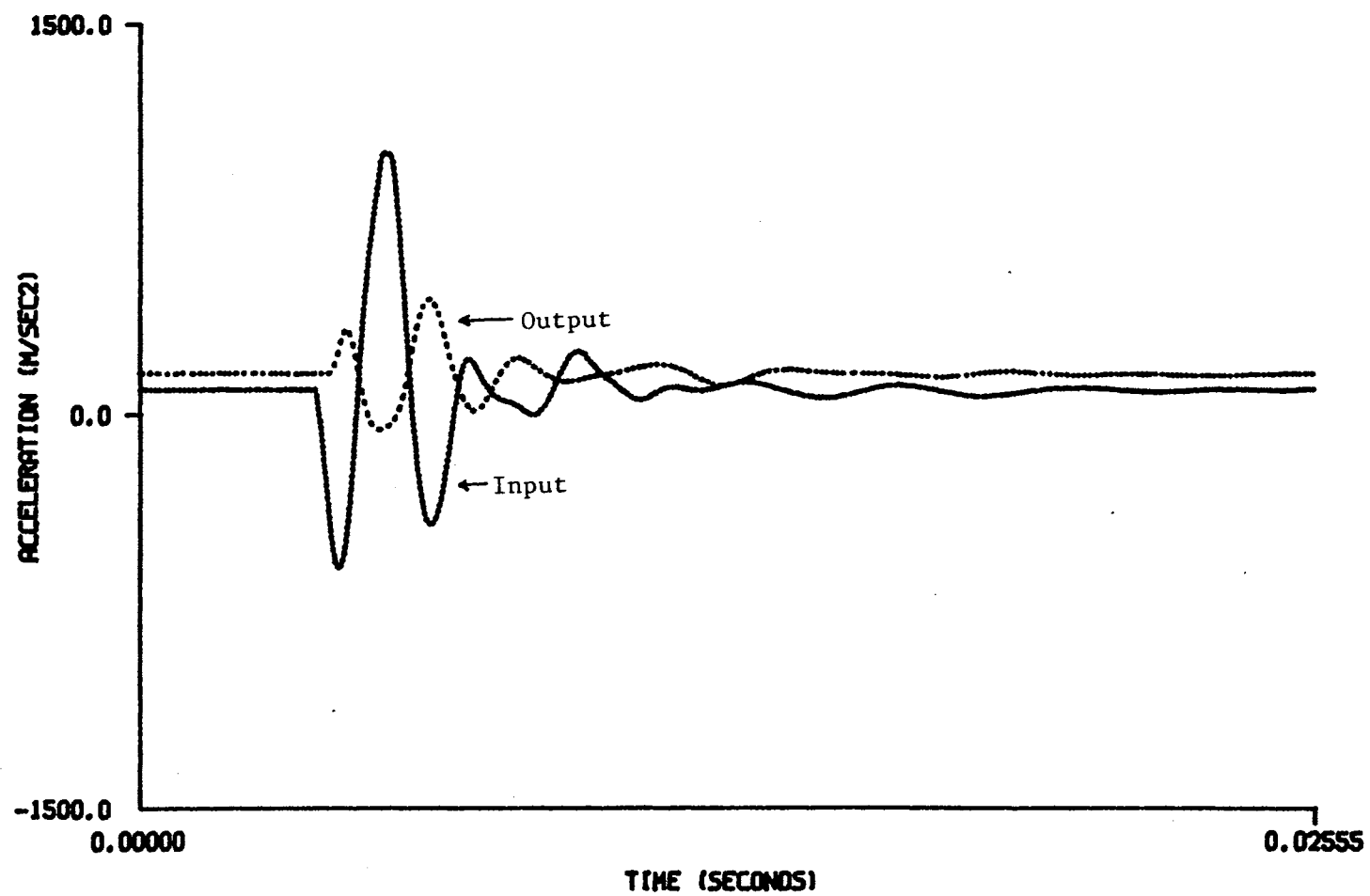


Figure 33. Horizontal Input and Horizontal Output at a Distance of 0.114 Meters

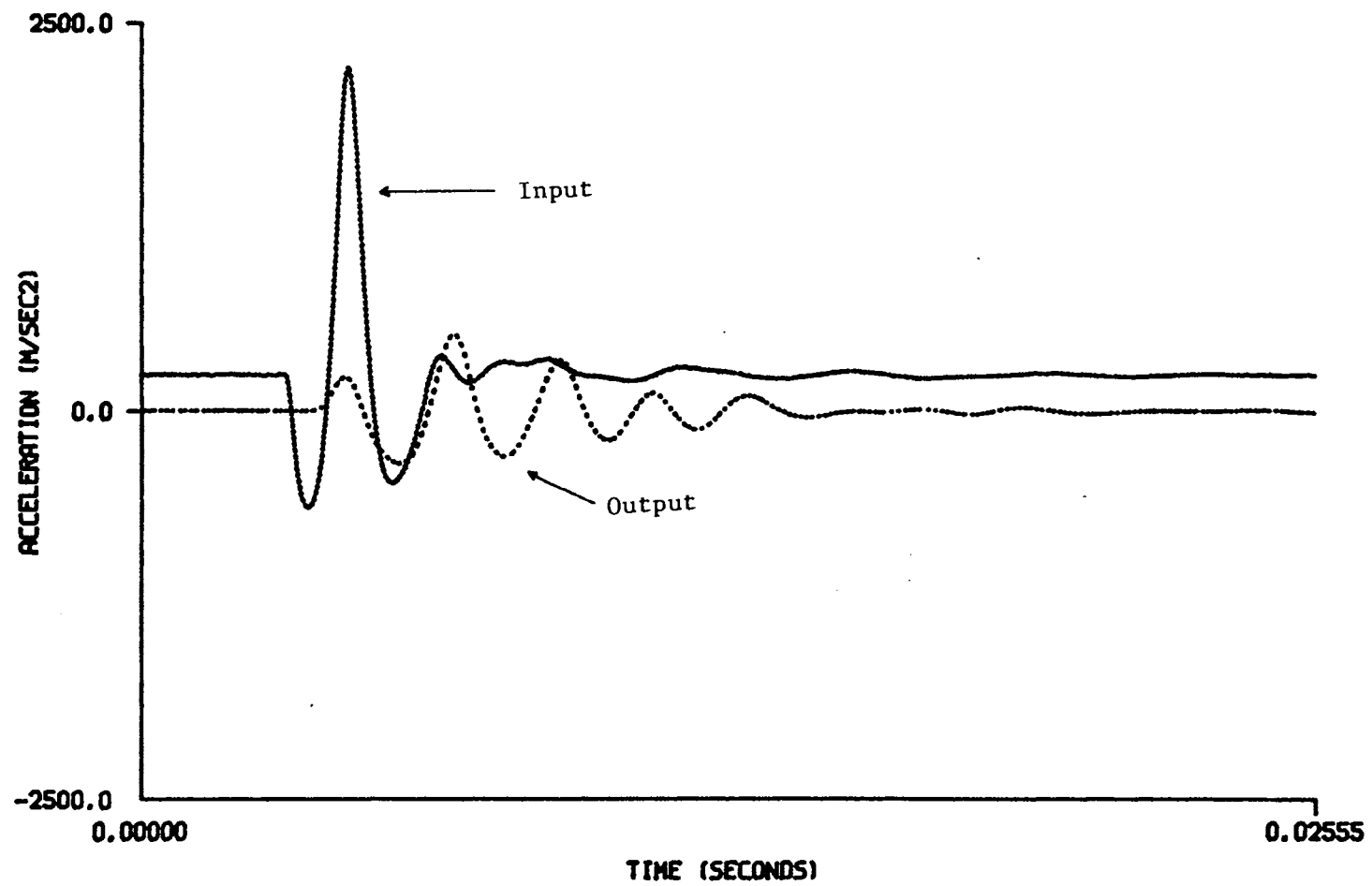


Figure 34. Horizontal Input and Vertical Output at a Distance of 0.227 Meters

Poisson's Ratio Determination

The soil mass used for the in-situ portion of this experiment was stressed on one face and the output due to that stress on a perpendicular face was recorded. From classical three-dimensional stress-strain analysis, the strain in any direction x, y, and z can be written as a function of the stress in one direction plus a combination of the stresses in the other two directions multiplied by a constant ν' . For example, the strain in the y direction can be written as follows:

$$\epsilon_y = \frac{\sigma_y}{E^*} - \nu' \frac{\sigma_x}{E^*} - \nu' \frac{\sigma_z}{E^*} \quad (24)$$

The stresses on the faces y and z are assumed to be equal to zero for this analysis since no input is made on either of these faces. This reduces equation (24) to the following form:

$$\epsilon_y = - \nu \frac{\sigma_x}{E^*} = - \nu \frac{\sigma_z}{E^*} \quad (25)$$

Use of the above equation provides a means by which Poisson's ratio for the soil mass can be found knowing the input stress and the strain at the output location.

The input stress, σ_i , is calculated by multiplying the mass of the soil block times the maximum compressive acceleration of the input waveform and dividing this quantity by the area of the face upon which the input was

made. The constant E^* is the dynamic modulus of elasticity of the soil mass based on the second order viscoelastic stress-strain equation developed by Kocher and Summers (1988) and is represented by the following equation:

$$E^* = E - \xi \omega^2 + j\alpha\omega \quad (26)$$

The excitation frequency is obtained from the input signal by determining the time at which the oscillatory portion of the signal starts and the time at which one cycle ends. The frequencies varied between input-output orientations due to the natural frequency of the soil block in the direction which the input was made. The difference in frequencies between input-output orientations is due to a difference in boundary conditions.

The values of α and ξ were obtained from the data concerning α and ξ as functions of moisture content and frequency. The excitation frequencies of each test for each input-output orientation are listed in Appendix B.

The maximum strain of the face perpendicular to the input is equal to the maximum displacement experienced by that face divided by one-half the length of the longitudinal axis of that face.

The recorded data consisted of an acceleration value and the time at which it occurred. By recording data in this manner, it was possible to obtain displacement values from the output waveform in a direction perpendicular to the input. This lateral displacement was converted to the

strain undertaken by that particular location on that face of the soil mass.

The procedure used for obtaining displacements from acceleration data for the one-dimensional case cannot be used for this analysis because the oscillatory portion of the signal was not symmetrical about the time axis. Converting acceleration values be numerically integrated twice.

Several integration methods including trapezoidal rule, Simpson's one-third rule and parabolic splines were tried. Because the oscillatory portion of the waveform approximated a sine wave, each method was used to integrate a typical sine wave from zero to π radians. The purpose of this was to determine the error in approximating the area under a sinusoidal curve. The analysis was performed by numerically integrating a sine wave of given amplitude and frequency from zero to π radians. This value was compared to an analytical result obtained by integrating the function $A \sin(\omega t)$. The process was repeated for another set of integration limits (0 to 2π radians) and a comparison was made between the three methods.

Simpson's one-third rule best approximated both areas of the sinusoidal curve and therefore was used to integrate the experimental data.

As the disk of the impulse generator struck the soil mass, a stress wave (body wave) propagated radially outward from the point of impact. As this waveform traveled from

its point of input the volume of soil it encountered increased. While the energy of the waveform remained constant, its energy density decayed. This decrease in energy density is called geometrical damping. The amplitude of the propagating waveform decreases in proportion to the distance r from the input source. The amplitude of a body wave decreases in proportion to the inverse of the distance, $1/r$ (Prakash, 1981).

The strain experienced at a certain location at a distance, r from the input source is directly proportional to the amplitude of the waveform at that point. Therefore, the strain, ϵ , at any location r from the input source becomes a function of the energy density decay of the input waveform.

Referring to equation (24), the value of ν' is also a function of the energy density decay of the input waveform. In this manner, the value of ν' is not a true value of Poisson's ratio of the soil mass but rather is a value of the apparent Poisson's ratio, i.e. the value of Poisson's ratio relative to the point at which the input was made.

At each output location from the input source, four stress levels were input and four strains were measured. This resulted in four apparent Poisson's ratio values at each of the five output locations. This data is listed in Appendix B. These values of apparent Poisson's ratio were averaged at each location and the results are shown in Table VIII.

Since the amplitude of the waveform decreases in proportion to $1/r$, the values of apparent Poisson's ratio should do likewise. From the theory of geometrical damping, the ratio of the amplitudes of the waveform at two locations r_1 and r_2 can be written as

$$\frac{A_2}{A_1} = \frac{r_1}{r_2} \quad (27)$$

TABLE VIII
AVERAGE VALUES OF APPARENT POISSON'S RATIO FOR EACH
DISTANCE r FROM THE SOURCE OF INPUT FOR ALL
THREE INPUT - OUTPUT ORIENTATIONS

Distance r from input, m	Input - Output Orientation		
	H - H	H - V	V - H
0.114	0.042	0.090	0.181
0.144	0.035	0.064	0.160
0.183	0.027	-----	0.145
0.227	0.018	0.021	0.088
0.274	0.016	0.012	0.076

Since v' is proportional to the amplitudes of the waveform at the two different output locations, equation (27) can be written as follows:

$$\frac{\nu'_2}{\nu'_1} = \frac{r_1}{r_2} \quad (28)$$

The following table presents the calculated and theoretical values of apparent Poisson's ratio for each of the three input-output orientations.

TABLE IX
COMPARISON OF CALCULATED VALUES OF APPARENT POISSON'S RATIO
AND THEORETICAL VALUES BASED ON GEOMETRICAL DAMPING
FOR ALL INPUT-OUTPUT ORIENTATIONS

H - H	H - V	V - H	Theoretical Value
1.20	1.40	1.13	1.26
1.27	-	1.10	1.27
1.55	-	1.64	1.24
1.07	1.75	1.15	1.21

By regressing the values of apparent Poisson's ratio against the distance from the input source, the effect of the geometrical damping is removed and a true value of Poisson's ratio can be attained for each input-output orientation of the soil mass. Figures 35, 36, and 37 show the values of apparent Poisson's ratio plotted against $1/r$. Table X gives the intercept and slope of each of the

equations relating to distance, r . The coefficients of determination are 0.98, 0.97, and 0.90 respectively. The slope of each of these lines is the true value of Poisson's ratio for that particular input-output orientation.

TABLE X
VALUES OF THE INTERCEPT, I AND THE SLOPE, S OF THE
REGRESSION $= I + S/r$ FOR EACH OF THE THREE
INPUT - OUTPUT ORIENTATIONS

Input - Output Orientation	Intercept	Slope
H - H	-3.5E-03	5.4E-03
H - V	-4.6E-02	1.6E-02
V - H	6.4E-03	2.1E-02

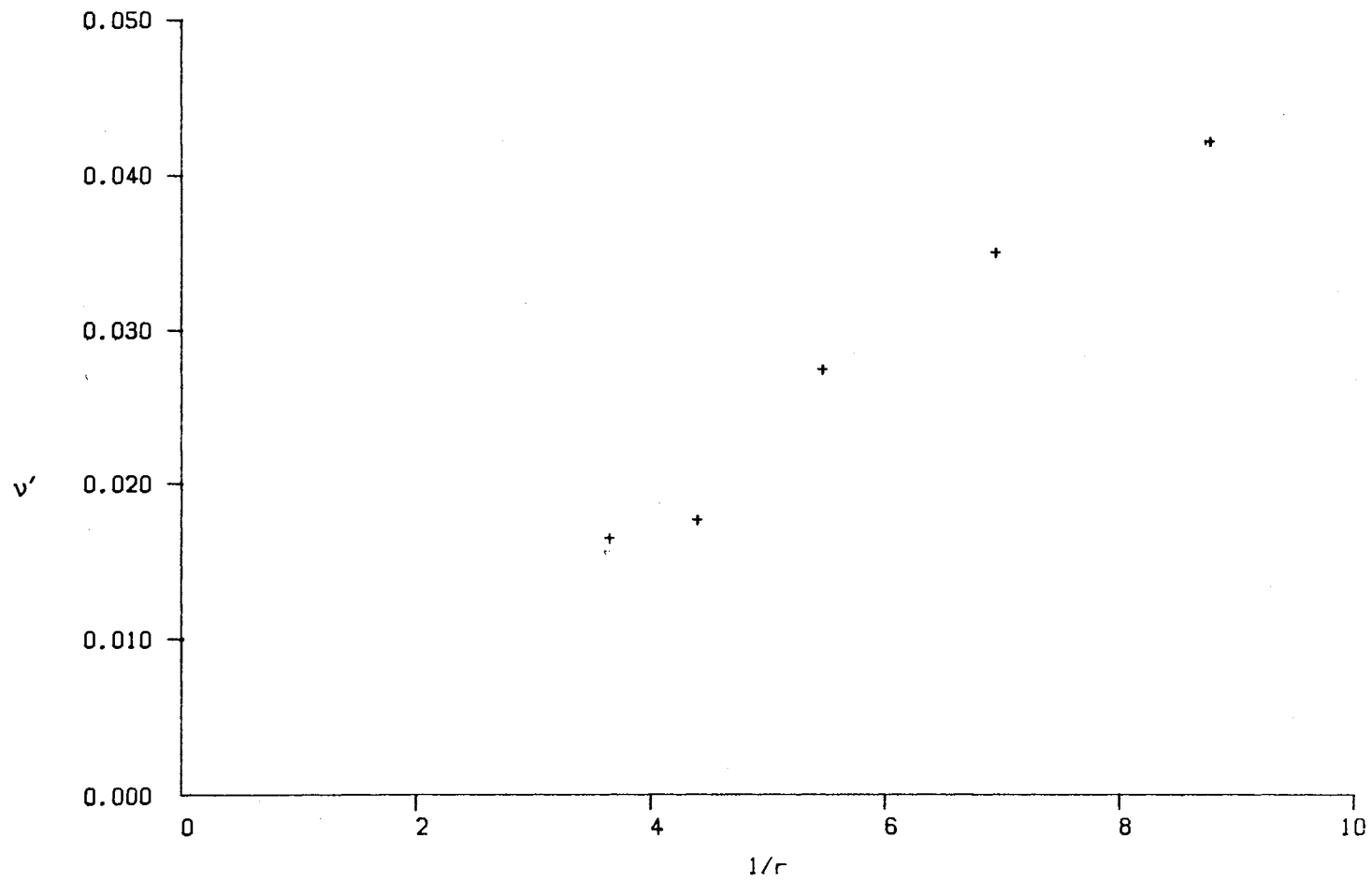
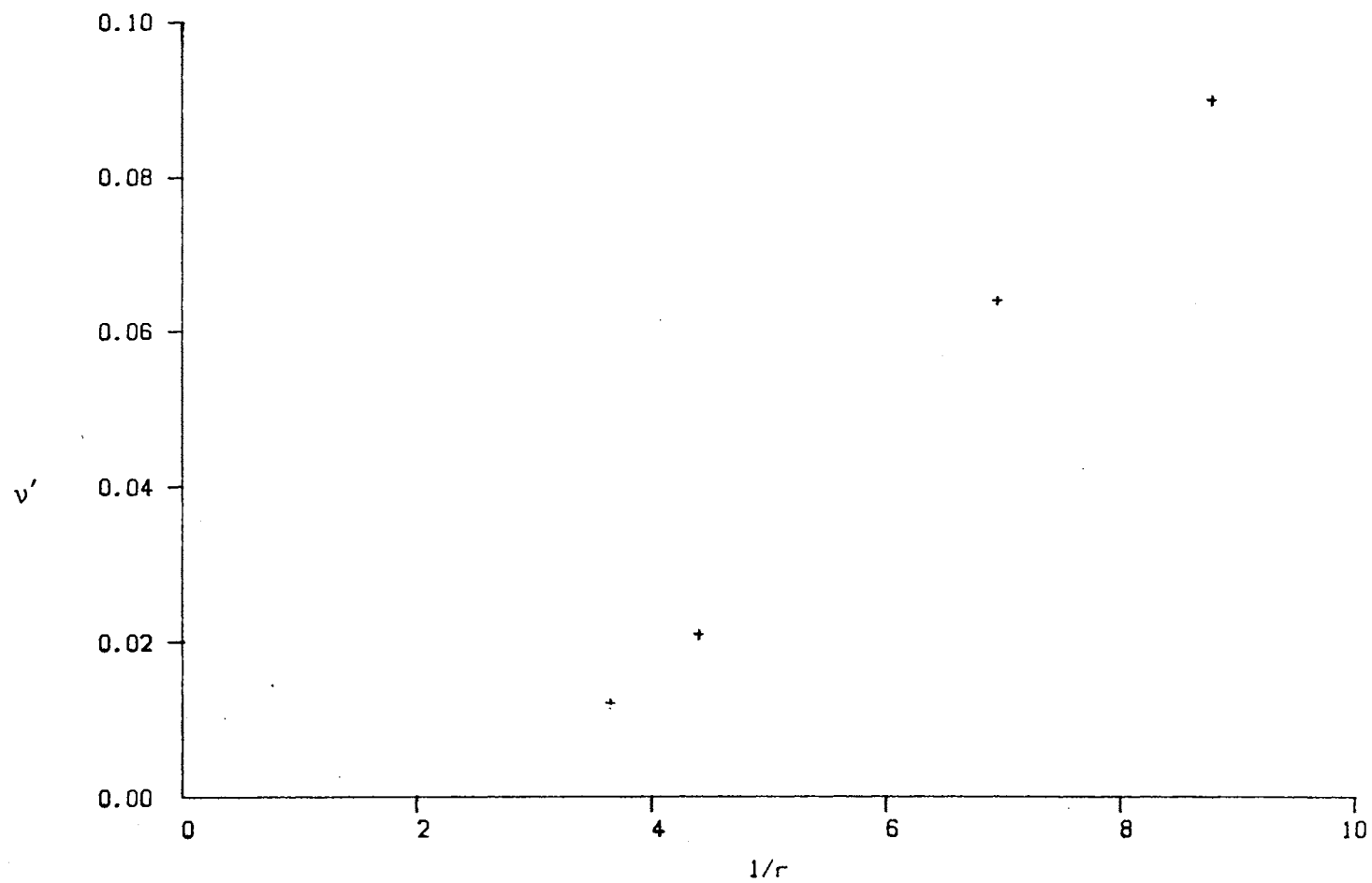
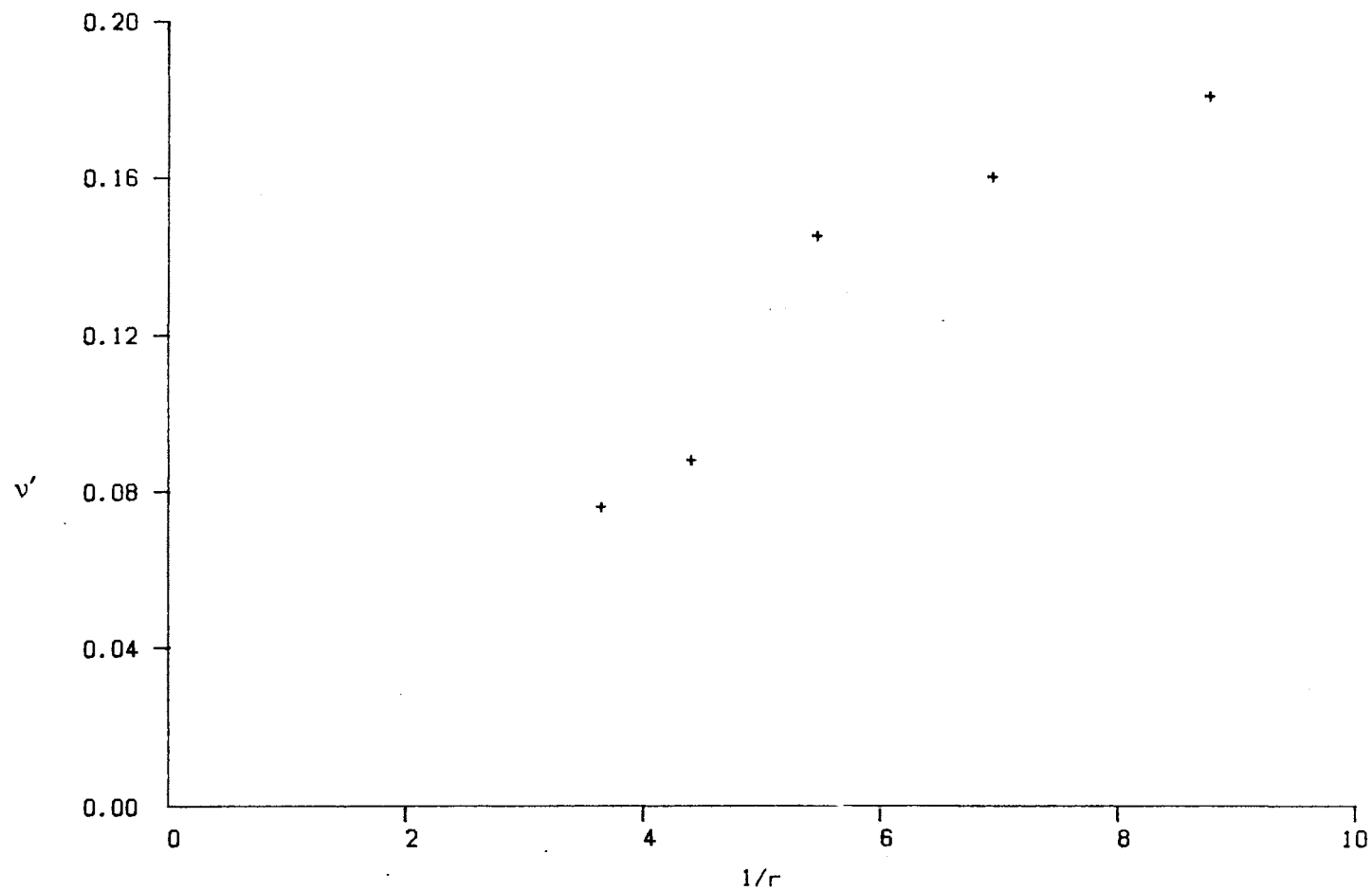


Figure 35. Variation of Apparent Poisson's Ratio with the Inverse Distance for the Horizontal Input-Horizontal Output Orientation



36. Variation of Apparent Poisson's Ratio with the Inverse Distance for the Horizontal Input-Vertical Output Orientation



37. Variation of Apparent Poisson's Ratio with the Inverse Distance for the Vertical Input-Horizontal Output Orientation

CHAPTER VI

CONCLUSIONS

Cylindrical soil samples of varying moisture content were tested at different frequencies ranging from 300 Hz to 2000 Hz. The tests involved measuring the accelerations of the top and bottom of each sample in order to determine the stress-strain behavior of soil. The concept of measuring soil accelerations subject to sinusoidal excitation was extended to three-dimensional in-situ testing. This experimentation consisted of recording accelerations due to an input source and its output response on a plane perpendicular to the input. This was done for input and output in both horizontal and vertical directions. Specific conclusions are:

1. Moisture content does not have a significant effect on the deformation of soil through the range of moisture contents tested except at those tested at a frequency of 300 Hz. This is evidenced by the values of the stresses and strains attained as moisture content varied within a certain frequency. The values of α and ξ at frequencies of 800 to 2000 Hz showed little or no variation with moisture content and the hypothesis

that moisture content did not play a role could not be rejected at any standard level of significance for most values of α and ξ . Frequency variation within a particular moisture content has a much more pronounced effect on stress-strain behavior than moisture content variation with a certain frequency.

2. Subject to conditions of varying amplitude and frequency, the soil tested through the range of moisture contents did not yield and achieve plastic deformation nor could a plausible failure criterion be established.
3. A relationship, $\nu' = f(1/r)$, based on the geometrical damping of propagating waves modeled the relative deformation of the soil in three dimensions at various distances from an input source. This model provided a means to determine a true value of Poisson's ratio for the soil.
4. Use of an impulse generator proved adequate in obtaining information concerning in-situ soil deformation of a parallelepiped soil mass in three dimensions.

CHAPTER VII

RECOMMENDATIONS FOR FURTHER RESEARCH

The research undertaken in this study has provided important information concerning soil deformation. Additional research in certain areas will help complement this study. These are as follows:

1. Both the one-dimensional experimentation and the three-dimensional study (in-situ experimentation) were conducted at the research facility at Chickasha, Oklahoma. Investigation of differing soil types, present at other locations in Oklahoma, on soil deformation subject to the same range of frequencies and moisture contents would be helpful.
2. The soil used for this study had not been tilled or worked for a period of one year prior to testing. The effect of compaction on both the one-dimensional and in-situ portions of this study is needed.
3. The range of frequencies achieved for the in-situ experimentation was limited to 250 to 500 Hz. The results obtained from the one-dimensional experimentation suggest that large deformations

exist at low frequencies. Due to these findings, it is felt that investigation of frequencies in the range of 50-250 Hz might deform soil as to achieve plastic deformation or possibly failure.

4. The soil samples were all tested at room temperature. The effect of temperature variation (5°C - 30°C) on soil deformation subject to varying frequencies and moisture contents would be useful. Heating or cooling the samples to achieve the desired temperature might alter the moisture content of the sample. Therefore, this testing would need to be done immediately after the samples are removed from the ground, so that minimal loss of moisture occurs.
5. The findings of the one-dimensional experimentation reflect a need for additional stress-strain testing at lower ($<13.0\%$) moisture contents. It is felt that the magnitude of the stress-strain values might change significantly at lower moisture contents. This should be examined for frequencies of 500 to 2000 Hz.

LITERATURE REVIEWED

- Arthur, J. R. F. and B. K. Menzies. 1972. Inherent anisotropy in a sand. *Geotechnique* 22(1):115-128.
- Arya, V. K., K. K. Debnath and N. S. Bhatnager. 1980. The spherical vessel with anisotropic creep properties considering large strains. *International Journal of Non-linear Mechanics* 15:185-193.
- Baladi, G. Y. and B. Rohani. 1977. Liquefaction potential of dams and foundations. Report 3. Development of an elastic-plastic constitutive relationship for saturated sand. U. S. Army Engineer Waterways Experiment Station Research Report S-76-2.
- Baladi, G. Y. and B. Rohani. 1978. Liquefaction potential of dams and foundations. Report 5. Development of a constitutive relation for simulating the response of saturated cohesionless soil. U. S. Army Engineer Waterways Experiment Station Research Report S-76-2.
- Baladi, G. Y. 1979. An effective stress model for ground motion calculations. U. S. Army Engineer Waterways Experiment Station Technical Report SL-79-7.
- Baladi, G. Y. and B. Rohani. 1982. An elastic-viscoplastic constitutive model for earth materials. U. S. Army Engineer Waterways Experiment Station Technical Report SL-82-10.
- Banerjee, P. K., A. S. Stipho and N. B. Yousif. 1981. A simple analytical model of the bi-axial stress strain behavior of anisotropically consolidated clays. *Proceedings of the Implementation of Computer Procedures and Stress-Strain Laws in Geotechnical Engineering* pp. 535-549.
- DeRoock, B. and A. W. Cooper. 1967. Relation between propagation velocity of mechanical waves through soil and soil strength. *TRANSACTIONS of the ASAE* 10(4):471-474.
- Deuthler, H. 1932. Experimentelle Untersuchungen ueber die Abhaengigkeit, der Zugspannungen von Verformungsgeschwindigkeit. *Physikalische Zeitschrift* 33:247-296.

- Gill, W. R. 1959. The effects of drying on the mechanical strength of Lloyd clay. Soil Sci. Soc. of Amer. Proc. 23(4):255-267.
- Gill, W. R. and G. E. Vanden Berg. 1968. Soil dynamics in tillage and traction. USDA-ARS Agricultural Handbook No. 316. U. S. Government Printing Office, Washington, D. C.
- Green, G. E. and D. W. Readies. 1975. Boundary conditions, anisotropy and sample shape effects on the stress-strain behavior of sand in triaxial compression and plane strain. Geotechnique 25(2):333-356.
- Hansen, L. A. and G. W. Clough. 1982. The significance of clay anisotropy in finite element analyses of supported excavations. ASCE Application of Plasticity and Generalized Stress-Strain in Geotechnical Engineering pp. 73-92.
- Johnson, C. E., G. Murphy, W. G. Lovely, and R. L. Schafer. 1972. Identifying soil dynamic parameters for soil-machine systems. TRANSACTIONS of the ASAE 15(1):9-13.
- Khan, M. H. 1979. Three-dimensional stress-strain relationships of unsaturated soil under different stress paths. Ph.D. Thesis, University of Illinois, Champaign, Ill.
- Kitani, O. and S. P. E. Persson. 1967. Stress-strain relationships for soil with variable lateral strain. TRANSACTIONS of the ASAE 10(6):738-741, 745.
- Kocher, M. F. and J. D. Summers. 1988. Wave propagation theory for evaluating dynamic soil stress-strain models. TRANSACTIONS of the ASAE 31(3):683-694.
- Lade, P. V. and J. M. Duncan. 1975. Elastoplastic stress-strain theory for cohesionless soil. ASCE Journal of the Geotechnical Engineering Division 101(GT10):1037-1053.
- Lopes, F. R. and R. Feijoo. 1982. An approach to soil creep modelling. International Conference on Numerical Methods in Geomechanics pp. 189-195
- Malvern, L. E. 1951. The propagation of longitudinal waves of plastic deformation in a bar of material exhibiting a strain-rate effect. Journal of Applied Mechanics 18:203-208.

- Matsuoka, H. and T. Nakai. 1974. Stress-deformation and strength characteristics of soil under three different principal stresses. Proceedings of the Japanese Society of Civil Engineers 232:59-70.
- Matsuoka, H. 1976. On the significance of the "spatial mobilized plane". Soils and Foundations 16(1):91-100.
- Miura, S. and S. Toki. 1984. Elastoplastic stress-strain relationship for loose sands with anisotropic fabric under three-dimensional stress conditions. Soils and Foundations 24(2):43-57.
- Nakai, T. and H. Matsuoka. 1983. Constitutive equation for soils based on the extended concept of "spatial mobilized plane" and its application to finite element analysis. Japanese Society of Soil Mechanics and Foundation Engineering 23(4):87-105.
- Nakase, A. and T. Kamei. 1983. Undrained shear strength anisotropy of normally consolidated cohesive soils. Soils and Foundations 23(1):91-101.
- Ochiai, H. and P. V. Lade. 1983. Three-dimensional behavior of sand with anisotropic fabric. ASCE Journal of Geotechnical Engineering 109(10):1313-1328.
- Pisarenko, B. G. 1984. Propagation of strain waves in non-Hookian media with yield delay. Strength of Materials 15(6):842-849.
- Prakash, S. 1981. Soil dynamics. McGraw-Hill. New York, NY 10016.
- Prandtl, L. 1928. Ein gedankenmodell zur kinetischen Theorie der festen Koerper. Zeitschrift fur angewandte Mathematik und Mechanik 8:85-106.
- Prevost, J. H. and K. Hoeg. 1975. Effective stress-strain-strength model for soils. ASCE Journal of the Geotechnical Engineering 101(GT3):259-280
- Prevost, J. H. and K. Hoeg. 1977. Plasticity model for undrained stress-strain behavior. Proceedings of the International Conference on Soil Mechanics and Foundation Engineering 1:255-261.
- Prevost, H. J., T. J. R. Hughes, M. F. Cohen. 1980. Analysis of gravity offshore structure foundations. Journal of Petroleum Technology 32(2):199-209.

- Prevost, J. H. 1980. Mechanics of continuous porous media. International Journal of Engineering Science 18:787-800.
- Prevost, J. H. 1985. A simple plasticity theory for frictional cohesionless soils. Soil Dynamics and Earthquake Engineering 4(1):9-17.
- Ram, R. B. and C. P. Gupta. 1972. Relationship between rheological coefficients and soil parameters in compression test. TRANSACTIONS of the ASAE 15(6):1054-1058.
- Richter, T. 1979. Nonlinear consolidation models for finite element computations. Third International Conference on numerical Methods in Geomechanics pp. 181-190.
- Rohani, B. 1972. Damping capacity of soil during dynamic loading. Report 1. Review of mathematical material models. U. S. Army Engineer Waterways Experiment Station Miscellaneous Paper S-72-11.
- Shackel, B. 1973. An engineering approach to defining three dimensional stress-strain relationships. Conference on Stress and Strain in Engineering pp. 26-31.
- Smith, G. M., Y. C. Pao and J. D. Fickes. 1978. Determination of a dynamic model for urethane prosthetic compounds. Experimental Mechanics 18(10):389-395.
- Sokolovsky, V. V. 1948. The propagation of elastic-viscous-plastic waves in bars. Prikladnaia Matematika i Mekhanika 12:261-280
- Vanden Berg, G. E. 1961. Requirements for a soil mechanics. TRANSACTIONS of the ASAE 4(2):234-238.
- Vasin, R. A., V. S. Lenskii and E. V. Lenskii. 1975. Dynamic correlation between stress and strains. Problems of the Dynamics of Elastoplastic Media pp. 7-38.
- Yuen, C. M. K., K. Y. Lo, J. H. L. Palmer and G. A. Leonards. 1978. A new apparatus for measuring the principal strains in anisotropic clays. Geotechnical Testing Journal 1(1):24-33.

APPENDIXES

APPENDIX A

ONE-DIMENSIONAL ACCELERATION DATA

FREQUENCY = 300 Hz
VERTICAL ORIENTATION

MOISTURE 43.0% CONTENT, % SATURATION, DENSITY (WB)	LAMBDA *10 ⁶	ACCLN. RATIO	PHASE ANGLE rad	ALPHA	XI
13.1%	17	1.58	-0.243	6533	-6.58
43.0%	37	1.71	-0.395	6287	-4.75
1666 (kg/m ³)	59	2.15	-0.607	4342	-3.31
	55	2.01	-1.130	4083	-1.78
17.1%	13	2.53	-0.567	3207	-3.40
62.9%	23	2.82	-0.788	2974	-2.77
1847	36	3.10	-1.400	2377	-1.83
	47	3.16	-1.500	2228	-1.74
	62	3.11	-1.780	1890	-1.50
	87	2.77	-2.380	1135	-1.10
	134	2.30	-2.780	581	-0.87
17.9%	15	1.84	-0.295	3352	-3.75
63.8%	24	2.02	-0.378	3045	-3.16
1839	31	2.47	-0.589	2488	-2.30
	39	3.35	-1.191	1740	-1.40
	54	3.16	-2.043	1116	-0.83
	59	3.32	-2.031	1090	-0.86
	103	2.45	-2.647	572	-0.54
17.2%	12	2.18	-0.418	2795	-2.18
60.7%	22	2.84	-0.776	2200	-1.15
1830	47	2.70	-2.078	1233	0.01
	55	2.72	-2.180	1109	0.05
	61	2.60	-2.236	1058	0.08
	95	1.96	-2.845	386	0.37
	116	1.86	-2.960	230	0.41
	126	1.76	-3.070	87	0.46
14.9%	14	2.01	-0.327	4136	-4.68
49.1%	24	2.88	-0.724	3010	-2.69
1702	63	1.31	-2.806	702	-0.02

20.0%
68.7%
1874

9	3.31	-0.921	1855	-1.62
19	3.68	-1.352	1554	-1.22
30	3.65	-1.534	1456	-1.09
60	2.90	-2.028	1230	-0.72
85	2.32	-2.300	1038	-0.50
144	0.80	-2.590	852	0.34

FREQUENCY = 800 Hz
VERTICAL ORIENTATION

MOISTURE CONTENT, % SATURATION, DENSITY (WB)	LAMBDA *10 ⁶	ACCLN. RATIO	PHASE ANGLE rad	ALPHA	XI
16.0%	1	1.28	-2.732	1969	-0.90
54.3%	2	1.26	-2.744	1921	-0.89
1772 (kg/m ³)	2	1.30	-2.748	1926	-0.90
16.6%	3	1.20	-2.785	1806	-1.16
65.9%	9	1.06	-2.830	1641	-1.03
1870	20	0.94	-2.922	1184	-0.90
	32	0.92	-3.118	1129	-0.88
16.8%	4	0.51	-3.060	1411	-0.01
46.7%	9	0.49	-3.023	1653	-0.05
1626	18	0.45	-3.106	1472	0.08
	29	0.42	-3.208	1529	0.12
	36	0.41	-3.241	1477	0.14
	57	0.44	-3.529	1072	0.20
17.2%	4	0.89	-2.943	902	-0.72
51.6%	9	0.86	-3.017	600	-0.70
1711					
15.1%	3	1.45	-2.577	1839	-0.96
	6	1.39	-2.634	1681	-0.93
	10	1.28	-2.702	1515	-0.87
	20	1.15	-2.798	1161	-0.80
	33	1.09	-2.979	588	-0.76
	34	1.05	-3.043	328	-0.74
19.8%	4	0.71	-3.037	766	-0.75
66.4%	9	0.70	-3.083	418	-0.72
1790	18	0.72	-3.105	305	-0.72

FREQUENCY = 1000 Hz
VERTICAL ORIENTATION

MOISTURE CONTENT, % SATURATION, DENSITY (WB)	LAMBDA *10 ⁶	ACCLN. RATIO	PHASE ANGLE rad	ALPHA	XI
16.8%	1	0.31	-4.944	1481	-0.18
58.3%	3	0.28	-4.986	1493	-0.17
1785 (kg/m ³)	5	0.24	-5.091	1478	-0.15
	9	0.18	-5.240	1466	-0.13
	12	0.17	-5.288	1463	-0.12
	17	0.14	-5.370	1455	-0.10
16.4%	1	0.99	-3.317	278	-0.38
67.9%	2	0.95	-3.253	203	-0.39
1870	6	0.88	-3.544	655	-0.36
	12	0.79	-3.721	779	-0.32
	18	0.68	-3.868	1067	-0.30
	23	0.63	-3.968	1123	-0.26
	37	0.49	-4.236	1212	-0.22
16.4%	2	0.78	-3.618	260	-0.06
51.4%	6	0.64	-4.042	388	-0.04
1694	11	0.46	-4.371	502	-0.01
	18	0.36	-4.427	528	-0.00
	22	0.32	-4.517	539	0.00
	36	0.23	-4.663	554	0.00
	45	0.20	-4.727	558	0.03
	56	0.17	-4.774	557	0.04
	59	0.16	-4.927	560	0.04
17.3%	3	0.81	-3.597	396	-0.18
51.0%	6	0.75	-3.878	502	-0.15
1718	12	0.62	-4.297	572	-0.12
	18	0.52	-4.458	617	-0.09
	23	0.45	-4.658	621	-0.82
	37	0.32	-4.856	629	-0.04
	45	0.28	-4.962	626	-0.03
	58	0.24	-4.967	628	-0.03
	62	0.22	-5.072	629	-0.03

18.5%	2	1.00	-3.022	733	-1.04
79.6%	4	1.03	-3.037	640	-1.07
1958	6	1.03	-3.063	479	-1.03
	8	1.03	-3.155	82	-0.29
	11	1.00	-3.276	104	-0.23
	18	0.92	-3.549	305	-0.22
	23	0.89	-3.641	355	-0.22
	28	0.89	-3.430	324	-0.18
	45	0.72	-4.164	526	-0.17
	74	0.48	-4.447	532	-0.14
21.7%	2	0.61	-4.980	482	-0.05
61.5%	6	0.45	-5.245	473	-0.02
1756	12	0.35	-5.408	476	-0.01
	19	0.31	-5.463	480	0.07
	23	0.27	-5.573	472	0.05
	37	0.22	-5.789	445	0.03
	45	0.20	-5.828	449	0.04

FREQUENCY = 1300 Hz
VERTICAL ORIENTATION

MOISTURE CONTENT, % SATURATION, DENSITY (WB)	LAMBDA *10 ⁶	ACCLN. RATIO	PHASE ANGLE rad	ALPHA	XI
14.5%	1	0.58	-3.043	1435	-0.40
53.4%	3	0.56	-3.092	1269	-0.34
1809 (kg/m ³)	7	0.54	-3.118	1381	-0.30
	10	0.51	-3.122	1672	-0.27
	13	0.51	-3.186	1520	-0.24
	21	0.44	-3.226	1800	-0.18
	25	0.43	-3.353	1705	-0.15
17.0%	1	0.60	-3.341	1183	-0.37
64.8%	3	0.60	-3.416	1211	-0.34
1872	7	0.61	-3.412	1175	-0.34
	10	0.62	-3.622	1135	-0.28
	13	0.63	-3.692	1095	-0.27
	21	0.54	-4.189	1093	-0.19
	26	0.49	-4.321	1100	-0.18
	33	0.44	-4.519	1066	-0.15
17.1%	1	0.65	-3.398	983	-0.35
62.6%	3	0.65	-3.440	992	-0.34
1847	7	0.64	-3.724	995	-0.32
	10	0.59	-4.048	1085	-0.23
	13	0.56	-4.131	1092	-0.21
	20	0.43	-4.433	1095	-0.18
	25	0.37	-4.614	1098	-0.15
	32	0.33	-4.667	1099	-0.15
	37	0.29	-4.714	1097	-0.14
17.3%	1	0.55	-3.267	434	-0.17
64.9%	3	0.54	-3.305	499	-0.16
1859	6	0.54	-3.457	585	-0.13
	10	0.52	-3.685	641	-0.10
	13	0.49	-3.921	644	-0.08
	21	0.37	-4.303	662	-0.04
	32	0.27	-4.600	657	-0.02
	37	0.25	-4.638	654	-0.02

21.5%	1	0.31	-5.416	368	-0.04
68.3%	3	0.24	-5.5	397	-0.03
1853	7	0.22	-5.447	424	-0.02
	10	0.17	-5.548	445	-0.01
	13	0.16	-5.575	467	-0.00
	21	0.12	-5.610	470	-0.00
	26	0.11	-5.681	468	-0.00
	33	0.10	-5.677	470	0.00
	38	0.10	-5.649	471	0.00
22.6%	1	0.72	-4.862	669	-0.20
64.3%	3	0.72	-4.896	659	-0.20
1700	4	0.65	-5.006	659	-0.19
	6	0.57	-5.188	626	-0.17
	10	0.48	-5.295	635	-0.16
	12	0.45	-5.276	671	-0.16
	18	0.35	-5.517	626	-0.13
	17	0.37	-5.423	662	-0.14
	33	0.26	-5.701	630	-0.10
	38	0.23	-5.797	618	-0.09

FREQUENCY = 1500 Hz
VERTICAL ORIENTATION

MOISTURE CONTENT, % SATURATION, DENSITY (WB)	LAMBDA *10 ⁶	ACCLN. RATIO	PHASE ANGLE rad	ALPHA	XI
15.3%	1	0.48	-5.095	610	-0.13
46.0%	2	0.37	-5.126	686	-0.12
1705 (kg/m ³)	5	0.30	-5.289	675	-0.10
	8	0.25	-5.365	695	-0.09
	10	0.23	-5.391	700	-0.08
	16	0.17	-5.469	738	-0.07
	19	0.15	-5.542	737	-0.06
15.5%	1	0.60	-4.909	956	-0.16
55.6%	2	0.52	-5.028	969	-0.14
1776	5	0.41	-5.172	996	-0.12
	8	0.34	-5.252	1023	-0.10
	9	0.30	-5.314	1027	-0.09
	15	0.23	-5.413	1066	-0.07
	19	0.21	-5.365	1151	-0.06
	23	0.17	-5.453	1148	-0.05
18.0%	1	0.66	-3.930	760	-0.04
53.3%	2	0.62	-4.211	765	-0.26
1769	5	0.53	-4.498	768	-0.00
	8	0.44	-4.902	687	0.02
	9	0.40	-5.005	675	0.02
	15	0.31	-5.116	711	0.04
	19	0.27	-5.227	697	0.05
	23	0.25	-5.178	746	0.05
	26	0.23	-5.331	691	0.06
18.1%	1	0.48	-4.547	580	-0.07
61.1%	2	0.41	-4.701	591	-0.06
1809	5	0.32	-4.815	627	-0.04
	8	0.27	-4.892	635	-0.04
	9	0.24	-4.994	642	-0.03
	15	0.19	-5.067	651	-0.02
	18	0.16	-5.100	654	-0.01
	24	0.14	-5.124	659	-0.01
	27	0.13	-5.140	667	-0.01

20.6%	1	0.36	-5.549	728	-0.14
67.6%	2	0.35	-5.543	740	-0.14
1828	5	0.30	-5.618	746	-0.14
	8	0.27	-5.677	759	-0.12
	10	0.26	-5.712	760	-0.11
	15	0.23	-5.799	757	-0.10
	19	0.21	-5.870	756	-0.10
21.5%	1	0.22	-5.294	518	-0.08
62.8%	2	0.20	-5.393	508	-0.07
1750	5	0.17	-5.320	558	-0.07
	7	0.16	-5.318	556	-0.07
	9	0.16	-5.378	553	-0.06
	15	0.13	-5.358	548	-0.06
	19	0.12	-5.535	540	-0.05
	23	0.12	-5.500	542	-0.05
	26	0.11	-5.535	537	-0.56

FREQUENCY = 1700 Hz
VERTICAL ORIENTATION

MOISTURE CONTENT, % SATURATION, DENSITY (WB)	LAMBDA *10 ⁶	ACCLN. RATIO	PHASE ANGLE rad	ALPHA	XI
14.5%	1	0.75	-4.244	725	-0.18
50.2%	2	0.69	-4.440	738	-0.17
1720 (kg/m ³)	4	0.59	-4.720	730	-0.15
	6	0.49	-4.919	724	-0.13
	8	0.46	-4.888	773	-0.13
	12	0.36	-5.168	720	-0.11
	16	0.33	-5.256	705	-0.10
	20	0.28	-5.355	703	-0.09
14.7%	1	0.69	-4.245	1241	-0.20
57.7%	2	0.64	-4.427	1228	-0.18
1850	4	0.58	-4.569	1229	-0.17
	6	0.50	-4.683	1261	-0.15
	8	0.48	-4.743	1246	-0.14
	12	0.39	-5.016	1175	-0.11
	15	0.35	-5.067	1196	-0.10
	19	0.31	-5.184	1153	-0.09
	22	0.28	-5.226	1170	-0.08
15.8%	1	0.20	-5.733	693	-0.07
51.7%	2	0.18	-5.825	721	-0.06
1742	4	0.15	-5.781	747	-0.06
	6	0.13	-5.787	779	-0.06
	8	0.13	-5.825	789	-0.05
	13	0.11	-5.878	798	-0.04
	16	0.09	-5.930	902	-0.04
	20	0.08	-5.972	810	-0.03
	22	0.08	-5.997	812	-0.03

16.3%	1	0.66	-4.450	724	-0.17
62.1%	2	0.62	-4.572	717	-0.16
1771	7	0.41	-5.120	668	-0.12
	9	0.38	-5.068	715	-0.12
	13	0.32	-5.182	719	-0.11
	18	0.26	-5.296	722	-0.10
	23	0.23	-5.386	716	-0.09
	24	0.22	-5.489	666	-0.08
17.8%	1	0.50	-5.263	664	-0.14
53.3%	2	0.44	-5.356	658	-0.13
1723	4	0.40	-5.331	711	-0.13
	6	0.34	-5.544	634	-0.11
	8	0.33	-5.598	619	-0.11
	13	0.26	-5.788	587	-0.09
	16	0.23	-5.879	583	-0.08
	20	0.21	-5.959	573	-0.07
18.4%	1	0.56	-4.218	909	-0.11
55.4%	2	0.54	-4.321	895	-0.10
1681	4	0.44	-4.556	907	-0.10
	6	0.38	-4.655	924	-0.08
	8	0.34	-4.724	948	-0.06
	13	0.25	-4.910	953	-0.04
	15	0.23	-4.960	955	-0.03
	19	0.20	-5.020	958	-0.03
	22	0.19	-5.095	965	-0.03

FREQUENCY = 2000 Hz
VERTICAL ORIENTATION

MOISTURE CONTENT, % SATURATION, DENSITY (WB)	LAMBDA *10 ⁶	ACCLN. RATIO	PHASE ANGLE rad	ALPHA	XI
16.4%	1	0.34	-4.911	1117	-0.12
	3	0.28	-4.986	1141	0.11
	5	0.24	-5.092	1140	-0.10
	6	0.23	-5.132	1139	-0.09
	9	0.18	-5.240	1142	-0.08
	12	0.16	-5.288	1138	-0.07
	14	0.14	-5.323	1136	-0.07
	17	0.13	-5.370	1132	-0.07
16.9%	1	0.31	-5.401	1281	-0.18
	3	0.25	-5.714	1102	-0.15
	4	0.23	-5.777	1119	-0.15
	6	0.22	-5.804	1127	-0.14
	9	0.18	-5.923	1142	-0.12
	12	0.15	-6.024	1152	-0.10
	15	0.14	-6.073	1157	-0.10
	16	0.14	-6.091	1162	-0.29
17.1%	1	0.12	-5.553	977	-0.06
	3	0.11	-5.615	989	-0.05
	5	0.10	-5.603	998	-0.05
	6	0.10	-5.651	1002	-0.04
	9	0.08	-5.659	1007	-0.04
17.2%	1	0.65	-3.790	1334	-0.29
	2	0.66	-3.892	1282	-0.28
	4	0.66	-4.029	1250	-0.26
	6	0.61	-4.269	1224	-0.24
	8	0.60	-4.389	1196	-0.22
	13	0.49	-4.642	1216	-0.19
	15	0.43	-4.708	1227	-0.18
	20	0.37	-4.837	1245	-0.16
	22	0.35	-4.951	1248	-0.16

18.0%

1	0.19	-5.742	877	-0.01
3	0.15	-5.773	958	-0.09
5	0.13	-5.884	958	-0.08

FREQUENCY = 300 Hz
HORIZONTAL ORIENTATION

MOISTURE CONTENT, % SATURATION, DENSITY (WB)	LAMBDA *10 ⁶	ACCLN. RATIO	PHASE ANGLE rad	ALPHA	XI
17.2%	12	2.22	-0.510	4132	-3.46
57.5%	26	2.47	-0.721	3802	-2.68
1815 (kg/m ³)	34	2.78	-1.031	3211	-1.96
	41	2.85	-1.254	2910	-1.61
	47	2.89	-1.240	2889	-1.64
	95	2.54	-2.176	1627	-0.73
	106	2.53	-2.333	1355	-0.67
17.7%	6	4.16	-1.210	1927	-1.97
51.3%	26	2.50	-2.126	1654	-0.75
1710	78	1.31	-2.506	1212	-0.23
	109	1.46	-3.021	232	-0.07
18.6%	9	3.22	-1.033	2667	-1.46
58.7%	20	3.42	-1.529	2169	-0.91
1726	136	0.77	-3.445	145	1.80
19.2%	9	3.59	-1.030	2247	-2.05
61.2%	29	2.64	-2.017	1753	-0.95
1803	43	2.26	-2.198	1581	-0.72
	76	1.77	-2.359	1439	-0.44
	115	1.50	-2.464	1305	-0.25
	145	1.38	-2.522	1214	-0.16
	193	1.27	-2.658	965	-0.03
	256	1.09	-2.723	857	0.10
	335	0.99	-2.817	678	0.20
19.6%	12	2.57	-0.464	3200	-4.75
69.8%	22	3.33	-0.752	2645	-3.76
1865	78	2.07	-2.226	1813	-1.69
	67	1.11	-2.594	1279	-0.88

20.2%	8	4.00	-1.208	2228	-3.24
68.7%	20	3.37	-1.900	1863	-2.50
1818	56	2.09	-2.448	1350	-1.81
	111	1.57	-2.976	351	-1.43

FREQUENCY = 800 Hz
HORIZONTAL ORIENTATION

MOISTURE CONTENT, % SATURATION, DENSITY (WB)	LAMBDA *10 ⁶	ACCLN. RATIO	PHASE ANGLE rad	ALPHA	XI
17.1%	4	0.97	-2.887	1324	-0.96
51.1%	9	0.88	-3.018	665	-0.86
1886 (kg/m ³)	19	0.74	-3.237	675	-0.57
	30	0.61	-3.419	682	-0.43
	37	0.57	-3.501	685	-0.16
	58	0.46	-3.768	668	-0.12
	72	0.42	-3.864	691	-0.08
	90	0.38	-4.046	695	-0.06
	103	0.35	-4.165	692	-0.04
18.3%	4	1.13	-2.918	1339	-1.26
63.2%	9	1.02	-3.101	248	-1.14
1863	22	0.85	-3.303	210	-0.17
	29	0.74	-3.514	504	-0.14
	36	0.74	-3.454	526	-0.12
	58	0.69	-4.175	581	-0.05
	69	0.60	-4.401	619	-0.01
	91	0.45	-4.578	660	0.04
	105	0.37	-4.630	667	0.01
18.6%	4	0.93	-2.953	1133	-1.24
62.0%	10	0.96	-3.011	806	-1.16
1790	18	0.93	-3.093	305	-1.11
21.4%	4	0.63	-3.269	246	-0.28
70.1%	9	0.61	-3.274	296	-0.26
1820	18	0.59	-3.410	433	-0.23
	32	0.61	-3.884	435	-0.20
	36	0.62	-3.899	423	-0.18
	54	0.54	-4.222	421	-0.17
	72	0.48	-4.432	418	-0.17
	120	0.34	-4.750	422	-0.17

21.4%	4	0.79	-3.594	578	-0.36
78.1%	9	0.83	-4.101	579	-0.28
1857	18	0.63	-4.567	616	-0.22
	32	0.47	-4.813	638	-0.18
	37	0.47	-4.836	632	-0.17
	54	0.36	-5.009	622	-0.15
	72	0.31	-5.153	619	-0.13
	100	0.25	-5.242	617	-0.12

FREQUENCY = 1000 Hz
HORIZONTAL ORIENTATION

MOISTURE CONTENT, % SATURATION, DENSITY (WB)	LAMBDA *10 ⁶	ACCLN. RATIO	PHASE ANGLE rad	ALPHA	XI
16.9%	3	0.82	-2.912	1016	-0.54
60.2%	6	0.78	-2.994	664	-0.50
1816 (kg/m ³)	12	0.73	-3.121	97	-0.45
	18	0.69	-3.265	110	-0.02
	23	0.66	-3.457	244	-0.01
	36	0.56	-3.806	368	-0.00
	45	0.50	-4.046	447	0.03
	57	0.43	-4.201	452	0.03
	61	0.41	-4.277	454	0.03
17.1%	2	0.78	-2.861	1288	-0.68
47.5%	6	0.75	-2.912	1064	-0.65
1646	11	0.72	-2.962	839	-0.63
	18	0.71	-3.035	506	-0.61
	36	0.65	-3.300	152	-0.16
	47	0.60	-3.586	358	-0.14
	47	0.60	-3.594	353	-0.14
17.9%	2	1.05	-3.244	124	-0.29
68.8%	5	1.14	-3.399	245	-0.26
1897	13	0.94	-4.261	629	-0.18
	18	0.75	-4.504	648	-0.17
	23	0.66	-4.613	740	-0.14
	37	0.47	-4.850	812	-0.12
	46	0.39	-4.910	849	-0.08
	57	0.34	-5.023	852	-0.78
	63	0.32	-5.013	861	-0.07
18.2%	2	0.77	-3.293	321	-0.32
58.7%	6	0.72	-3.437	589	-0.30
1748	11	0.67	-3.581	780	-0.25
	18	0.65	-3.763	828	-0.24
	23	0.63	-3.958	872	-0.20
	36	0.47	-4.340	900	-0.18
	45	0.38	-4.517	903	-0.12
	56	0.35	-4.547	904	-0.11
	60	0.34	-4.631	910	-0.11

20.3%	2	0.77	-3.306	216	-0.27
71.9%	6	0.82	-3.411	275	-0.25
1916	11	0.88	-3.630	437	-0.18
	18	0.84	-4.001	452	-0.17
	27	0.73	-4.295	473	-0.16
	49	0.57	-4.611	495	-0.14
	60	0.50	-4.743	499	-0.13
20.5%	2	0.62	-3.556	896	-0.31
68.4%	6	0.64	-3.614	833	-0.29
1796	11	0.68	-4.122	776	-0.27
	23	0.54	-4.725	655	-0.14
	41	0.37	-5.030	660	-0.12
	46	0.33	-5.129	655	-0.11
	57	0.30	-5.179	653	-0.10
	61	0.28	-5.192	647	-0.09

FREQUENCY = 1300 Hz
HORIZONTAL ORIENTATION

MOISTURE CONTENT, % SATURATION, DENSITY (WB)	LAMBDA *10 ⁶	ACCLN. RATIO	PHASE ANGLE rad	ALPHA	XI
16.7%	1	0.71	-4.810	544	-0.17
54.1%	3	0.55	-4.923	612	-0.15
1783 (kg/m ³)	7	0.41	-5.153	636	-0.14
	11	0.34	-5.152	669	-0.12
	13	0.31	-5.192	693	-0.12
	21	0.23	-5.348	702	-0.09
	26	0.19	-5.395	707	-0.08
	33	0.17	-5.458	710	-0.07
	38	0.16	-5.385	712	-0.07
16.9%	1	0.86	-4.041	827	-0.29
57.4%	4	0.81	-4.318	838	-0.26
1732	7	0.70	-4.568	863	-0.23
	11	0.56	-4.887	897	-0.19
	13	0.50	-4.887	897	-0.19
	21	0.38	-5.118	890	-0.16
	27	0.34	-5.162	903	-0.15
	37	0.28	-5.285	906	-0.13
18.4%	1	0.67	-4.708	705	-0.20
57.2%	3	0.58	-4.822	728	-0.19
1749	7	0.48	-5.016	719	-0.17
	11	0.41	-5.154	708	-0.15
	14	0.38	-5.242	694	-0.14
	22	0.30	-5.421	672	-0.12
	27	0.27	-5.506	662	-0.11
	34	0.24	-5.610	649	-0.10
	39	0.21	-5.707	637	-0.09
18.6%	1	0.78	-3.776	989	-0.33
64.9%	3	0.78	-3.863	996	-0.29
1867	7	0.74	-4.139	1017	-0.28
	10	0.63	-4.466	1011	-0.25
	13	0.59	-4.610	1000	-0.22
	21	0.49	-4.780	1007	-0.20
	26	0.45	-4.872	1012	-0.18
	33	0.39	-4.998	1015	-0.18
	38	0.34	-5.092	1014	-0.17

19.6%	1	0.76	-4.726	500	-0.16
72.6%	3	0.61	-4.978	502	-0.15
1783	6	0.46	-5.174	518	-0.13
	12	0.35	-5.300	540	-0.11
	20	0.28	-5.425	500	-0.10
	24	0.26	-5.409	578	-0.09
	29	0.23	-5.535	548	-0.08
	37	0.19	-5.591	567	-0.07
	44	0.18	-5.658	564	-0.07

FREQUENCY = 1500 Hz
HORIZONTAL ORIENTATION

MOISTURE CONTENT, % SATURATION, DENSITY (WB)	LAMBDA *10 ⁶	ACCLN. RATIO	PHASE ANGLE rad	ALPHA	XI
16.7%	1	0.41	-4.783	685	-0.11
57.8%	2	0.32	-4.941	694	-0.09
1850(kg/m ³)	5	0.26	-5.021	728	-0.08
	8	0.22	-4.920	812	-0.08
	10	0.20	-5.059	812	-0.08
	15	0.16	-5.108	789	-0.06
	19	0.15	-5.096	817	-0.05
	24	0.13	-5.241	819	-0.05
	27	0.12	-5.258	822	-0.05
17.1%	1	0.59	-4.932	818	-0.18
60.4%	2	0.49	-5.054	840	-0.17
1815	5	0.39	-5.148	891	-0.15
	8	0.34	-5.245	876	-0.14
	10	0.30	-5.269	917	-0.13
	16	0.23	-5.370	857	-0.11
	19	0.21	-5.430	942	-0.10
	24	0.18	-5.518	942	-0.09
17.4%	3	0.21	-5.445	751	-0.09
66.4%	5	0.18	-5.490	764	-0.08
1886	8	0.16	-5.564	760	-0.06
	11	0.15	-5.499	779	-0.06
	21	0.10	-5.643	806	-0.05
	26	0.10	-5.610	829	-0.05
	28	0.09	-5.651	832	-0.04
17.6%	1	0.62	-4.068	1049	-0.20
63.3%	2	0.57	-4.260	1058	-0.18
1858	5	0.52	-4.419	1046	-0.17
	8	0.44	-4.618	1049	-0.14
	10	0.41	-4.689	1043	-0.14
	15	0.32	-4.867	1056	-0.11
	19	0.28	-4.933	1058	-0.10
	23	0.26	-4.977	1066	-0.09
	27	0.23	-5.024	1066	-0.09

18.3%	1	0.81	-3.719	972	-0.31
70.3%	2	0.82	-3.862	988	-0.30
1874	5	0.83	-4.075	979	-0.27
	8	0.77	-4.331	986	-0.24
	10	0.73	-4.386	1012	-0.24
	15	0.58	-4.689	1043	-0.20
	19	0.52	-4.799	1051	-0.19
	24	0.44	-5.020	995	-0.17
	27	0.42	-5.059	1000	-0.16
18.5%	1	0.31	-5.723	511	-0.10
70.7%	3	0.27	-5.695	572	-0.09
1919	5	0.27	-5.617	611	-0.10
	9	0.24	-5.597	642	-0.09
	11	0.22	-5.637	681	-0.08
	17	0.18	-5.709	701	-0.07
	21	0.18	-5.698	715	-0.07
	26	0.16	-5.745	717	-0.07

FREQUENCY = 1700 Hz
HORIZONTAL ORIENTATION

MOISTURE CONTENT, % SATURATION, DENSITY (WB)	LAMBDA *10 ⁶	ACCLN. RATIO	PHASE ANGLE rad	ALPHA	XI
16.5%	1	0.73	-4.526	1047	-0.21
56.9%	2	0.66	-4.613	1086	-0.20
1821 (kg/m ³)	4	0.59	-4.741	1096	-0.43
	6	0.53	-4.850	1100	-0.18
	8	0.49	-4.924	1089	-0.17
	13	0.40	-5.206	1003	-0.14
	16	0.36	-5.179	1074	-0.14
	20	0.30	-5.413	975	-0.11
	23	0.29	-5.342	1044	-0.11
16.8%	1	0.67	-4.712	800	-0.19
54.7%	2	0.60	-4.785	833	-0.18
1683	4	0.51	-5.023	796	-0.16
	6	0.47	-5.087	793	-0.15
	8	0.44	-5.152	779	-0.14
	13	0.36	-5.325	764	-0.13
	15	0.32	-5.356	784	-0.12
	20	0.30	-5.454	755	-0.12
	22	0.28	-5.518	743	-0.11
17.8%	1	0.34	-5.089	2090	-1.00
67.3%	2	0.32	-5.216	845	0.11
1882	4	0.28	-5.271	860	-0.10
	6	0.24	-5.304	886	-0.09
	7	0.23	-5.274	927	-0.09
	12	0.19	-5.380	927	-0.07
	15	0.17	-5.414	933	-0.07
	19	0.14	-5.434	964	-0.06
	21	0.14	-5.409	990	-0.06

17.9%	1	0.58	-4.580	982	-0.18
71.1%	2	0.53	-4.672	989	-0.17
1914	4	0.47	-4.781	998	-0.16
	6	0.41	-4.905	993	-0.15
	8	0.39	-4.956	981	-0.14
	16	0.28	-5.217	957	-0.11
	20	0.25	-5.273	957	-0.11
	23	0.24	-5.390	905	-0.10
20.1%	1	0.32	-5.581	734	-0.42
75.5%	2	0.30	-5.709	669	-0.13
1846	4	0.29	-5.758	663	-0.12
	6	0.27	-5.814	655	-0.12
	7	0.26	-5.824	653	-0.12
	12	0.23	-5.990	657	-0.10

FREQUENCY = 2000 Hz
HORIZONTAL ORIENTATION

MOISTURE CONTENT, % SATURATION, DENSITY (WB)	LAMBDA *10 ⁶	ACCLN. RATIO	PHASE ANGLE rad	ALPHA	XI
16.5%	1	0.26	-5.845	1027	-0.14
48.3%	2	0.24	-5.872	1042	-0.13
1678 (kg/m ³)	3	0.24	-6.015	935	-0.13
	5	0.22	-5.956	1035	0.12
16.7%	1	0.30	-5.715	846	-0.13
62.5%	3	0.25	-5.905	802	-0.12
1843	5	0.23	-5.891	825	-0.11
17.3%	1	0.38	-5.154	1146	-0.13
70.5%	2	0.35	-5.263	1100	-0.13
1915	3	0.34	-5.199	1180	-0.13
	5	0.30	-5.240	1201	-0.12
	6	0.28	-5.334	1151	-0.11
	9	0.23	-5.425	1177	-0.09
	12	0.21	-5.419	1213	-0.09
	15	0.19	-5.448	1235	-0.08
	17	0.17	-5.500	1231	-0.07
18.3%	1	0.15	-5.231	2301	1.17
64.3%	3	0.14	-5.231	2233	1.09
1844	6	0.11	-5.352	2601	0.95
	9	0.10	-5.360	2570	0.81
	12	0.09	-5.407	2495	0.75
	15	0.08	-5.416	2569	0.69
	17	0.07	-5.437	2627	0.68
18.9%	1	0.12	-5.620	3892	0.90
58.3%	3	0.11	-5.663	3576	0.85
1729	5	0.09	-5.681	3858	0.76
	9	0.07	-6.696	3822	0.59
	12	0.06	-5.703	4264	0.51
	15	0.05	-5.712	3708	0.49

20.3%	1	0.17	-5.832	3479	1.03
70.5%	3	0.16	-5.841	3523	0.96
1870	5	0.15	-5.853	3665	0.91
	9	0.11	-5.867	4189	0.68
	12	0.10	-5.877	4484	0.61
	15	0.09	-5.882	4432	0.57
	19	0.01	-5.916	3795	0.62

APPENDIX B

THREE-DIMENSIONAL IN-SITU DATA

EXPERIMENTAL VALUES OF FREQUENCY, STRAIN AND APPARENT
POISSON'S RATIO FOR THE HORIZONTAL INPUT-
HORIZONTAL OUTPUT ORIENTATION

Distance between Input and Output, meters	Frequency, Hertz	Strain, meters/ meter	Apparent Poisson's Ratio
0.114	454.5	1.54E-03	0.034
	465.0	1.79E-03	0.045
	487.8	1.77E-03	0.039
	500.0	1.85E-03	0.050
0.144	444.3	9.49E-04	0.028
	454.6	1.43E-03	0.035
	476.2	1.67E-03	0.031
	487.2	1.21E-03	0.044
0.183	454.5	8.09E-04	0.026
	465.0	1.03E-03	0.028
	476.2	1.35E-03	0.026
	476.2	1.61E-03	0.030
0.227	465.0	3.34E-04	0.010
	487.8	4.44E-04	0.011
	500.0	5.39E-04	0.013
	526.3	1.03E-03	0.025
0.274	476.2	4.18E-04	0.016
	476.2	5.41E-04	0.017
	487.8	5.41E-04	0.016
	487.8	5.51E-04	0.017

EXPERIMENTAL VALUES OF FREQUENCY, STRAIN AND APPARENT
POISSON'S RATIO FOR THE HORIZONTAL INPUT-
VERTICAL OUTPUT ORIENTATION

Distance between Input and Output, meters	Frequency, Hertz	Strain, meters/ meter	Apparent Poisson's Ratio
0.114	487.8	1.64E-03	0.034
	476.2	3.30E-03	0.117
	472.4	3.65E-03	0.124
	454.2	3.72E-03	0.094
0.144	464.0	1.53E-03	0.081
	487.8	2.08E-03	0.055
	474.6	2.54E-03	0.061
	476.2	2.92E-03	0.059
0.227	454.6	6.37E-04	0.027
	512.5	6.39E-04	0.024
	526.3	7.82E-04	0.024
	540.2	1.03E-03	0.028
0.274	512.8	2.73E-04	0.012
	512.8	2.93E-04	0.010
	526.3	4.13E-04	0.012
	526.3	4.50E-04	0.014

EXPERIMENTAL VALUES OF FREQUENCY, STRAIN AND APPARENT
POISSON'S RATIO FOR THE VERTICAL INPUT-
HORIZONTAL OUTPUT ORIENTATION

Distance between Input and Output, meters	Frequency, Hertz	Strain, meters/ meter	Apparent Poisson's Ratio
0.114	307.6	2.15E-03	0.127
	312.6	3.83E-03	0.160
	317.4	4.65E-03	0.187
	322.6	6.03E-03	0.252
0.144	277.7	3.65E-03	0.141
	298.4	4.59E-03	0.159
	317.4	5.41E-03	0.176
	333.3	5.94E-03	0.197
0.183	273.9	3.20E-03	0.124
	285.7	3.59E-03	0.140
	298.8	3.46E-03	0.140
	303.0	4.14E-03	0.170
0.227	273.9	1.57E-03	0.080
	277.7	1.78E-03	0.089
	281.5	1.99E-03	0.100
	285.7	1.55E-03	0.084
0.274	277.7	1.02E-03	0.077
	277.7	1.13E-03	0.065
	285.7	1.07E-03	0.077
	298.4	1.27E-03	0.084

2
VITA

Richard Glenn Nelson

Candidate for the Degree of
Doctor of Philosophy

Thesis: INVESTIGATION OF FREQUENCY AND MOISTURE CONTENT ON
THE DEFORMATION CHARACTERISTICS OF SOIL

Major Field: Mechanical and Agricultural Engineering

Biographical:

Personal Data: Born in Minot, North Dakota, January 9,
1958, the son of Glenn Jay and Barbara Jane
Nelson.

Education: Graduated from Tulsa Memorial High School,
Tulsa, Oklahoma, May, 1976; received Bachelor of
Science degree in Mechanical Engineering from
Oklahoma State University in May, 1981; received
Master of Science degree in Mechanical Engineering
from Oklahoma State University in July, 1982;
completed requirements for the Doctor of
Philosophy degree at Oklahoma State University in
December, 1989.

Professional Experience: Project Engineer, Garrett
Airesearch, Los Angeles, California, June, 1982 to
November, 1982; Graduate Research Assistant,
Department of Agricultural Engineering, Oklahoma
State University, January, 1983 to December, 1987;
Graduate Teaching Assistant, Department of
Agricultural Engineering, Oklahoma State
University, January, 1986 to December, 1986;
Instructor, Department of Mathematics, Oklahoma
State University, August, 1986 to December, 1986.
Passed the Engineer-in-Training Exam, Fall 1981.
Student Member of the American Society of
Agricultural Engineers. Member of Phi Mu Epsilon.